Advection-Diffusion-Reaction Modeling of *Bacteroidales* in Estuaries with a Specific Application to the San Pablo Bay

By

ANTHONY JAMES MCDONALD
B.S. (University of California, Davis) 2006

THESIS

Submitted in partial satisfaction of the requirements for the degree of

MASTER OF SCIENCE

in

Civil and Environmental Engineering

in the

OFFICE OF GRADUATE STUDIES

of the

UNIVERSITY OF CALIFORNIA

DAVIS

Approved:

Committee in Charge

2007

Table of Contents

Introduction 1

Chapter 1: Internet Sources for Model Calibration Data 3

Chapter 2: Review of *Bacteroidales* Modeling Research 7

2.1: Introduction to the Literature Review 7

2.2: Purpose of the Review 9

2.3: Development of the Fate and Transport Model for Bacteria 10

2.4: Release of Bacteria from the Source 12

2.5: Overland Transport of Bacteria from Their Sources to Water Bodies 17

2.6: Partitioning of Bacteria Between Soluble and Sorbed Phases 20

2.7: Survival of Bacteria once Released into the Environment 21

2.8: Summary of the Literature Review Findings 32

2.9: Concluding Remarks on the Literature Review 33

Chapter 3: One-Dimensional Advection-Dispersion-Reaction Modeling 35

3.1: Introduction and Purpose of the 1-D A-D-R Model 35

3.2: Model Setup 36

3.3: Model Testing 44

3.4: Modeling Results 47

3.5: Concluding Remarks on the 1-D A-D-R Model 56

Chapter 4: Semi-Implicit Three-Dimensional Flow Modeling 58

4.1: Introduction to the S-I 3-D Flow Model 58

4.2: The Si3D Input File and Dictionary of Terminology 62

4.3: Coarsening Bathymetric Data for Input into the Si3D Program 63

4.4: Results of the 1000-Meter San Francisco Bay 1-Day Test Run 70

Conclusion 81

Bibliography 84

Appendix A: List of Internet Sources for Model Calibration Data 87

Appendix B: FORTRAN 77 Program for 1-D A-D-R Finite-Difference Models 109

Appendix C: Sample Si3D Input File 114

Appendix D: Dictionary of Terminology Used in Si3D 115

Appendix E: FORTRAN 77 Program for Coarsening NOS's SF Bay DEM 121

List of Tables and Figures

Figure 1.1: Proposed set of ten monthly *Bacteroidales* sampling locations 4

Figure 2.1: C/C_0 vs. $k\Delta Q$ relation using the SWAT and HSPF models 14

Figure 2.2: Observed and predicted manure effluent curves for various salinities 16

Figure 2.3: Effect of flow volumes on the temporal concentration of *E. coli* 18

Figure 2.4: Delivery ratio *DR* as a function of distance *D* from a water body 20

Figure 2.5: Sensitivity of temporal bacterial survival to the decay rate constant k 22

Figure 2.6: Demonstration of the stepwise decay model 24

Figure 2.7: Sensitivity of decay rate k to temperature T according to $k = k_{20}\theta^{T-20}$ 25

Figure 2.8: Effect of temperature and solar radiation 27

Figure 2.9: Mean monthly water temperature and cumulative precipitation 29

Figure 2.10: River-wide logistic regression results for ruminant markers 29

Figure 2.11: Seasonal variation in persistence in situ and in the laboratory 31

Figure 2.12: Effect of temp., filtration or cyc. addition on persistence of bacteria 31

Figure 3.1: Fully implicit scheme advection model tested against a step function 48

Table 3.1: Root mean squared error values for all models convergence tested 50

Figure 3.2: Results of fully implicit scheme dispersion 53

Figure 3.3: Results of fully implicit advection, fully explicit dispersion and decay 54

Figure 3.4: Results of Neumann boundary condition with fully explicit dispersion 56

Figure 4.1: San Francisco Bay DEM at original thirty-meter resolution 68

Figure 4.2: San Francisco Bay DEM increased to 240-meter resolution 69

Figure 4.3: 1000-meter bathymetric model of the San Francisco Bay 71

Figure 4.4: Velocity field at the free surface during a high slack tide in SF Bay 73

Figure 4.5: Velocity field at the free surface during an ebb tide in SF Bay 74

Figure 4.6: Velocity field at the free surface during a low slack tide in SF Bay 75

Figure 4.7: Velocity field at the free surface during a flood tide in SF Bay 76

Figure 4.8: Velocity profile at Carquinez Strait during high slack tide in SF Bay 77

Figure 4.9: Velocity profile at Golden Gate during high slack tide in SF Bay 77

Figure 4.10: Velocity profile at Carquinez Strait during ebb tide in SF Bay 78

Figure 4.11: Velocity profile at Golden Gate during ebb tide in SF Bay 78

Figure 4.12: Velocity profile at Carquinez Strait during low slack tide in SF Bay 79

Figure 4.13: Velocity profile at Golden Gate during low slack tide in SF Bay 79

Figure 4.14: Velocity profile at Carquinez Strait during flood tide in SF Bay 80

Figure 4.15: Velocity profile at Golden Gate during flood tide in SF Bay 80

Figure A.1: BDAT-EMP sampling locations 89

Figure A.2: NOAA-NDBC sampling locations 103

Figure A.3: SFEI-CISNet sampling locations 108

Acknowledgements

Many thanks to my thesis committee chair, Professor Fabián Bombardelli, for his continuous guidance and advice during the course of my research these past fifteen months. I also thank my two other thesis committee members, Professors Stefan Wuertz and Timothy Ginn, for their prompt review of the final version of this work.

Thank you also to the University of California, Davis, Department of Civil and Environmental Engineering for providing me with a research appointment which also covered all university registration fees as well as the funding agency, the Cooperative Institute for Coastal and Estuarine Environmental Technology, which provided funding for my research appointment during the summer.

Special acknowledgement is given to Doctor Peter Smith, who has kindly provided us access to the current source code for his semi-implicit, three-dimensional, finite-difference model for estuarine circulation, also known as Si3D, which was the topic of his Ph.D. dissertation and is a central element of this research project as well. Doctor Smith has collaborated with us and given access to the current model that he and his colleagues are developing for the San Francisco Bay and Estuary.

Finally, I want to thank all those who have supported me in this endeavor, especially my parents, Michael and Ann McDonald, who have provided me with the necessary motivation and encouragement to complete this degree.

Introduction

This thesis provides an overview of the methodology used in modeling *Bacteroidales* concentrations within an estuarine environment. *Bacteroidales* is an order of anaerobic fecal bacteria which contains four families. Recently, *Bacteroidales* have come into use as an indicator for the presence of pathogens. According to recent research, *Bacteroidales* may serve as a reliable predictor of pathogenic bacteria in general (Shanks et al., 2006). Measuring *Bacteroidales* only gives an historical record of their concentrations; however, models can be employed to predict future *Bacteroidales* concentrations as well as hypothetical ones. Such models can also provide much utility for determining appropriate total maximum daily loads or TMDLs allowable for meeting local water quality standards.

Flow modeling and advection-diffusion-reaction modeling, as with any computational simulation, requires initial conditions as well as boundary information to be supplied in order to accurately simulate *Bacteroidales* concentrations. The Internet sources for model calibration data described in Chapter 1 and listed in Appendix A are places which store flow and tidal data, water quality data as well as bathymetric and weather data pertaining to the San Francisco Bay, Delta and their immediate proximity. The literature review in Chapter 2 summarizes the current scientific advances regarding the measuring and modeling of *Bacteroidales* within estuarine environments. The more technical side of this thesis, contained in Chapter 3, explains the modeling of *Bacteroidales* concentrations through the use of one-dimensional advection-dispersion-reaction finite-differencing models with constant parameters. The final section, Chapter 4, is an introduction to semi-implicit, three-dimensional flow modeling, and how it can be applied to model *Bacteroidales* concentrations in the San Pablo Bay.

Chapter 1: Internet Sources for Model Calibration Data

Modeling *Bacteroidales* concentration within estuaries requires both a flow model and an advection-diffusion-reaction model. An accurate estuarine flow model will first require a good bathymetric model. This model must be resolved enough to represent all important features of the estuary, including straits, channels, islands and shoals. At least one thousand-meter resolution is needed to represent the Carquinez Strait; however, higher resolution would be necessary to capture the finer details of this strait. Boundaries need to be at locations that can accommodate the available data. If there is no nearby information, data must be adapted from sources farther away. The model boundaries require flow rate, water surface elevation and salinity data. This information is needed at small enough intervals to represent the tidal cycle. Hourly or fifteen-minute data is sufficient enough to capture these changes. In addition to providing boundary information, flow, stage and salinity data within the model's extents can be compared with its results for calibration purposes. An A-D-R model can be applied to the flow model to represent *Bacteroidales* concentrations. Boundary and calibration data will be needed for these concentrations as well; however, due to the difficulty of obtaining such information, *Bacteroidales* concentrations cannot be expected to be obtained at the same frequency as flow, stage and salinity data. The following figure shows a proposed set of locations in which Professor Wuertz's team from the Department of Civil and Environmental Engineering at the University of California, Davis, will take samples for *Bacteroidales* testing. This process is complex and is only expected to be executed at monthly intervals. Weather data may prove to be useful information for identifying *Bacteroidales* source release events.

Figure 1.1: Proposed set of ten monthly *Bacteroidales* sampling locations

An index of Internet data sources for water quality, flow and weather data for the San Francisco Bay and Estuary has been provided in Appendix A in order to provide sources for adequate modeling data. This all-encompassing list reports the data parameters which were measured, along with their frequencies, periods and locations. The list is sorted alphabetically by Internet source. The Bay Delta and Tributaries Project (http://bdat.ca.gov/) contains monthly and semimonthly water quality data over many of the past thirty years at many different locations around the bay. The California Data

Exchange Center (http://cdec.water.ca.gov/) has hourly water quality, flow and weather data over many of the past twenty years at many different locations around the bay. The Center for Integrative Coastal Observation, Research and Education (http://www.cicore.org/) has water quality and weather data about every five minutes over the past few years at a few locations in the San Francisco Bay. The California Irrigation Management Information System (http://wwwcimis.water.ca.gov/) operates weather stations which have been recording hourly weather data over the past four to twenty-two years at many locations around the bay. The Interagency Ecological Program (http://iep.water.ca.gov/) has tracked the mean daily flow at a few different locations in the delta for fifty-one years and has recorded hourly water quality and flow data over many of the past twenty-four years at many different locations around the bay. The National Estuarine Research Reserve System (http://nerrs.noaa.gov/) collects water quality and weather data in the Suisun Marsh every fifteen minutes since August 2006. The National Data Buoy Center (http://ndbc.noaa.gov/) collects six-minute and hourly weather data over the past few years at many locations within the bay and surrounding ocean. The National Geophysical Data Center's Marine Geology and Geophysics division (http://www.ngdc.noaa.gov/mgg/) has a Geophysical Data System which contains ninety-meter resolution coastal bathymetry. The National Ocean Service's Estuarine Bathymetry division (http://estuarinebathymetry.noaa.gov/) collected bathymetric data at thirty-meter resolution for the entire San Francisco Bay. The NOAA: Tides and Currents (http://tidesandcurrents.noaa.gov/) has six-minute and hourly water and weather data for much of the past fourteen years at many locations within the bay. The San Francisco Estuary Institute's (http://www.sfei.org/) CISNet study has monthly water quality data for about one year for many locations within the San Pablo Bay and Marsh. Finally, the San Francisco Bay and Delta region of the USGS (http://sfbay.wr.usgs.gov/) has ten-meter resolution bathymetric data for the entire delta and Suisun Bay.

Chapter 2: Review of *Bacteroidales* Modeling Research

2.1: Introduction to the Literature Review

Estuaries are the receiving waters for rivers and streams before they enter the ocean and are a collecting place where these continental waters mix with seawater. Many estuaries in the world receive very large amounts of freshwater, especially those that are the receiving waters for large and vast basins like the one of the great valley of California. These estuaries have great potential for harboring high levels of pathogens as well as other microbes. Pathogens mainly come from human and animal feces, and many of these sources remain unregulated or are poorly regulated.

Pathogens are specific causative agents of disease, such as bacteria or viruses. Some pathogens can be life threatening. They are most often contracted through direct ingestion of contaminated food or water. This health risk has caused officials to look into remediation options for keeping water bodies at safer levels, as far as human health is concerned. Bacteria such as *E. coli*, *enterococci* and *Bacteroidales* indicate the presence of these disease causing agents. Regulatory agencies have identified allowable concentrations of fecal pathogen indicators; however, many water bodies are not meeting these minimum standards for human health safety, causing many beaches and other public swimming areas to close because of the elevated risk of contracting disease through exposure due to accidental ingestion.

Traditionally, *E. coli* and *enterococci* have been used as pathogenic indicators; however, they have been found to grow and persist in extraintestinal environments such as lakes, rivers and soils (Shanks et al., 2006). These traditional indicators are not a reliable measurement of recent pathogenic contamination if they proliferate or persist in places where the pathogens they represent do not. For indicator bacteria to be a reliable measure of pathogens, they should persist and be present at concentrations that are proportional to the concentrations of the pathogens they represent. Recently, scientists have introduced anaerobic fecal bacteria belonging to the order *Bacteroidales* as an indicator for pathogenic or microbial contamination within water bodies. Shanks' study has found that *Bacteroidales* do not proliferate outside the intestine the same way that *E. coli* does and, therefore, may be a more reliable indicator of pathogenic contamination.

Pathogenic contamination sources may be localized or spread out, i.e., point sources or distributed sources. Livestock manure, bird guano, industrial runoff, sewage spills and animal feces can all contribute to the concentration of pathogens at a particular location within a water body at any given time. High runoff events provide a fast and efficient transport mechanism for getting pathogens from their source to surface water systems, especially if they have to cover a long distance to get there.

Point measurements of pathogenic indicators such as *E. coli*, *enterococci* and *Bacteroidales* are mechanisms currently used to determine if a water body has acceptable levels of pathogenic contamination, from a human health perspective. Professor Wuertz of the Civil and Environmental Engineering Department at the University of California, Davis, is currently conducting a study that is taking measurements of *Bacteroidales* at specific locations within the San Pablo Bay. See Figure 1.1 for a proposed set of ten monthly sampling locations. Measuring *Bacteroidales* concentrations is a lengthy and complicated process and has a limited frequency in which it can reasonably be done. In many cases, limited numbers of measurements must be trusted to predict pathogenic contamination levels throughout a large or extensive water body. Clearly, measurements alone do not provide sufficient information to know the true contamination levels at all places within a water body at any given time. A better understanding of where pathogens and microbes are coming from, where they are being transported to and where they ultimately end up will give a better idea of the true contamination levels throughout a system. In this thesis, it is argued that numerical simulation can assist with observations to determine the fate and transport of pathogens.

2.2: Purpose of the Review

The purpose of this review is to investigate the sources, methods of transport and ultimate fate of *Bacteroidales* as they exist and die off while traveling within surface water systems. This review includes an investigation into the various sources of pathogens and *Bacteroidales*, as well as an investigation into the causes and methods of release from the source. Once released from the source by events such as rainfall, *Bacteroidales* often must travel great distances over land before entering water bodies. Understanding this mode of transport gives a better idea of how *Bacteroidales* are entering water bodies from their various sources. Once inside a water body, it is helpful to know how *Bacteroidales* are traveling within the system and whether they travel as individual suspended particles, congeal together into larger masses or attach themselves to sediment particles. Understanding these transport processes will give a better idea of how *Bacteroidales* are traveling within water bodies. Finally, it is useful to know the settling, mortality or decay rates of *Bacteroidales* while within large water bodies. Understanding all these separate phenomena should provide a comprehensive basis for the development of a model for predicting actual concentration levels of *Bacteroidales* at any given place or time without the benefit of actual measurements at that particular location. This review should give the basis for how the presence of *Bacteroidales* may be modeled and predicted within the San Pablo Bay, California.

2.3: Development of the Fate and Transport Model for Bacteria

Transport models are useful for obtaining concentrations of fecal pathogens outside the spaces and times in which their indicator bacteria were measured. *Bacteroidales* can be a good indicator of fecal borne pathogen concentrations because, according to studies like Shanks et al. (2006), they have been found to persist at concentrations that are proportional to the pathogenic concentrations we are interested in. The use of a three-dimensional transport model will aid in understanding where waterborne bacterial concentrations are headed and where they will ultimately end up. Such a transport model is based upon a finite-difference estimation of the three-dimensional advection-diffusion-reaction equation. The A-D-R equation is designed to give temporal variation in concentration at particular points in space, and conceptually, it is made up of the four terms illustrated as follows.

$$\textit{concentration change} + \textit{advection} = \textit{diffusion} + \textit{sources/sinks} \tag{2.1}$$

Equation 2.1 is a simplification of the following differential equation:

$$\frac{\partial \overline{C}}{\partial t} + \overline{u}\frac{\partial \overline{C}}{\partial x} + \overline{v}\frac{\partial \overline{C}}{\partial y} + \overline{w}\frac{\partial \overline{C}}{\partial z} = \frac{\partial}{\partial x}\left(D_{Txx}\frac{\partial \overline{C}}{\partial x}\right) + \frac{\partial}{\partial y}\left(D_{Tyy}\frac{\partial \overline{C}}{\partial y}\right) + \frac{\partial}{\partial z}\left(D_{Tzz}\frac{\partial \overline{C}}{\partial z}\right) - k\overline{C} \tag{2.2}$$

where $\overline{C}$ is the local, turbulence averaged *Bacteroidales* concentration; $\overline{u}$, $\overline{v}$ and $\overline{w}$ are the average velocities in the *x*, *y* and *z* directions, respectively; D_{Txx}, D_{Tyy} and D_{Tzz} are the primary components of the diffusion/dispersion tensor; *k* is the decay or mortality rate constant, and *t* is the time coordinate. Smith (1997) developed a flow model based upon the solution to the layer-integrated, three-dimensional Navier-Stokes equations, which he used to analyze water flows that are within the extents of San Francisco, San Pablo and Suisun Bays. By incorporating the A-D-R equation into Smith’s model, it can be adapted to simulate the transport of *Bacteroidales* suspended within the waters of San Pablo Bay. *Bacteroidales* that are bonded together in masses or adsorbed to suspended sediment may be included as well; however, the model must be adapted to simulate the settling rate for these particles, since a certain number of them will reach the bottom of the bay and die there without being resuspended.

Analyzing just the concentration change vs. sources/sinks part of Equation 2.2 gives the following simplified equation which neglects the influences of advection and diffusion.

$$\frac{d\overline{C}}{dt} = -k\overline{C} \tag{2.3}$$

This is a first-order ordinary differential equation, and after removing the turbulence averaging, its solution in terms of local concentration is the following relation, where C_0 represents the original concentration C at $t = 0$. This equation is known as Chick's Law (1908).

$$C = C_0 e^{-kt} \tag{2.4}$$

2.4: Release of Bacteria from the Source

Animal feces are one of the main sources of bacteria and pathogens within surface waters. They include dog and bird feces as well as cow manure and other ruminant sources. In many cases, these feces are laying on the ground with a certain concentration of intestinal bacteria and pathogens. These bacteria and pathogens will more or less remain with the feces until released through a significant precipitation or runoff event. Considering this release phenomenon, various models have been developed for the simulation of source release during a runoff event. Two such models are found in the Soil and Water Assessment Tool (SWAT) developed by Sadeghi and Arnold (2002) and the Hydrological Simulation Program–FORTRAN (HSPF) developed by Bicknell et al.

(1997). The release equation based upon the Soil and Water Assessment Tool is the following linear equation:

$$C = C_0 k \Delta Q \tag{2.5}$$

where C is the concentration of bacteria released during the runoff event; C_0 is the original concentration of bacteria stored at the source and is assumed to be constant; k is the release rate, also assumed constant, and ΔQ is the cumulative total runoff. This model suggests that all of the bacteria are released (i.e., $C = C_0$) once $k\Delta Q$ reaches a value of one. The release equation based upon the Hydrological Simulation Program–FORTRAN (HSPF) uses the following exponential relationship.

$$C = C_0\left(1 - e^{-k\Delta Q}\right) \tag{2.6}$$

Figure 2.1 compares how these two models perform. The SWAT model releases all of the bacteria by the time $k\Delta Q$ reaches a value of one. This occurs when the ratio C/C_0 equals one, meaning that all the original concentration has been released. When $k\Delta Q$ reaches one, the HSPF model has only released 63% of the original bacterial concentration and does not reach 99% release until $k\Delta Q$ is 4.6.

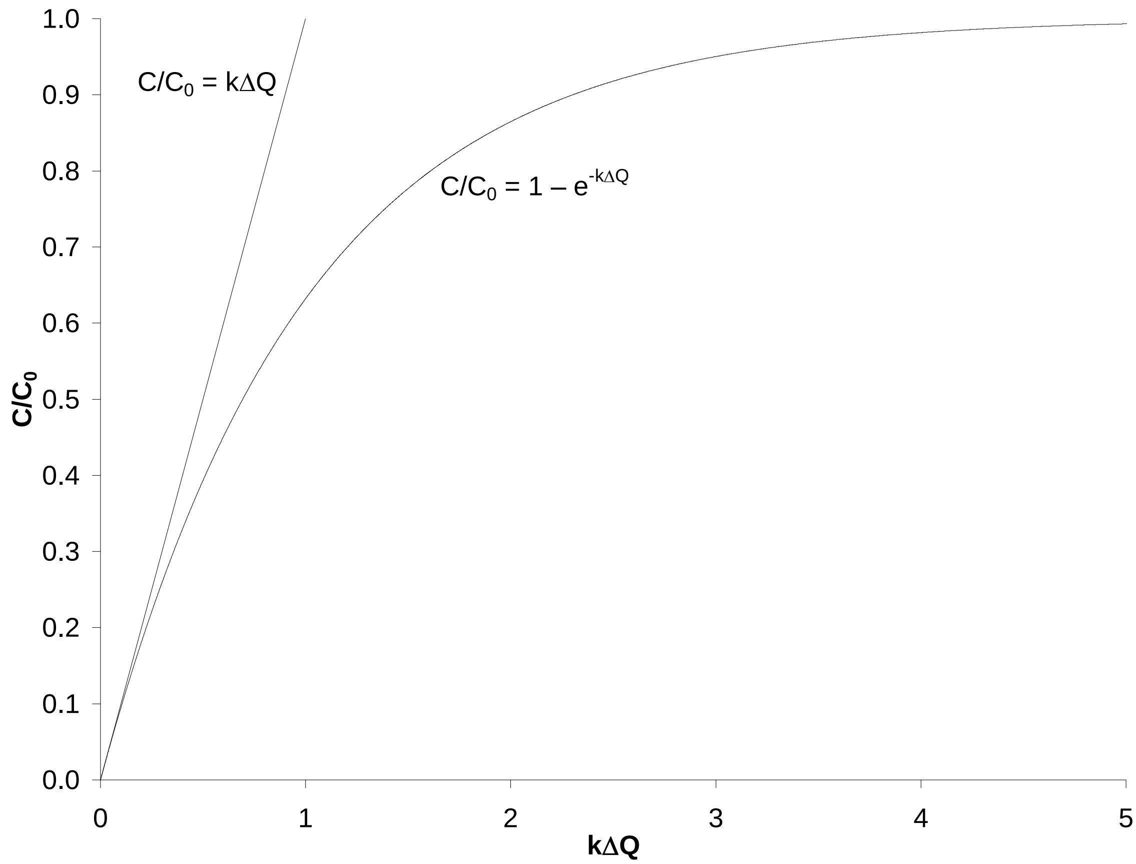

Figure 2.1: Comparison of the C/C_0 vs. $k\Delta Q$ relation from the SWAT model (Equation 5) vs. the HSPF model (Equation 6)

Pachepsky et al. (2006) reviewed an equation that was given by Vadas et al. (2004) in their study of a method to predict dissolved phosphorus in runoff from surface-applied manures. The following relation in terms of bacterial concentration is based upon that equation:

$$C = C_0 \alpha \left(\frac{\rho_w q}{M_d} t \right)^{\beta} \tag{2.7}$$

where C is the number of bacteria released during the event; C_0 is the original number of bacteria stored in the surface manure; M_d is the mass of manure per unit area; ρ_w is the water density; q is the runoff rate, and t is time. Bradford and Schijven (2002) developed studies to determine the release behavior of *Cryptosporidium* oocysts and *Giardia* cysts from dairy calf manure to waters of various salinities. They fitted the data they obtained with a relation similar to the following equation:

$$C = C_0\left(1 - \frac{1}{(1+\alpha\beta t)^{1/\beta}}\right) \tag{2.8}$$

where C is the number of bacteria released during the event; C_0 is the original number of bacteria stored in the surface manure; $\alpha = 0.0005EC^{-0.127}$, and $\beta = 4.95e^{0.097EC}$, where EC is the electrical conductivity of the water. Bradford and Schijven created the following plot in Figure 2.2, which fits their model with measured data for various solution salinities.

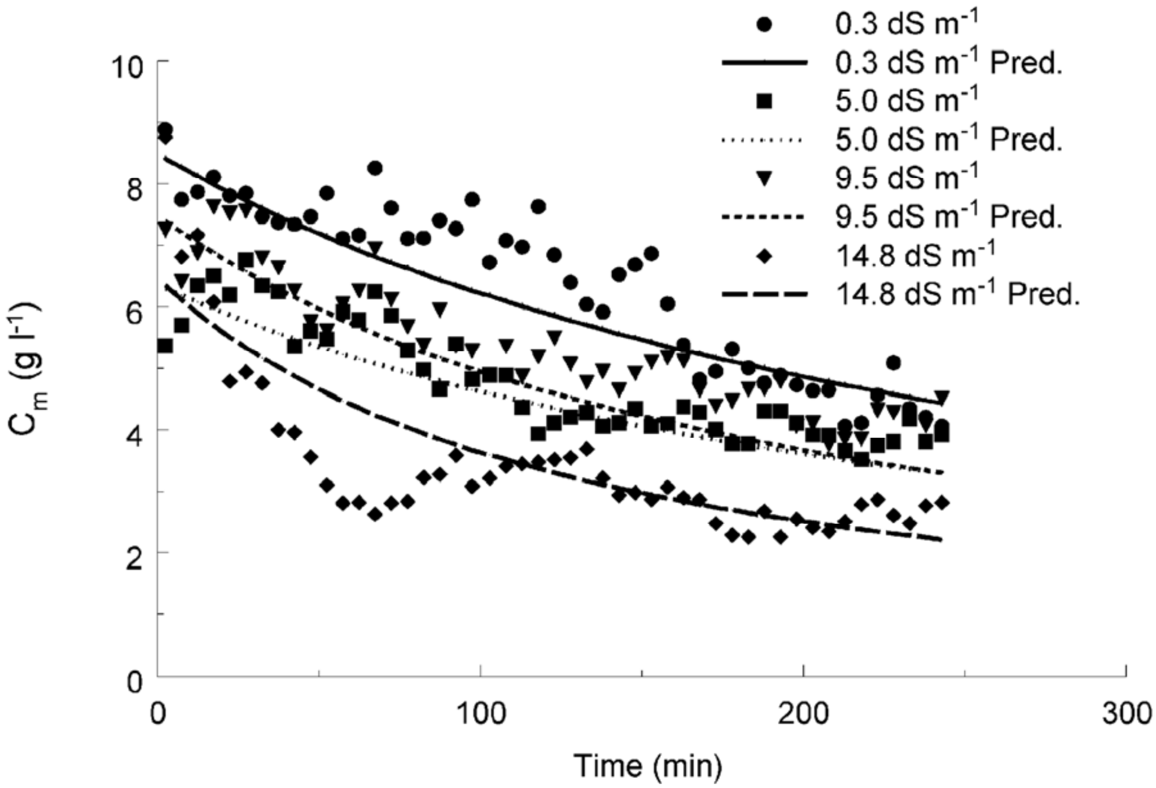

Figure 2.2: A plot of representative observed and predicted manure effluent curves for the various solution salinities (Bradford and Schijven, 2002)

Muirhead et al. (2005) studied the processes by which bacteria, specifically *E. coli*, may attach themselves to each other in cell masses or simply attach themselves to particles. From their study of these processes, they suggest that *E. coli* cells may enter the soil-surface runoff during rainfall events as highly mobile unattached cells with long survival times. This may serve as an explanation for the occurrence of high background concentrations of *E. coli* in surface runoff.

2.5: Overland Transport of Bacteria from Their Sources to Water Bodies

During overland transport from the source to a large water body, bacteria can settle out of suspension and accumulate on the ground; whereas, a runoff event can resuspend previously settled bacteria. Tian et al. (2002) developed a model for spatial and temporal changes of microbial contaminants on grazing farmlands. They suggest that the daily resuspension rate *RS* should be defined by the following equation:

$$RS = 1 - \exp\left(\frac{V_0 - V}{Q_0}\right), \quad V > V_0 \qquad (2.9)$$

where V is the daily flow volume; V_0 is the minimum flow volume required for resuspension, and Q_0 is a control parameter for the resuspension rate *RS*. Figure 2.3 demonstrates Tian's model and the use of Equation 2.9 by illustrating the effect of flow volume on temporal *E. coli* concentrations at the outlet of a hypothetical grazing land catchment.

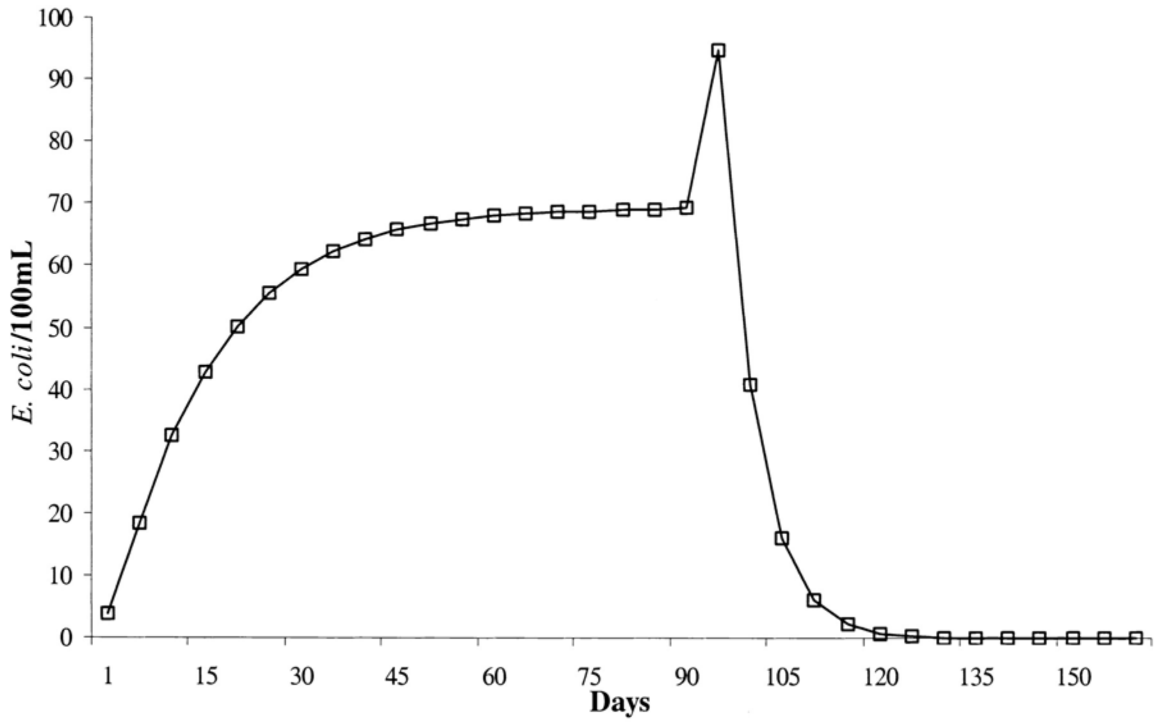

Figure 2.3: Effect of flow volume on temporal *E. coli* concentration; a low flow volume was used for the first ninety days; then a high flow volume was applied for the remainder (Tian et al., 2002)

As seen in Figure 2.3, the model by Tian et al. (2002) produced reasonable results when evaluating the effect of flow volume on the concentration of *E. coli*. This result shows that *E. coli* concentration at the outlet jumped immediately after the flow volume increased, due to catchment flushing. The model indicated that the period for catchment-wide cleanup was about one month. Tian's model is consistent with other studies regarding resuspension rates.

Vegetated buffer strips and wetlands remove bacteria from runoff water and trap bacteria that are attached to sediment particles (Pachepsky et al., 2006). Moore et al. (1988), in their evaluation of coliform concentrations in runoff from various animal waste management systems, developed an equation for the percent removal of bacteria *PR*:

$$PR = 11.8 + 4.3R \tag{2.10}$$

where *R* is the ratio of the filter strip width, m, to the slope, %. It is clear here that percent removal follows a linear relationship with the filter strip width, and full removal of the bacteria occurs when the filter strip width, expressed in terms of meters, is at least 20.51 times wider than the slope, expressed in terms of a percentage.

Tian et al. (2002), who studied spatial and temporal modeling of microbial contaminants on grazing farmlands, based the delivery ratio *DR* of bacteria upon the distance *D* of the source from the water body:

$$DR = \frac{a_L}{D} \tag{2.11}$$

where a_L is a land use parameter. Figure 2.4 shows that the delivery ratio is high at short distances and quickly drops to a lower level at longer distances.

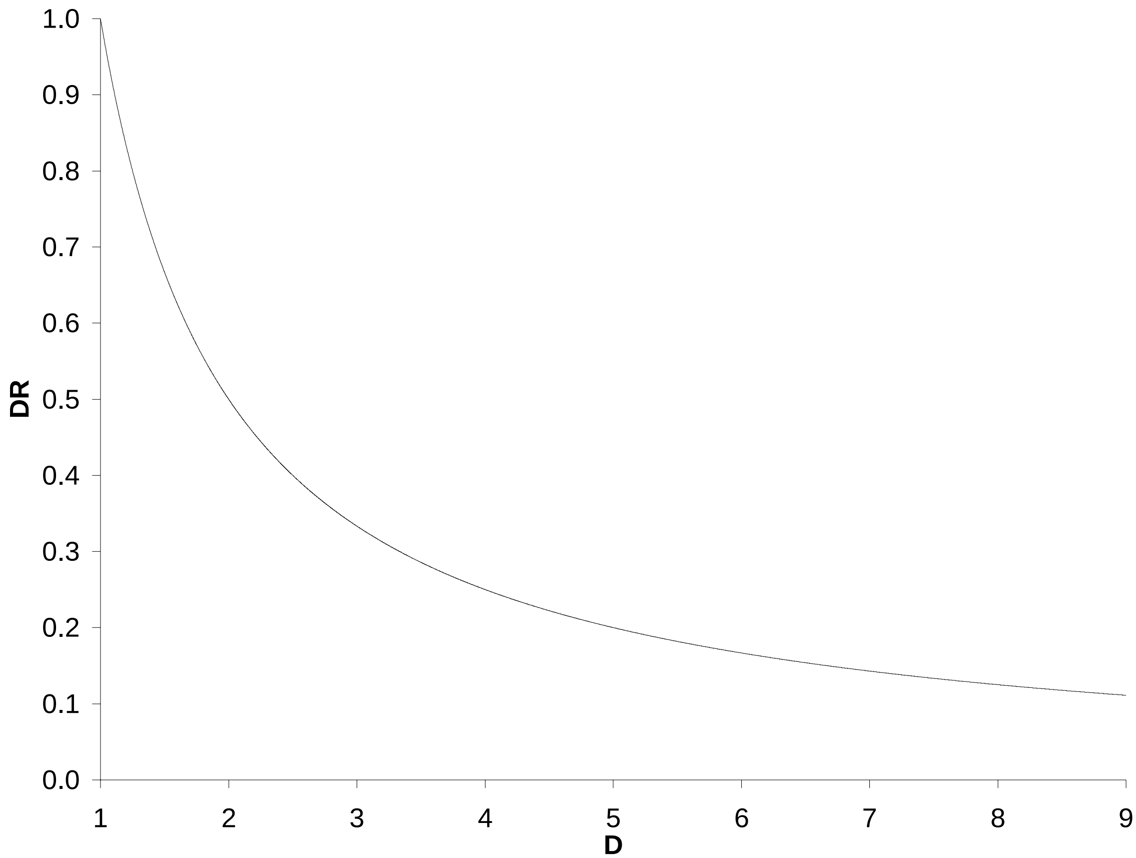

Figure 2.4: Delivery ratio *DR* as a function of distance *D* from water body ($a_L = 1$)

2.6: Partitioning of Bacteria Between Soluble and Sorbed Phases

According to the Benham et al. (2006) overview and the Pachepsky et al. (2006) review of existing fate and transport models, fecal bacteria can be partitioned into soluble and sorbed phases. This partitioning applies to their initial release from the source, overland and subsurface transport as well as stream and bed transport. SWAT (Sadeghi and Arnold, 2002) and HSPF (Bicknell et al., 1997) assume the following linear partitioning relationship:

$$S = K_d C \tag{2.12}$$

where S is the amount of adsorbed bacteria in runoff, measured as count/g; K_d is the partitioning coefficient, and C is the concentration of bacteria in runoff, measured as count/mL. Pachepsky et al. (2006) found K_d values of 10 and 70 mL/g to be reasonable. According to Hagedorn et al. (1978), clay content is the leading factor for determining K_d; however, according to Bengtsson (1989), relationships between K_d and clay content are uncertain.

The Muirhead et al. (2005) study of *E. coli* adsorption found that the percentages of *E. coli* cells that were attached to particles varied but tended to be low, with an overall mean of only eight percent of bacteria attaching to particles. They also found that the majority of *E. coli* cells not attached to particles were transported individually in suspension and not in groups of cell masses.

2.7: Survival of Bacteria once Released into the Environment

A comprehensive study of the survival or mortality rate of *Bacteroidales* usually begins with the widely used Chick's Law (1908). Chick, in his investigation of the laws of disinfection, suggested this first-order exponential decay relation for bacteria given in Equation 2.4 of the model development section. This equation is reproduced here for convenience.

$$C = C_0 e^{-kt} \tag{2.4}$$

For this case of bacterial survival, C is the bacterial concentration at time t; C_0 is the original bacterial concentration, and k is the decay rate constant. Crane and Moore (1986), in their review of enteric bacterial decay models, found k values for *E. coli* to rage between 0.1 and 2 day^{-1}. Figure 2.5 shows the sensitivity of temporal bacterial survival to the decay rate constant k. When k = 2 day^{-1}, 98% of the initial concentration is lost within the first two days; whereas, when k = 0.1 day^{-1}, it takes nearly seven days for the initial concentration to reduce by one half.

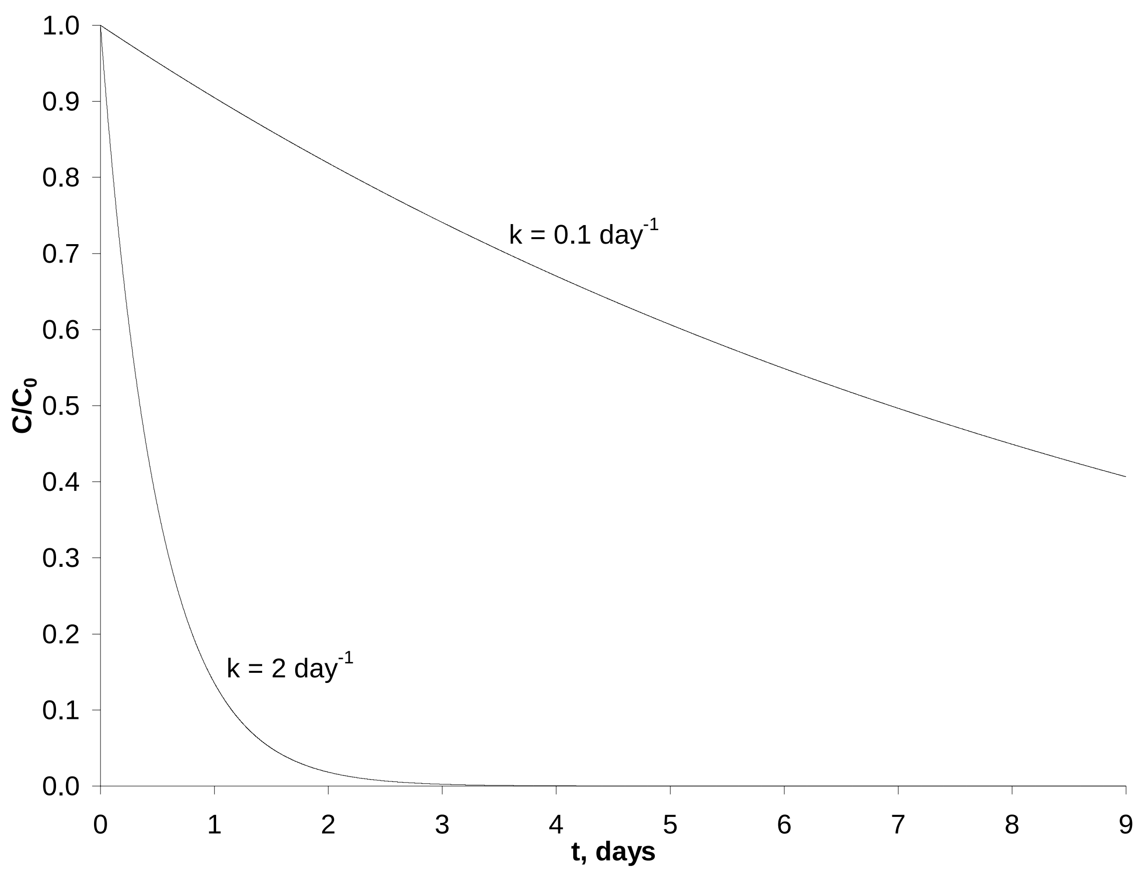

Figure 2.5: Sensitivity of temporal bacterial survival to the decay rate constant k

Crane and Moore also suggest that the decay rate k can change over time. For instance, a high initial death rate may be followed by slower long term decay. They propose the following stepwise model which changes the decay rate from k_1 to k_2 at time t_1.

$$C = \begin{cases} C_0 e^{-k_1 t}, & t < t_1 \\ C_0 e^{-k_2 t}, & t \geq t_1 \end{cases} \tag{2.13}$$

This model is illustrated in Figure 2.6, and it is clear that the initial decay rate of 2 day^{-1} eliminates 99.8% of the initial concentration in the first three days; whereas, die-off is more gradual after that due to the decay rate constant reducing to 0.5 day^{-1}.

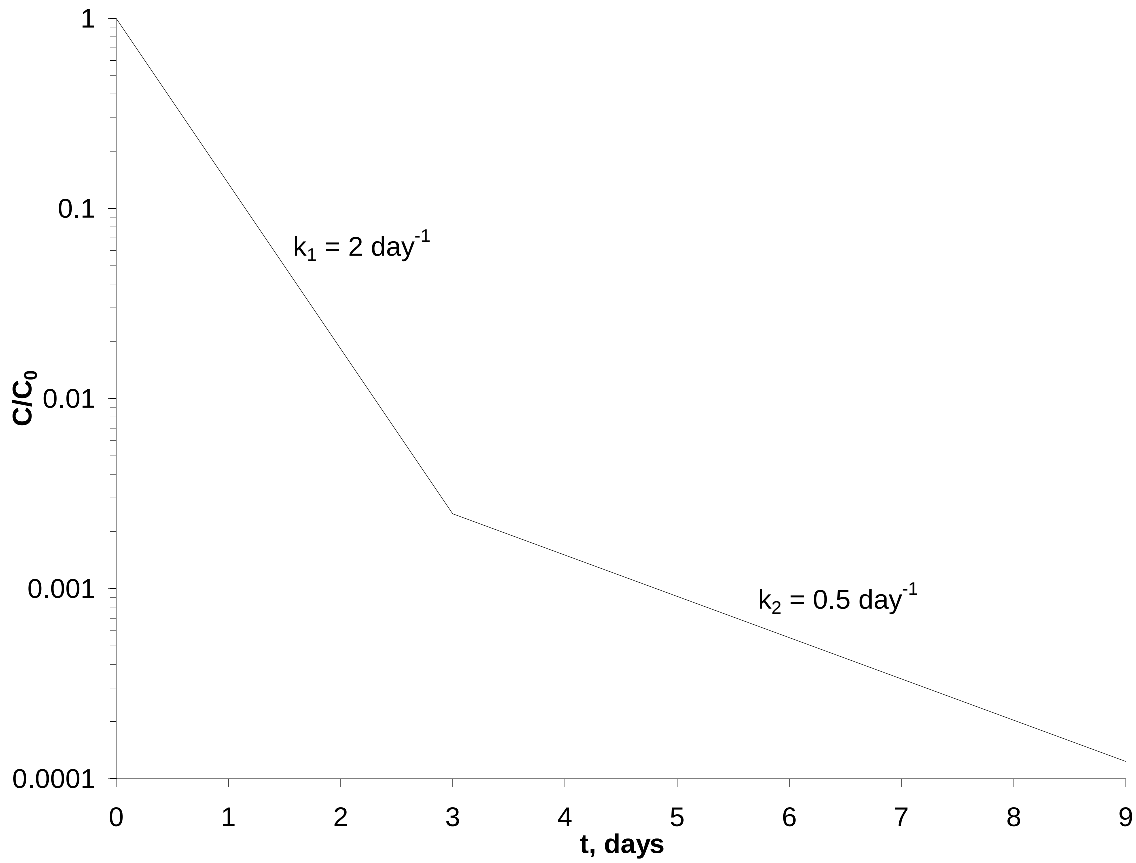

Figure 2.6: Demonstration of the stepwise decay model in Equation 2.13 using a high initial decay rate for the first three days followed by more gradual decay thereafter

According to the review of modeling enteric bacterial decay by Crane and Moore (1986) and as reviewed by Benham et al. (2006) and Pachepsky et al. (2006), the T_{20} equation suggests the following temperature correction for the decay rate k:

$$k = k_{20}\theta^{T-20} \tag{2.14}$$

where k is the decay rate at temperature T; k_{20} is the decay rate at 20 °C, and θ is the temperature correction factor. Typically, θ is about 1.07 and is independent of the surroundings; whereas, k_{20} varies depending upon the environment. Figure 2.7 displays the results of a sensitivity analysis performed on the T_{20} equation along a range of temperatures which is expected to be found in the San Pablo Bay.

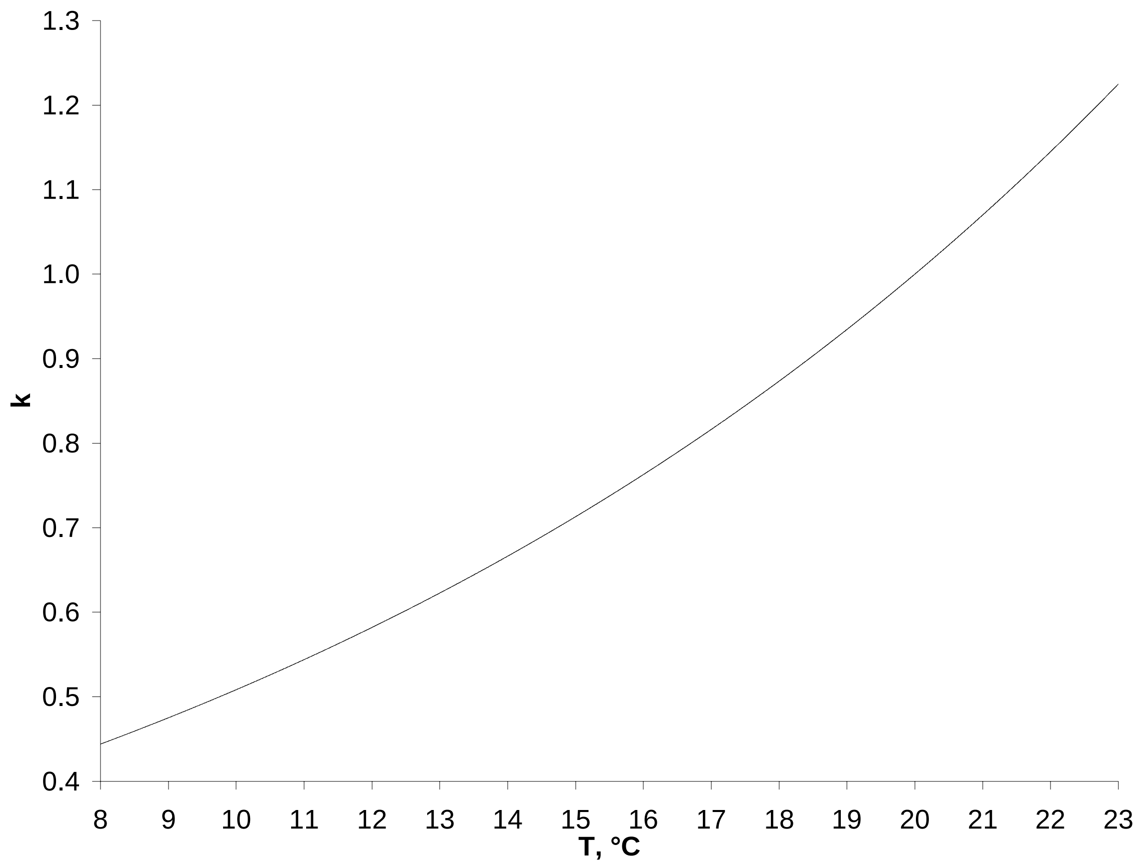

Figure 2.7: Sensitivity of decay rate k to temperature changes according to $k = k_{20}\theta^{T-20}$

Figure 2.7 uses an arbitrary k_{20} value of one, and as a result, k varies from 0.44 at 8 °C to 1.23 at 23 °C. There is a significantly large variance in decay rate between the warmer, summertime bay temperature and the colder, winter temperature; therefore, these warmer temperatures may result in a decay rate which is nearly three times greater than it would be at the colder bay temperatures, according to the T_{20} equation.

The model by Tian et al. (2002) suggests the following temperature and solar radiation correction for decay rate k:

$$k = \frac{T}{a_T} + \frac{R}{a_R} \tag{2.15}$$

k is the decay rate at temperature T and solar radiation R; a_T is the inactivation rate by temperature, and a_R is the inactivation rate by solar radiation. The k-T-R relationship of Equation 2.15 is demonstrated in Figure 2.8, as the decay rate k is balanced against a constant *E. coli* stocking rate. A low k value was applied for the first ninety days, followed by a high k value for the next ninety days. The resulting *E. coli* count was modeled and plotted against time to show the effect which different temperature and solar radiation values have on total *E. coli* population.

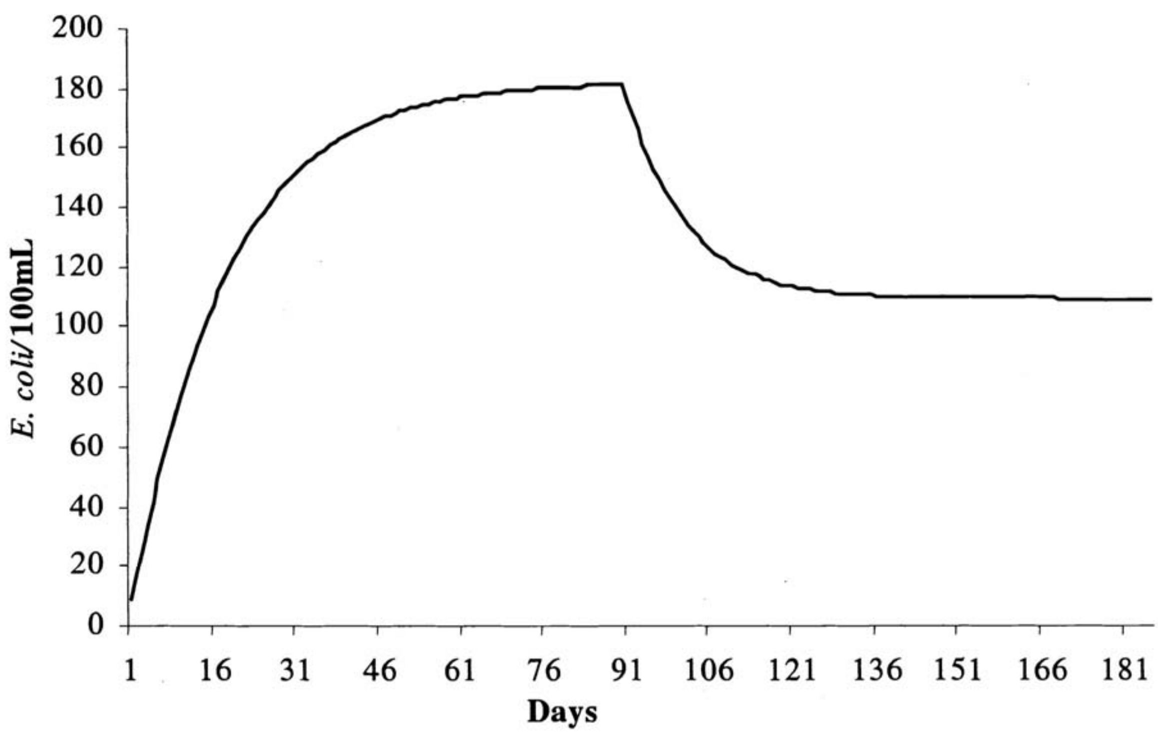

Figure 2.8: Effect of temperature and solar radiation on *E. coli* count; a low treatment was applied for the first ninety days, and a high treatment was applied thereafter (Tian et al., 2002)

The particular temperature and radiation values for this model were selected to represent typical climate conditions in New Zealand. At the low temperature and radiation conditions, the *E. coli* concentration was able to reach 180 *E. coli*/100 mL. However, the sudden change to high temperature and radiation caused the *E. coli* population to drop quickly and ultimately reach a steady state near 110 *E. coli*/100 mL. Steady state is reached as the decay rate, which varies with total *E. coli* population, reaches a balance with the constant stocking rate of *E. coli*. This stocking rate is what prevents the *E. coli* population from disappearing completely. No matter how high the decay rate *k* may be, any positive stocking rate will balance out the decay before the *E. coli* population completely dies off.

The study by Shanks et al. (2006) compared the detection of *E. coli* vs. *Bacteroidales*. They performed a two-year study within the Tillamook Basin, Oregon, at thirty sites within the bay and five tributaries. One finding of this study was that there was a forty percent greater prevalence of ruminant *Bacteroidales* markers from sources such as cow manure, than there was of human markers. The most important finding of this study, however, was that there were large inconsistencies between the trends of *E. coli* counts and *Bacteroidales* markers. More specifically, they found a significant positive relationship between *E. coli* count and both water temperature and turbidity as well as a negative relationship between *E. coli* count and pH. Their study had found *E. coli* to grow and persist outside the intestine, especially at higher temperatures.

Shanks et al. (2006) found many inconsistencies between *E. coli* counts and the presence of *Bacteroidales* markers. Mainly, the *Bacteroidales* markers did not follow the same seasonal variations that the *E. coli* counts did. *Bacteroidales* were also found to be more sensitive to temperature increases than *E. coli* was. However, on the other hand, Shanks et al. (2006) found evidence to suggest that higher salinity has less of a detrimental effect on *Bacteroidales* than it does on *E. coli*, possibly making it a better indicator of pathogen levels, assuming certain types of these pathogens are able to persist in salt water environments at similar rates as *Bacteroidales* markers.

One of the most striking *E. coli* vs. *Bacteroidales* findings of the Shanks et al. (2006) study was that *E. coli* counts were the highest in the dry summer months and decreased during precipitation events; whereas, *Bacteroidales* marker levels decreased during the dry summer months and were the highest during the first rainfall event in the fall. The annual precipitation cycle is shown in Figure 2.9, and in Figure 2.10, it can be seen that the probability of detecting ruminant *Bacteroidales* markers fell to its lowest point in the summer, corresponding to a time when water temperature was at its highest and precipitation was at its lowest. Indications from this study also show that *Bacteroidales* markers do not grow and persist outside the intestine at rates in which *E. coli* does, especially at higher temperatures.

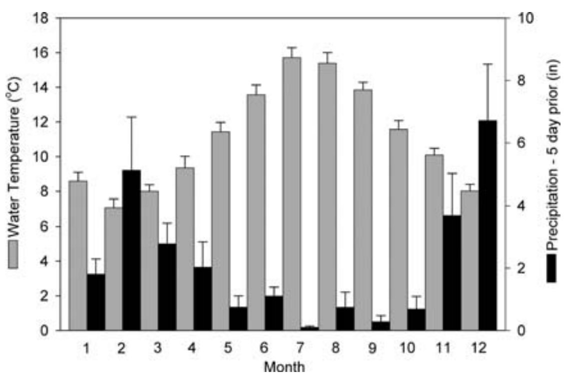

Figure 2.9: Mean monthly values for water temperature and cumulative precipitation for the 5 days leading up to and including the day of a sampling event. The error bars indicate 95% confidence intervals. (Shanks et al., 2006)

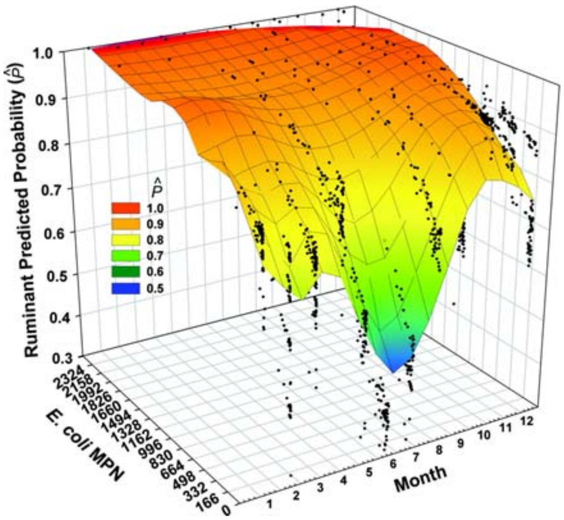

Figure 2.10: River-wide logistic regression results for ruminant markers. A Loess smoother at 0.3 sampling proportion and first-degree polynomial was applied to the solution of the regression model. (Shanks et al., 2006)

Walters and Field (2006) specifically studied the extraintestinal growth of fecal bacteria. They obtained *Bacteroidales vulgatus* ATCC 4245 as well as the control organism *Fulvimarina pelagi* HTCC 2506, plus they collected sewage influent from the Corvallis Wastewater Reclamation Plant in Oregon. They incubated the sewage at the in situ temperature of 21 °C under aerobic conditions for 4, 8, 12 and 24 hours. They found that *Bacteroidales* can grow for up to twenty-four hours in sewage when preparations are incubated aerobically at the in situ temperature of sewage, and the markers persist for at least twenty-four hours under the same conditions. The Walters and Field (2006) study also found that there was growth of *Bacteroidales* cells during aerobic incubation of sewage influent and suggests that *Bacteroidales* may be able to persist and grow in low-oxygen refuges in streams, lakes, estuaries and bays. They also observed that some of the factors that influence the growth of extraintestinal *Bacteroidales* include predation, ambient water temperature, UV radiation and sediment adsorption.

Kreader (1998) evaluated the persistence of PCR-detectable *Bacteroides distasonis* in surface water by dispersing whole human feces into water from the Ohio River and incubating them in laboratory flasks or in diffusion chambers in situ. She found that the persistence of PCR-detectable *Bacteroides distasonis* depended upon temperature and predation. She found an inverse relationship between *Bacteroides distasonis* survival and temperature. Specifically, she found that the molecular signal for *Bacteroides distasonis* persisted for at least two weeks at 4 °C, four to five days at 14 °C, one to two days at 24 °C and only one day at 30 °C in the Ohio River water. These findings indicate that there is a positive relationship between temperature and mortality rate of *Bacteroides distasonis* and is consistent with the findings of other studies regarding *Bacteroidales*, namely Shanks et al. (2006); furthermore, these findings validate the T_{20} equation. In filtered water lacking predators, the persistence of *Bacteroides distasonis* at 24 °C was extended by at least one week. Figures 2.11 and 2.12 show the relative abundance of these markers during Kreader's study.

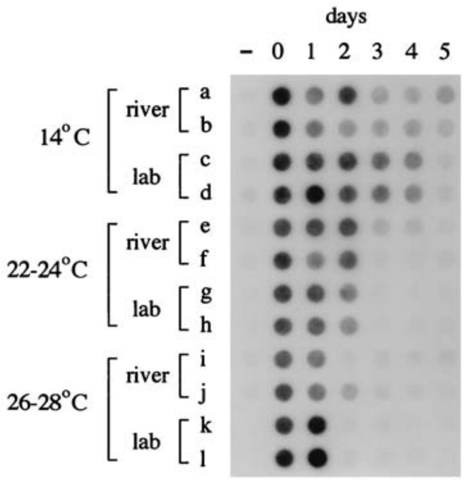

Figure 2.11: Seasonal variation in persistence in situ and in the laboratory using raw river water. Samples taken before addition of feces (day -), immediately after addition of feces (day 0) and after incubation for 1 to 5 days. Experiments ran from 24 to 29 April (rows *a* and *b*), from 5 to 10 May (rows *c* and *d*), from 6 to 11 June (rows *e* to *h*) and from 6 to 13 July (rows *i* to *l*), all in 1995. Surface water temperatures in the river were 14, 14, 22 to 24 and 26 to 28°C, respectively. Rows *a*, *b*, *e*, *f*, *i* and *j* are samples taken from diffusion chambers incubated in the river. Rows *c*, *d*, *g*, *h*, *k* and *l* are samples from flasks incubated in the lab at the indicated temperatures. (Kreader, 1998)

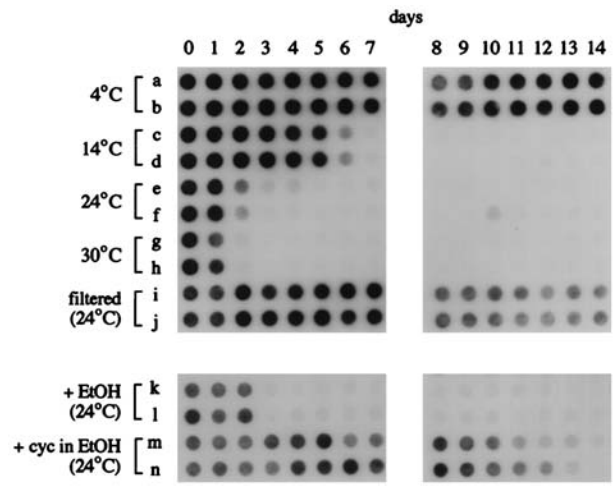

Figure 2.12: Effect of temperature, filtration or cycloheximide (cyc.) addition on persistence of PCR-detectable bacteria. Samples were taken immediately after addition of feces (day 0) and after incubation for 1 to 14 days at the indicated temperatures. For rows *a* to *h* and *k* to *n*, raw river water was used. For rows *i* and *j*, filtered water was filtered through a 0.45-mm filter with a 500-ml Millipore filtration unit before addition of feces. For rows *k* and *l*, 0.5 ml of ethanol (EtOH) and for rows *m* and *n*, 0.5 ml of 25-mg/ml cycloheximide in ethanol was added per 50 ml of river water before addition of feces. (Kreader, 1998)

Seurinck et al. (2005) collected fecal samples from human, dog, horse, cow, chicken and pig sources. The fecal samples were collected in sterile recipients and stored at -20 °C. They collected water samples from a freshwater canal, septic waste collecting trucks and domestic wastewater treatment plant influent. The water samples were filtered through a 0.22-mm filter. They performed aerobic incubation of the human-specific *Bacteroides* marker (HF183) and found that it persisted in freshwater for up to twenty-four days at 4 and 12 °C and up to eight days at 28 °C in fresh river water. These findings are consistent with those of Kreader (1998) in that they confirm the positive relationship between temperature and *Bacteroides* mortality rate.

2.8: Summary of the Literature Review Findings

Fecal borne bacteria and pathogens originate in the intestine and are washed overland and into waterways by precipitation and runoff events. Bacteria and pathogens remain near the fecal matter as it lies on dry ground. A runoff event may wash away part or all of the bacteria and pathogens originally present. *Bacteroidales* can be a reasonable measure of fecal pathogen loads, assuming they have similar decay rates and exhibit concentrations proportional to those of fecal pathogens.

The overland transport of bacteria between its source and neighboring surface water system depends on the size of the catchment area, the distance to the neighboring waterway, the size and amount of rainfall/runoff events and the presence of wetlands or filtration systems. Depending upon these conditions, bacterial concentrations may build up over time within a catchment area and be flushed away later by a significant runoff event.

While within surface runoff or waterways, bacteria may adsorb to particles or be transported in suspension. There have not been clear and consistent findings on actual adsorption rates. Most bacteria that are being transported in suspension are moving individually and not in cell masses (Muirhead et al., 2005). Adsorption rates may be related to the amount of clay particles present; however, no clear relationship has been found.

Bacteroidales markers may be detectable anywhere from one day to a few weeks, depending upon the conditions. The general tendency is that *Bacteroidales* persist longer in colder environments, corresponding to lower decay rate constants at lower temperatures, verifying the T_{20} equation (Kreader, 1998; Seurinck et al., 2005). Solar radiation, in addition to higher temperatures, increases *Bacteroidales* decay rate (Tian et al., 2002).

This information regarding the sources, fate and transport of *Bacteroidales* can be applied to the general advection-diffusion-reaction equation to model *Bacteroidales* as they travel within an estuary.

2.9: Concluding Remarks on the Literature Review

This review gives the basis of knowledge necessary for identifying the sources, transport mechanisms and fate of *Bacteroidales* within an estuarine system, so as to give a better understanding of their concentration and the pathogen levels they represent. It provides the background needed to create a fate and transport model that can be used to predict bacterial concentrations at spaces and times that are beyond the frequency of the measurements, in order that we can more fully know the true concentrations of these bacteria at all spaces and times within an estuary. The actual parameter values that are to be used in the transport model, such as source locations and concentrations, release rates and times, partitioning coefficients and settling rates as well as decay or mortality rates, cannot be specifically known from this review; however, values for these parameters can be adjusted during model calibration, as the model results are fitted against measured data.

Chapter 3: One-Dimensional Advection-Dispersion-Reaction Modeling

3.1: Introduction and Purpose of the 1-D A-D-R Model

The one-dimensional advection-dispersion-reaction equation with constant velocity, dispersivity and decay rate parameters may be used as a simple model for the transport and fate of *Bacteroidales* in water bodies where depth and width are not as important as length, for instance, river reaches. Such a model is useful to compare with river observations in order to determine proper dispersivities and decay rates. This 1-D A-D-R equation was approximated using finite-differencing schemes for the advection, dispersion and reaction terms of the A-D-R equation. The eight advection models tested were backward (upwind) differences, Lax dissipative scheme, Lax-Wendroff scheme, leap-frog scheme, fully implicit scheme, McCormack's scheme, Fromm's scheme and the generalized box explicit scheme. The three dispersion models tested were the fully explicit scheme, fully implicit scheme and the Crank-Nicolson scheme. Similarly, the three reaction models tested were also the fully explicit, fully implicit and Crank-Nicolson schemes, and they simulate first-order decay.

Each of the above advection models can be combined with each dispersion model and each reaction model to approximate advection-dispersion-reaction phenomena in a multitude of ways. The A-D-R model is implemented stepwise, in an iterative fashion, across space and time to obtain a solution for this physical behavior. All the different schemes vary in complexity, with backward (upwind) differences and the fully explicit schemes being the most simple of them all. Generally speaking, increased model complexity requires more computer time for each computational step; however, it often saves total computing time by requiring fewer spatial and temporal steps to reach a reasonable solution. All of these different models were implemented in FORTRAN 77 and tested for accuracy and stability. The main purpose is to determine the A-D-R scheme along with the spatial and temporal step size combination that satisfies accuracy and stability in the fewest number of computations. The ideal scheme and step size combination, chosen in terms of accuracy and efficiency, would certainly be the best model for simulating *Bacteroidales* concentrations within the San Pablo Bay.

3.2: Model Setup

This section outlines the methodology used to set up a one-dimensional advection-dispersion-reaction model, where the following theoretical relation is to be modeled.

$$\frac{\partial c}{\partial t} + u\frac{\partial c}{\partial x} = D\frac{\partial^2 c}{\partial x^2} - \lambda c \tag{3.1}$$

In this equation, c = concentration; x = distance; t = time; u = velocity; D = dispersivity, and λ = decay rate. u, D and λ are assumed to be constant. For the purpose of this model, the A-D-R equation is divided into its three different terms: advection, dispersion and reaction.

Advection Term

The advective part of the A-D-R equation is defined by the following relation.

$$\frac{\partial c}{\partial t} = -u\frac{\partial c}{\partial x} \tag{3.2}$$

This advection equation is approximated by the following eight models taken from Koutitas (1988). In the following modeling equations, the integers *i* and *n* represent the current spatial and temporal positions, respectively. $i - 1$ and $i + 1$ represent the previous and next spatial positions, and the same applies for $n - 1$ and $n + 1$. Finally, Δx and Δt are the spatial and temporal step sizes.

Model 1: Backward (upwind) differences

$$\frac{c_i^{n+1} - c_i^n}{\Delta t} = \frac{-u}{\Delta x}\left(c_i^n - c_{i-1}^n\right) \tag{3.3}$$

Model 2: Lax dissipative scheme

$$\frac{\theta c_i^{n+1} - \frac{1-\theta}{2}\left(c_{i+1}^n + c_{i-1}^n\right)}{\Delta t} = \frac{-u}{2\Delta x}\left(c_{i+1}^n - c_{i-1}^n\right) \tag{3.4}$$

The weighting factor θ for this scheme varies between zero and one, excluding zero.

Model 3: Lax-Wendroff scheme

$$\frac{c_i^{n+1} - c_i^n}{\Delta t} = \frac{-u}{2\Delta x}\left(c_{i+1}^n - c_{i-1}^n\right) + \frac{u^2 \Delta t}{\Delta x^2}\left(c_{i+1}^n - 2c_i^n + c_{i-1}^n\right) \tag{3.5}$$

Model 4: Leap-frog scheme

$$\frac{c_i^{n+1} - c_i^{n-1}}{2\Delta t} = \frac{-u}{2\Delta x}\left(c_{i+1}^n - c_{i-1}^n\right) \tag{3.6}$$

Model 5: Fully implicit scheme

$$\frac{c_i^{n+1} - c_i^n}{\Delta t} = \frac{-u}{4\Delta x}\left(c_{i+1}^{n+1} + c_{i+1}^n - c_{i-1}^{n+1} - c_{i-1}^n\right) \tag{3.7}$$

Model 6: McCormack's scheme

$$\frac{c_i^{n'} - c_i^n}{\Delta t} = \frac{-u}{\Delta x}\left(c_{i+1}^n - c_i^n\right) \tag{3.8}$$

$$\frac{c_i^{n+1} - \frac{1}{2}\left(c_i^{n'} + c_i^n\right)}{\Delta t} = \frac{-u}{\Delta x}\left(c_i^{n'} - c_{i-1}^{n'}\right) \tag{3.9}$$

The above two equations combine as follows.

$$\frac{c_i^{n+1}-c_i^n}{\Delta t}=\frac{-u}{2\Delta x}\left(c_{i+1}^n+c_i^n-2c_{i-1}^n\right)+\frac{u^2\Delta t}{\Delta x^2}\left(c_{i+1}^n-2c_i^n+c_{i-1}^n\right) \tag{3.10}$$

Model 7: Fromm's scheme

$$\frac{c_i^{n+1}-c_i^n}{\Delta t}=\frac{-u}{4\Delta x}\left(c_{i+1}^n-c_{i-1}^n+c_i^n-c_{i-2}^n\right)+\frac{u^2\Delta t}{4\Delta x^2}\left(c_{i+1}^n-2c_i^n+c_{i-1}^n\right)$$
$$+\frac{u^2\Delta t-2u\Delta x}{4\Delta x^2}\left(c_{i-2}^n-2c_{i-1}^n+c_i^n\right) \tag{3.11}$$

Model 8: Generalized box explicit scheme

$$(1-\theta)\left(\frac{c_i^{n+1}-c_i^n}{\Delta t}\right)+\theta\left(\frac{c_{i-1}^{n+1}-c_{i-1}^n}{\Delta t}\right)=\frac{-u}{2\Delta x}\left(c_i^{n+1}-c_{i-1}^{n+1}+c_i^n-c_{i-1}^n\right) \tag{3.12}$$

The weighting factor θ for this scheme varies between zero and one, inclusive. All of the above eight advection models are explicit, meaning c^{n+1} is solved completely in terms of c^n and c^{n-1}, except for the fully implicit scheme and the generalized box explicit scheme which are both implicit models.

Dispersion Term

The dispersive part of the A-D-R equation is defined by the following equation.

$$\frac{\partial c}{\partial t} = D\frac{\partial^2 c}{\partial x^2} \tag{3.13}$$

This dispersion equation can be approximated by centered finite differences as suggested by Koutitas (1988).

$$\frac{c_i^{n+1} - c_i^n}{\Delta t} = (1-\alpha)\frac{D}{\Delta x^2}\left(c_{i+1}^n - 2c_i^n + c_{i-1}^n\right) + \alpha\frac{D}{\Delta x^2}\left(c_{i+1}^{n+1} - 2c_i^{n+1} + c_{i-1}^{n+1}\right) \tag{3.14}$$

The weighting factor α for this scheme varies between zero and one, inclusive, and is used to specify whether the model is fully explicit, fully implicit or any combination in between.

$\alpha = 0$ indicates that the model is fully explicit and is written as follows.

$$\frac{c_i^{n+1} - c_i^n}{\Delta t} = \frac{D}{\Delta x^2}\left(c_{i+1}^n - 2c_i^n + c_{i-1}^n\right) \tag{3.15}$$

$\alpha = 1$ indicates that the model is fully implicit, and this case is represented by the following equation.

$$\frac{c_i^{n+1} - c_i^n}{\Delta t} = \frac{D}{\Delta x^2}\left(c_{i+1}^{n+1} - 2c_i^{n+1} + c_{i-1}^{n+1}\right) \tag{3.16}$$

However, $\alpha = 0.5$ means the model is an exact average of the explicit and implicit models. This case is called a Crank-Nicolson scheme and is written as follows.

$$\frac{c_i^{n+1} - c_i^n}{\Delta t} = \frac{D}{2\Delta x^2}\left(c_{i+1}^n - 2c_i^n + c_{i-1}^n\right) + \frac{D}{2\Delta x^2}\left(c_{i+1}^{n+1} - 2c_i^{n+1} + c_{i-1}^{n+1}\right) \tag{3.17}$$

Reaction Term

The reactive part of the A-D-R equation is the following first-order decay relationship.

$$\frac{dc}{dt} = -\lambda c \tag{3.18}$$

This reaction equation can be approximated by the following finite-differencing scheme.

$$\frac{c_i^{n+1} - c_i^n}{\Delta t} = -(1-\beta)\lambda c_i^n - \beta\lambda c_i^{n+1} \tag{3.19}$$

The weighting factor β for this scheme varies between zero and one, inclusive, and like α, it is used to specify whether the model is fully explicit, fully implicit or any combination in between.

$\beta = 0$ indicates a fully explicit scheme which is written as follows.

$$\frac{c_i^{n+1} - c_i^n}{\Delta t} = -\lambda c_i^n \tag{3.20}$$

β = 1 indicates a fully implicit scheme. This model is represented as follows.

$$\frac{c_i^{n+1} - c_i^n}{\Delta t} = -\lambda c_i^{n+1} \tag{3.21}$$

When β = 0.5, the model is an exact average of the explicit and implicit models, creating the Crank-Nicolson scheme, which is written as follows.

$$\frac{c_i^{n+1} - c_i^n}{\Delta t} = -\frac{\lambda}{2} c_i^n - \frac{\lambda}{2} c_i^{n+1} \tag{3.22}$$

Any of the advection models may be combined with any of the dispersion models and any of the reaction models to approximate the full advection-dispersion-reaction equation.

The explicit forms of finite-differencing schemes must satisfy the following stability criteria for advection and dispersion, respectively.

$$u \frac{\Delta t}{\Delta x} < 1 \tag{3.23}$$

$$D\frac{\Delta t}{\Delta x^2} < \frac{1}{2} \tag{3.24}$$

The implicit forms of the finite-differencing schemes, however, are stable for all Δx and Δt and, therefore, do not need to satisfy the above stability criteria.

All models sweep once through every spatial position for every forward advancement in time. For explicit models, c_i^{n+1} is solved for each spatial position during each temporal advancement. For implicit models, the coefficients a_i, b_i, c_i and d_i of the equation $a_i c_{i-1}^{n+1} + b_i c_i^{n+1} + c_i c_{i+1}^{n+1} = d_i$ are first found for each spatial position during each temporal advancement; a_1 and c_N are both set equal to zero, and the following tridiagonal matrix is obtained from this system of equations.

$$\begin{bmatrix} b_1 & c_1 & 0 & 0 & 0 \\ a_2 & b_2 & c_2 & 0 & 0 \\ 0 & a_3 & b_3 & \cdot & 0 \\ 0 & 0 & \cdot & \cdot & c_{N-1} \\ 0 & 0 & 0 & a_N & b_N \end{bmatrix} \begin{bmatrix} x_1 \\ x_2 \\ \cdot \\ \cdot \\ x_N \end{bmatrix} = \begin{bmatrix} d_1 \\ d_2 \\ \cdot \\ \cdot \\ d_N \end{bmatrix} \tag{3.25}$$

The tridiagonal matrix algorithm, also known as the Thomas algorithm, is applied to the coefficients a_i, b_i, c_i and d_i to solve c_i^{n+1} for each spatial position during each temporal advancement. The FORTRAN 77 source code used to implement all these different finite-differencing models is contained in Appendix B.

3.3: Model Testing

Three different problems were devised to test the models. In order to satisfy advection and dispersion stability criteria for all explicit models, the temporal step size was always chosen to satisfy both the advection and dispersion stability criteria of Equations 3.23 and 3.24, respectively, for the particular Δx, u and D combination that was being tested.

First, all of the advection models were tested against the advancement of a sharp, unit step front at constant velocity u. It is a variation of the Heaviside unit step function, and its analytical solution is as follows.

$$c = \begin{cases} 1, & x \le ut \\ 0, & x > ut \end{cases} \tag{3.26}$$

The models were also tested using the Dirac delta function centered at $x = 0$ as the initial condition. Informally, the Dirac delta function can be described as a function that is zero everywhere but at the origin, where it is infinite. This condition is explained by Equation 3.27; however, it must also satisfy the identity in Equation 3.28.

$$\delta(x) = \begin{cases} \infty, & x = 0 \\ 0, & x \ne 0 \end{cases} \tag{3.27}$$

$$\int_{-\infty}^{\infty} \delta(x)\,dx = 1 \tag{3.28}$$

Applying the advection-dispersion-reaction equation to the Dirac delta function results in the following Gaussian function, which is also the analytical solution.

$$c = \frac{e^{-\lambda t - \frac{(x-ut)^2}{4Dt}}}{\sqrt{4\pi Dt}} \tag{3.29}$$

The eight advection models were tested against the advancing unit step front of Equation 3.26 for a time span of $t = 32$, using a spatial step size of $\Delta x = 1$ and a velocity of $u = 1$. A constant concentration of $c = 1$ was used at the left-hand boundary; whereas, a constant concentration of $c = 0$ was placed at the right-hand boundary. These are known as Dirichlet boundary conditions. Boundaries were placed at spatial locations of $x = \pm 100$ and 100. These boundary locations were placed far enough away so as not to have an appreciable effect on modeling the moving concentration front.

Convergence tests were performed on the models using the following initial condition to represent the Dirac delta function described by Equations 3.27 and 3.28.

$$c = \begin{cases} 1/\Delta x, & x = 0 \\ 0, & x \neq 0 \end{cases} \tag{3.30}$$

Convergence testing was performed on the three dispersion models for the same time span of $t = 32$, using a dispersivity of $D = 2$ and spatial step sizes of 2^2, 2^1, 2^0, 2^{-1}, 2^{-2}, 2^{-3}, 2^{-4}, 2^{-5} and 2^{-6}. Dirichlet boundary conditions of $c = 0$ were used at spatial locations of x

= ±48 because the theoretical concentration values at those places never rises above 10^{-5} during the course of the modeling period.

Convergence tests using the same Dirac delta initial condition in Equation 3.30 were also performed on all the different advection-dispersion-reaction model combinations for the same time span of t = 32 and dispersivity of D = 2, as well as a velocity of u = 1 and a decay rate of λ = 0.01. The same spatial step sizes of 2^2, 2^1, 2^0, 2^{-1}, 2^{-2}, 2^{-3}, 2^{-4}, 2^{-5} and 2^{-6} were also used. Dirichlet boundary conditions of c = 0 were used at spatial locations of x = -16 and 80 for these models since the theoretical concentration values at those places never crosses above 10^{-5} during the modeling period.

Similar convergence tests were performed for a case taken from Fletcher (1991), which uses a Neumann boundary condition that varies in time. In this particular case, advection and reactions are not present, meaning that only the dispersion term is needed from the A-D-R equation. Recalling the dispersion equation from before:

$$\frac{\partial c}{\partial t} = D \frac{\partial^2 c}{\partial x^2} \tag{3.13}$$

will be solved in the spatial interval $0.1 \leq x \leq 1$ using the following Neumann boundary condition at x = 0.1:

$$\frac{\partial c}{\partial x} = 2 - 2\pi \sin(0.05\pi) \exp\left[-D \left(\frac{\pi}{2} \right)^2 t \right] \tag{3.31}$$

and a Dirichlet boundary condition of $c = 2$ at $x = 1$. The three different dispersion models were tested for eleven incremental time spans between $t = 0$ and 9, inclusive, using a dispersivity of $D = 0.9$ and spatial step sizes of $0.9/2^1$, $0.9/2^2$, $0.9/2^3$, $0.9/2^4$, $0.9/2^5$, $0.9/2^6$, $0.9/2^7$, $0.9/2^8$ and $0.9/2^9$. The results were compared against the following analytical solution.

$$c = 2x + 4\cos(0.5\pi x)\exp\left[-D\left(\frac{\pi}{2}\right)^2 t\right] \tag{3.32}$$

Finally, the root mean squared error was calculated for all model and step size combinations tested. RMSE is defined here as follows:

$$RMSE = \sqrt{\frac{1}{N}\sum_{i=1}^{N}(c_i - c)} \tag{3.33}$$

where N = number of spatial steps; c_i = modeled concentration at the current spatial step i, and c = theoretical concentration value at the current spatial step.

3.4: Modeling Results

Figure 3.1 shows the results of the fully implicit scheme advection model tested against the advancing unit step function in Equation 3.26. The undulations and overshooting of the step function illustrate the scheme's inability to accurately model a sharp front. This overshooting problem does not occur for smoother fronts or cases which include significant amounts of dispersion. All eight models experienced some amount of overshooting of the concentration front; however, all but three of the models had undulations leading up to the front. These three models were backward (upwind) differences, Lax-Wendroff scheme and McCormack's scheme. According to Gibbs phenomenon, sharper front modeling comes with the cost of having more undulations, and conversely, models without any undulations leading up to the front will have a greater amount of overshoot.

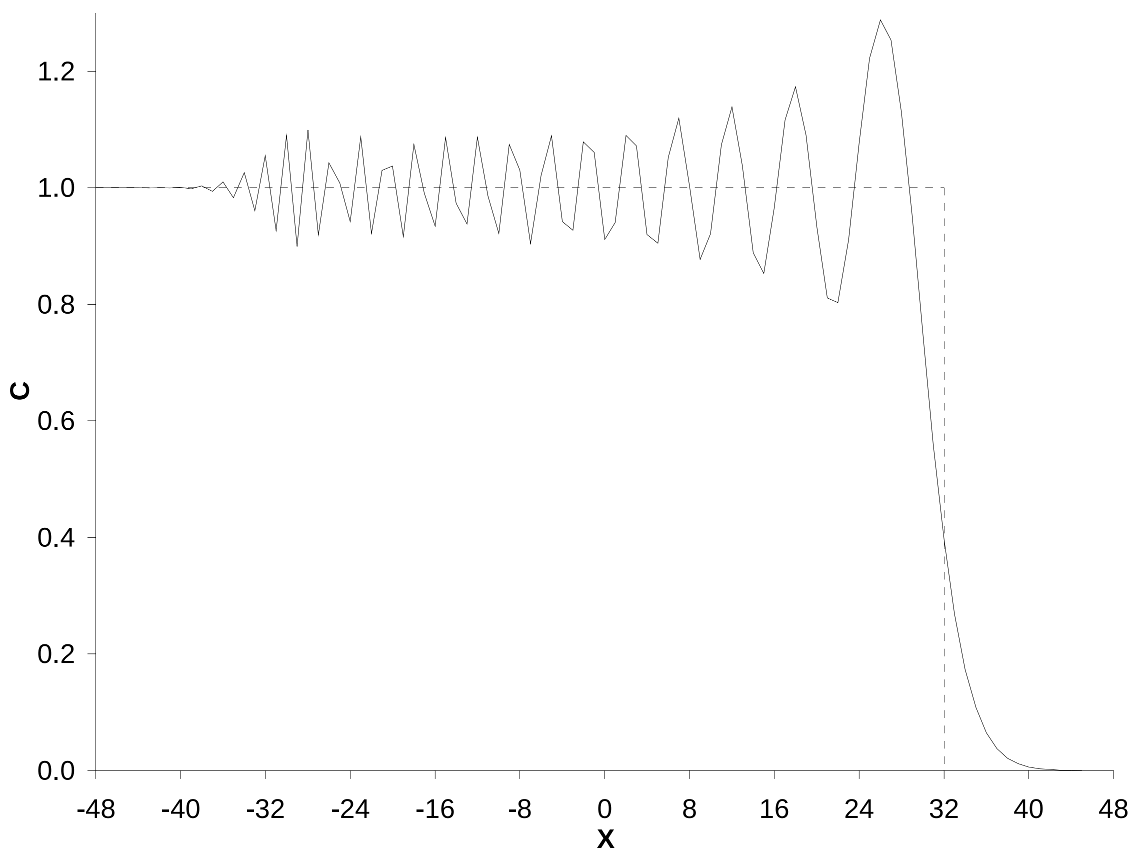

Figure 3.1: Fully implicit scheme advection model tested against an advancing unit step function (dashed line)

Convergence tests indicate that the fully implicit scheme was the most accurate advection model; the Crank-Nicolson scheme was the most accurate dispersion model, and the fully explicit scheme was the most accurate reaction model. The resulting root mean squared error values for all model combinations tested are found in Table 3.1. Most models were stable and convergent, meaning the RMSE decreased with decreasing step size; however, some models were unstable, and as the step size decreased, the RMSE became very large, so much so, that RMSE values above 10^{100} are represented in the table as "INF". Advection models 2 and 4 did not give accurate results with the fully explicit dispersion scheme ($\alpha = 0$), and model 8 did not give accurate results when $\theta = 0.5$ and $\alpha = 0$ as well as when $\theta = 1$. The Crank-Nicolson scheme ($\alpha = 0.5$) was the most accurate dispersion model; however, when combined with the advection models, sometimes the other dispersion schemes gave better results.

Table 3.1: Root mean squared error values for all models that were convergence tested

u=0	*t=32*	*D=2*	*λ=0*	$\Delta x=2^{2}$	$\Delta x=2^{1}$	$\Delta x=2^{0}$	$\Delta x=2^{-1}$	$\Delta x=2^{-2}$	$\Delta x=2^{-3}$	$\Delta x=2^{-4}$	$\Delta x=2^{-5}$	$\Delta x=2^{-6}$
		α=0		3.12E-04	7.49E-05	1.88E-05	4.77E-06	1.40E-06	7.92E-07	7.29E-07	7.21E-07	7.18E-07
		α=.5		2.02E-04	5.26E-05	1.34E-05	3.43E-06	1.12E-06	7.60E-07	7.26E-07	7.20E-07	7.18E-07
		α=1		7.50E-04	1.83E-04	4.56E-05	1.14E-05	2.94E-06	1.02E-06	7.44E-07	7.21E-07	7.18E-07
u=1	*t=32*	*D=2*	*λ=.01*	$\Delta x=2^{2}$	$\Delta x=2^{1}$	$\Delta x=2^{0}$	$\Delta x=2^{-1}$	$\Delta x=2^{-2}$	$\Delta x=2^{-3}$	$\Delta x=2^{-4}$	$\Delta x=2^{-5}$	$\Delta x=2^{-6}$
mod.1		*α=0*	*β=0*	5.21E+01	1.41E+04	2.11E-02	5.36E-04	2.90E-04	1.51E-04	7.66E-05	3.84E-05	1.91E-05
mod.1		*α=0*	*β=.5*	4.84E+01	1.26E+04	1.80E-02	1.73E-03	1.85E-03	1.93E-03	1.98E-03	2.00E-03	2.02E-03
mod.1		*α=0*	*β=1*	4.50E+01	1.12E+04	1.58E-02	4.01E-03	4.18E-03	4.29E-03	4.35E-03	4.38E-03	4.40E-03
mod.1		*α=.5*	*β=0*	2.83E-03	1.33E-03	9.01E-04	5.30E-04	2.88E-04	1.50E-04	7.65E-05	3.84E-05	1.91E-05
mod.1		*α=.5*	*β=.5*	2.88E-03	1.61E-03	1.61E-03	1.73E-03	1.85E-03	1.93E-03	1.98E-03	2.00E-03	2.02E-03
mod.1		*α=.5*	*β=1*	4.30E-03	3.56E-03	3.77E-03	4.01E-03	4.19E-03	4.29E-03	4.35E-03	4.38E-03	4.40E-03
mod.1		*α=1*	*β=0*	1.00E-03	1.22E-03	8.79E-04	5.25E-04	2.87E-04	1.50E-04	7.64E-05	3.84E-05	1.91E-05
mod.1		*α=1*	*β=.5*	1.64E-03	1.56E-03	1.61E-03	1.73E-03	1.85E-03	1.93E-03	1.98E-03	2.00E-03	2.02E-03
mod.1		*α=1*	*β=1*	3.77E-03	3.55E-03	3.77E-03	4.01E-03	4.19E-03	4.29E-03	4.35E-03	4.38E-03	4.40E-03
mod.2	*θ=.5*	*α=0*	*β=0*	3.58E+04	1.71E+23	1.05E+98	INF	INF	INF	INF	INF	INF
mod.2	*θ=.5*	*α=0*	*β=.5*	3.31E+04	1.58E+23	9.71E+97	INF	INF	INF	INF	INF	INF
mod.2	*θ=.5*	*α=0*	*β=1*	3.07E+04	1.47E+23	9.00E+97	INF	INF	INF	INF	INF	INF
mod.2	*θ=.5*	*α=.5*	*β=0*	5.33E-02	2.86E-02	2.73E-02	2.70E-02	2.70E-02	2.70E-02	2.70E-02	2.70E-02	2.70E-02
mod.2	*θ=.5*	*α=.5*	*β=.5*	5.07E-02	2.61E-02	2.48E-02	2.46E-02	2.46E-02	2.46E-02	2.46E-02	2.46E-02	2.46E-02
mod.2	*θ=.5*	*α=.5*	*β=1*	4.96E-02	2.45E-02	2.32E-02	2.30E-02	2.29E-02	2.29E-02	2.29E-02	2.29E-02	2.29E-02
mod.2	*θ=.5*	*α=1*	*β=0*	1.83E-02	1.13E-02	1.09E-02	1.08E-02	1.08E-02	1.08E-02	1.08E-02	1.08E-02	1.08E-02
mod.2	*θ=.5*	*α=1*	*β=.5*	2.08E-02	1.20E-02	1.13E-02	1.12E-02	1.12E-02	1.12E-02	1.12E-02	1.12E-02	1.12E-02
mod.2	*θ=.5*	*α=1*	*β=1*	2.42E-02	1.35E-02	1.25E-02	1.23E-02	1.23E-02	1.23E-02	1.23E-02	1.23E-02	1.23E-02
mod.2	*θ=1*	*α=0*	*β=0*	2.81E+00	3.31E+06	1.01E+31	INF	INF	INF	INF	INF	INF
mod.2	*θ=1*	*α=0*	*β=.5*	2.55E+00	3.00E+06	9.16E+30	INF	INF	INF	INF	INF	INF
mod.2	*θ=1*	*α=0*	*β=1*	2.31E+00	2.71E+06	8.29E+30	INF	INF	INF	INF	INF	INF
mod.2	*θ=1*	*α=.5*	*β=0*	1.15E-02	1.16E-02	1.16E-02	1.17E-02	1.17E-02	1.17E-02	1.17E-02	1.17E-02	1.17E-02
mod.2	*θ=1*	*α=.5*	*β=.5*	1.15E-02	1.16E-02	1.16E-02	1.17E-02	1.17E-02	1.17E-02	1.17E-02	1.17E-02	1.17E-02
mod.2	*θ=1*	*α=.5*	*β=1*	1.15E-02	1.16E-02	1.16E-02	1.17E-02	1.17E-02	1.17E-02	1.17E-02	1.17E-02	1.17E-02
mod.2	*θ=1*	*α=1*	*β=0*	1.15E-02	1.16E-02	1.16E-02	1.17E-02	1.17E-02	1.17E-02	1.17E-02	1.17E-02	1.17E-02
mod.2	*θ=1*	*α=1*	*β=.5*	1.15E-02	1.16E-02	1.16E-02	1.17E-02	1.17E-02	1.17E-02	1.17E-02	1.17E-02	1.17E-02
mod.2	*θ=1*	*α=1*	*β=1*	1.15E-02	1.16E-02	1.16E-02	1.17E-02	1.17E-02	1.17E-02	1.17E-02	1.17E-02	1.17E-02
mod.3		*α=0*	*β=0*	1.86E+03	1.13E+02	2.95E-04	7.45E-05	1.86E-05	5.57E-06	3.86E-06	3.85E-06	3.88E-06
mod.3		*α=0*	*β=.5*	1.77E+03	9.89E+01	1.86E-03	1.98E-03	2.02E-03	2.03E-03	2.03E-03	2.03E-03	2.03E-03
mod.3		*α=0*	*β=1*	1.68E+03	8.69E+01	4.20E-03	4.35E-03	4.39E-03	4.41E-03	4.41E-03	4.41E-03	4.41E-03
mod.3		*α=.5*	*β=0*	3.26E-01	9.53E-04	2.52E-04	6.35E-05	1.59E-05	5.08E-06	3.84E-06	3.85E-06	3.88E-06
mod.3		*α=.5*	*β=.5*	3.04E-01	1.61E-03	1.87E-03	1.98E-03	2.02E-03	2.03E-03	2.03E-03	2.03E-03	2.03E-03
mod.3		*α=.5*	*β=1*	2.84E-01	3.75E-03	4.20E-03	4.35E-03	4.39E-03	4.41E-03	4.41E-03	4.41E-03	4.41E-03
mod.3		*α=1*	*β=0*	2.91E-03	8.38E-04	2.24E-04	5.67E-05	1.43E-05	4.84E-06	3.84E-06	3.86E-06	3.88E-06
mod.3		*α=1*	*β=.5*	2.41E-03	1.59E-03	1.87E-03	1.99E-03	2.02E-03	2.03E-03	2.03E-03	2.03E-03	2.03E-03
mod.3		*α=1*	*β=1*	3.23E-03	3.76E-03	4.21E-03	4.35E-03	4.40E-03	4.41E-03	4.41E-03	4.41E-03	4.41E-03
mod.4		*α=0*	*β=0*	4.30E+03	7.44E+19	9.06E+84	INF	INF	INF	INF	INF	INF
mod.4		*α=0*	*β=.5*	3.94E+03	6.82E+19	8.32E+84	INF	INF	INF	INF	INF	INF
mod.4		*α=0*	*β=1*	3.60E+03	6.26E+19	7.64E+84	INF	INF	INF	INF	INF	INF
mod.4		*α=.5*	*β=0*	3.88E-02	3.78E-02	4.89E-02	6.77E-02	9.54E-02	1.35E-01	1.91E-01	2.70E-01	3.81E-01
mod.4		*α=.5*	*β=.5*	3.41E-02	3.39E-02	4.41E-02	6.12E-02	8.61E-02	1.22E-01	1.72E-01	2.43E-01	3.44E-01
mod.4		*α=.5*	*β=1*	3.02E-02	3.06E-02	3.99E-02	5.53E-02	7.78E-02	1.10E-01	1.55E-01	2.20E-01	3.11E-01
mod.4		*α=1*	*β=0*	2.23E-03	6.28E-04	1.65E-04	4.31E-05	1.24E-05	5.45E-06	4.18E-06	3.95E-06	3.90E-06
mod.4		*α=1*	*β=.5*	3.21E-03	2.15E-03	2.03E-03	2.03E-03	2.03E-03	2.03E-03	2.03E-03	2.03E-03	2.03E-03
mod.4		*α=1*	*β=1*	5.31E-03	4.48E-03	4.40E-03	4.40E-03	4.41E-03	4.41E-03	4.41E-03	4.41E-03	4.41E-03
mod.5		*α=0*	*β=0*	4.24E-04	1.45E-04	4.04E-05	1.12E-05	4.79E-06	3.98E-06	3.90E-06	3.89E-06	3.89E-06
mod.5		*α=0*	*β=.5*	1.98E-03	1.98E-03	2.01E-03	2.02E-03	2.03E-03	2.03E-03	2.03E-03	2.03E-03	2.03E-03
mod.5		*α=0*	*β=1*	4.35E-03	4.35E-03	4.39E-03	4.40E-03	4.41E-03	4.41E-03	4.41E-03	4.41E-03	4.41E-03
mod.5		*α=.5*	*β=0*	9.46E-04	1.88E-04	4.55E-05	1.25E-05	5.24E-06	4.10E-06	3.93E-06	3.90E-06	3.89E-06
mod.5		*α=.5*	*β=.5*	2.42E-03	2.03E-03	2.02E-03	2.02E-03	2.03E-03	2.03E-03	2.03E-03	2.03E-03	2.03E-03
mod.5		*α=.5*	*β=1*	4.72E-03	4.40E-03	4.39E-03	4.40E-03	4.41E-03	4.41E-03	4.41E-03	4.41E-03	4.41E-03
mod.5		*α=1*	*β=0*	2.11E-03	4.84E-04	1.18E-04	3.01E-05	8.77E-06	4.53E-06	3.98E-06	3.91E-06	3.89E-06
mod.5		*α=1*	*β=.5*	3.30E-03	2.13E-03	2.03E-03	2.03E-03	2.03E-03	2.03E-03	2.03E-03	2.03E-03	2.03E-03
mod.5		*α=1*	*β=1*	5.39E-03	4.48E-03	4.41E-03	4.40E-03	4.41E-03	4.41E-03	4.41E-03	4.41E-03	4.41E-03
mod.6		*α=0*	*β=0*	1.79E+04	7.95E+06	1.01E-02	1.02E-02	1.03E-02	1.03E-02	1.04E-02	1.04E-02	1.04E-02
mod.6		*α=0*	*β=.5*	1.72E+04	7.21E+06	1.10E-02	1.12E-02	1.13E-02	1.14E-02	1.14E-02	1.14E-02	1.14E-02
mod.6		*α=0*	*β=1*	1.65E+04	6.53E+06	1.24E-02	1.26E-02	1.28E-02	1.29E-02	1.29E-02	1.29E-02	1.29E-02
mod.6		*α=.5*	*β=0*	6.21E+00	1.00E-02	1.00E-02	1.02E-02	1.03E-02	1.03E-02	1.04E-02	1.04E-02	1.04E-02
mod.6		*α=.5*	*β=.5*	5.90E+00	1.08E-02	1.10E-02	1.12E-02	1.13E-02	1.14E-02	1.14E-02	1.14E-02	1.14E-02
mod.6		*α=.5*	*β=1*	5.60E+00	1.21E-02	1.24E-02	1.26E-02	1.28E-02	1.29E-02	1.29E-02	1.29E-02	1.29E-02
mod.6		*α=1*	*β=0*	1.53E-02	9.91E-03	1.00E-02	1.02E-02	1.03E-02	1.03E-02	1.04E-02	1.04E-02	1.04E-02
mod.6		*α=1*	*β=.5*	1.53E-02	1.07E-02	1.10E-02	1.12E-02	1.13E-02	1.14E-02	1.14E-02	1.14E-02	1.14E-02
mod.6		*α=1*	*β=1*	1.56E-02	1.20E-02	1.24E-02	1.26E-02	1.28E-02	1.29E-02	1.29E-02	1.29E-02	1.29E-02

mod.7		α=0	β=0	5.19E+01	1.39E+04	2.06E-02	5.09E-05	1.35E-05	5.09E-06	3.98E-06	3.89E-06	3.89E-06
mod.7		α=0	β=.5	4.82E+01	1.24E+04	1.77E-02	2.02E-03	2.03E-03	2.03E-03	2.03E-03	2.03E-03	2.03E-03
mod.7		α=0	β=1	4.48E+01	1.11E+04	1.56E-02	4.40E-03	4.41E-03	4.41E-03	4.41E-03	4.41E-03	4.41E-03
mod.7		α=.5	β=0	2.91E-03	4.64E-04	1.25E-04	3.34E-05	9.55E-06	4.56E-06	3.96E-06	3.90E-06	3.89E-06
mod.7		α=.5	β=.5	3.34E-03	2.05E-03	2.02E-03	2.02E-03	2.03E-03	2.03E-03	2.03E-03	2.03E-03	2.03E-03
mod.7		α=.5	β=1	5.02E-03	4.39E-03	4.39E-03	4.40E-03	4.41E-03	4.41E-03	4.41E-03	4.41E-03	4.41E-03
mod.7		α=1	β=0	9.29E-04	2.30E-04	6.63E-05	1.91E-05	6.71E-06	4.30E-06	3.96E-06	3.90E-06	3.89E-06
mod.7		α=1	β=.5	2.26E-03	2.05E-03	2.03E-03	2.03E-03	2.03E-03	2.03E-03	2.03E-03	2.03E-03	2.03E-03
mod.7		α=1	β=1	4.52E-03	4.41E-03	4.40E-03	4.40E-03	4.41E-03	4.41E-03	4.41E-03	4.41E-03	4.41E-03
mod.8	θ=0	α=0	β=0	3.61E-03	1.97E-03	1.11E-03	5.90E-04	3.04E-04	1.55E-04	7.76E-05	3.86E-05	1.92E-05
mod.8	θ=0	α=0	β=.5	3.08E-03	1.84E-03	1.60E-03	1.70E-03	1.84E-03	1.93E-03	1.98E-03	2.00E-03	2.02E-03
mod.8	θ=0	α=0	β=1	3.61E-03	3.36E-03	3.67E-03	3.97E-03	4.17E-03	4.29E-03	4.35E-03	4.38E-03	4.40E-03
mod.8	θ=0	α=.5	β=0	3.02E-03	1.91E-03	1.09E-03	5.84E-04	3.03E-04	1.54E-04	7.75E-05	3.86E-05	1.92E-05
mod.8	θ=0	α=.5	β=.5	2.55E-03	1.80E-03	1.59E-03	1.71E-03	1.84E-03	1.93E-03	1.98E-03	2.00E-03	2.02E-03
mod.8	θ=0	α=.5	β=1	3.31E-03	3.35E-03	3.67E-03	3.97E-03	4.17E-03	4.29E-03	4.35E-03	4.38E-03	4.40E-03
mod.8	θ=0	α=1	β=0	2.96E-03	1.87E-03	1.07E-03	5.79E-04	3.02E-04	1.54E-04	7.74E-05	3.86E-05	1.92E-05
mod.8	θ=0	α=1	β=.5	2.58E-03	1.78E-03	1.59E-03	1.71E-03	1.84E-03	1.93E-03	1.98E-03	2.00E-03	2.02E-03
mod.8	θ=0	α=1	β=1	3.42E-03	3.36E-03	3.67E-03	3.97E-03	4.17E-03	4.29E-03	4.35E-03	4.38E-03	4.40E-03
mod.8	θ=.5	α=0	β=0	1.10E+03	6.69E+25	INF	INF	INF	INF	INF	INF	INF
mod.8	θ=.5	α=0	β=.5	1.03E+03	6.16E+25	INF	INF	INF	INF	INF	INF	INF
mod.8	θ=.5	α=0	β=1	9.61E+02	5.67E+25	INF	INF	INF	INF	INF	INF	INF
mod.8	θ=.5	α=.5	β=0	2.46E-02	2.25E-02	4.99E-04	2.38E-04	1.16E-04	5.74E-05	2.88E-05	1.48E-05	8.17E-06
mod.8	θ=.5	α=.5	β=.5	2.24E-02	1.98E-02	2.07E-03	2.04E-03	2.03E-03	2.03E-03	2.03E-03	2.03E-03	2.03E-03
mod.8	θ=.5	α=.5	β=1	2.06E-02	1.78E-02	4.41E-03	4.41E-03	4.41E-03	4.41E-03	4.41E-03	4.41E-03	4.41E-03
mod.8	θ=.5	α=1	β=0	1.40E-03	8.10E-04	4.30E-04	2.20E-04	1.12E-04	5.63E-05	2.85E-05	1.47E-05	8.15E-06
mod.8	θ=.5	α=1	β=.5	2.42E-03	2.16E-03	2.06E-03	2.04E-03	2.03E-03	2.03E-03	2.03E-03	2.03E-03	2.03E-03
mod.8	θ=.5	α=1	β=1	4.55E-03	4.44E-03	4.41E-03	4.41E-03	4.41E-03	4.41E-03	4.41E-03	4.41E-03	4.41E-03
mod.8	θ=1	α=0	β=0	3.31E+17	6.61E+96	INF	INF	INF	INF	INF	INF	INF
mod.8	θ=1	α=0	β=.5	3.13E+17	6.34E+96	INF	INF	INF	INF	INF	INF	INF
mod.8	θ=1	α=0	β=1	2.96E+17	6.08E+96	INF	INF	INF	INF	INF	INF	INF
mod.8	θ=1	α=.5	β=0	3.41E+04	5.93E+24	5.04E+70	INF	INF	INF	INF	INF	INF
mod.8	θ=1	α=.5	β=.5	3.20E+04	5.38E+24	4.58E+70	INF	INF	INF	INF	INF	INF
mod.8	θ=1	α=.5	β=1	3.01E+04	4.88E+24	4.16E+70	INF	INF	INF	INF	INF	INF
mod.8	θ=1	α=1	β=0	3.34E-01	5.39E-03	1.90E-03	8.53E-04	4.83E+11	4.83E+66	INF	INF	INF
mod.8	θ=1	α=1	β=.5	3.08E-01	6.99E-03	3.54E-03	2.62E-03	1.05E+11	4.88E+66	INF	INF	INF
mod.8	θ=1	α=1	β=1	2.84E-01	9.30E-03	5.92E-03	5.02E-03	7.07E+11	3.35E+66	INF	INF	INF
u=0		D=.9	λ=0	$\Delta x=0.9/2^1$	$\Delta x=0.9/2^2$	$\Delta x=0.9/2^3$	$\Delta x=0.9/2^4$	$\Delta x=0.9/2^5$	$\Delta x=0.9/2^6$	$\Delta x=0.9/2^7$	$\Delta x=0.9/2^8$	$\Delta x=0.9/2^9$
	t=0.0	α=0		5.46E+00	5.40E+00	5.37E+00	5.35E+00	5.35E+00	5.34E+00	5.34E+00	5.34E+00	5.34E+00
	t=0.0	α=.5		5.46E+00	5.40E+00	5.37E+00	5.35E+00	5.35E+00	5.34E+00	5.34E+00	5.34E+00	5.34E+00
	t=0.0	α=1		5.46E+00	5.40E+00	5.37E+00	5.35E+00	5.35E+00	5.34E+00	5.34E+00	5.34E+00	5.34E+00
	t=0.9	α=0		7.18E-01	7.26E-01	7.26E-01	7.25E-01	7.25E-01	7.24E-01	7.24E-01	7.24E-01	7.24E-01
	t=0.9	α=.5		3.02E-01	3.24E-01	3.95E-01	4.37E-01	4.58E-01	4.69E-01	4.74E-01	4.77E-01	4.78E-01
	t=0.9	α=1		4.46E-01	7.09E-01	8.62E-01	9.44E-01	9.87E-01	1.01E+00	1.02E+00	1.03E+00	1.03E+00
	t=1.8	α=0		9.57E-02	9.80E-02	9.83E-02	9.83E-02	9.82E-02	9.81E-02	9.81E-02	9.81E-02	9.81E-02
	t=1.8	α=.5		3.65E-01	4.84E-01	5.46E-01	5.78E-01	5.95E-01	6.03E-01	6.07E-01	6.09E-01	6.10E-01
	t=1.8	α=1		6.09E-01	8.71E-01	1.02E+00	1.10E+00	1.14E+00	1.16E+00	1.18E+00	1.18E+00	1.18E+00
	t=2.7	α=0		1.29E-02	1.32E-02	1.33E-02	1.33E-02	1.33E-02	1.33E-02	1.33E-02	1.33E-02	1.33E-02
	t=2.7	α=.5		4.16E-01	5.21E-01	5.78E-01	6.08E-01	6.23E-01	6.31E-01	6.35E-01	6.37E-01	6.37E-01
	t=2.7	α=1		6.41E-01	8.98E-01	1.05E+00	1.13E+00	1.17E+00	1.19E+00	1.20E+00	1.21E+00	1.21E+00
	t=3.6	α=0		1.74E-03	1.79E-03	1.80E-03	1.80E-03	1.80E-03	1.80E-03	1.80E-03	1.80E-03	1.80E-03
	t=3.6	α=.5		4.22E-01	5.26E-01	5.83E-01	6.12E-01	6.27E-01	6.35E-01	6.39E-01	6.40E-01	6.41E-01
	t=3.6	α=1		6.45E-01	9.02E-01	1.05E+00	1.13E+00	1.17E+00	1.19E+00	1.20E+00	1.21E+00	1.21E+00
	t=4.5	α=0		2.35E-04	2.43E-04	2.44E-04	2.45E-04	2.44E-04	2.44E-04	2.44E-04	2.44E-04	2.44E-04
	t=4.5	α=.5		4.23E-01	5.26E-01	5.83E-01	6.13E-01	6.28E-01	6.35E-01	6.39E-01	6.41E-01	6.42E-01
	t=4.5	α=1		6.45E-01	9.03E-01	1.05E+00	1.13E+00	1.17E+00	1.19E+00	1.21E+00	1.21E+00	1.21E+00
	t=5.4	α=0		3.18E-05	3.29E-05	3.31E-05	3.31E-05	3.31E-05	3.31E-05	3.31E-05	3.31E-05	3.31E-05
	t=5.4	α=.5		4.23E-01	5.26E-01	5.83E-01	6.13E-01	6.28E-01	6.35E-01	6.39E-01	6.41E-01	6.42E-01
	t=5.4	α=1		6.45E-01	9.03E-01	1.05E+00	1.13E+00	1.17E+00	1.19E+00	1.21E+00	1.21E+00	1.21E+00
	t=6.3	α=0		4.30E-06	4.45E-06	4.49E-06	4.49E-06	4.49E-06	4.49E-06	4.48E-06	4.48E-06	4.48E-06
	t=6.3	α=.5		4.23E-01	5.26E-01	5.83E-01	6.13E-01	6.28E-01	6.35E-01	6.39E-01	6.41E-01	6.42E-01
	t=6.3	α=1		6.45E-01	9.03E-01	1.05E+00	1.13E+00	1.17E+00	1.19E+00	1.21E+00	1.21E+00	1.21E+00
	t=7.2	α=0		5.83E-07	6.03E-07	6.08E-07	6.09E-07	6.08E-07	6.08E-07	6.08E-07	6.08E-07	6.08E-07
	t=7.2	α=.5		4.23E-01	5.26E-01	5.83E-01	6.13E-01	6.28E-01	6.35E-01	6.39E-01	6.41E-01	6.42E-01
	t=7.2	α=1		6.45E-01	9.03E-01	1.05E+00	1.13E+00	1.17E+00	1.19E+00	1.21E+00	1.21E+00	1.21E+00
	t=8.1	α=0		7.90E-08	8.17E-08	8.24E-08	8.25E-08	8.24E-08	8.24E-08	8.24E-08	8.24E-08	8.24E-08
	t=8.1	α=.5		4.23E-01	5.26E-01	5.83E-01	6.13E-01	6.28E-01	6.35E-01	6.39E-01	6.41E-01	6.42E-01
	t=8.1	α=1		6.45E-01	9.03E-01	1.05E+00	1.13E+00	1.17E+00	1.19E+00	1.21E+00	1.21E+00	1.21E+00
	t=9.0	α=0		1.07E-08	1.11E-08	1.12E-08	1.12E-08	1.12E-08	1.12E-08	1.12E-08	1.12E-08	1.12E-08
	t=9.0	α=.5		4.23E-01	5.26E-01	5.83E-01	6.13E-01	6.28E-01	6.35E-01	6.39E-01	6.41E-01	6.42E-01
	t=9.0	α=1		6.45E-01	9.03E-01	1.05E+00	1.13E+00	1.17E+00	1.19E+00	1.21E+00	1.21E+00	1.21E+00

Figure 3.2 shows test results for the case of fully implicit scheme dispersion ($\alpha = 1$) using a spatial step size of $\Delta x = 2^{-6}$. Results were compared against the analytical solution at all of the following time spans: 0, 3.2, 6.4, 9.6, 12.8, 16, 19.2, 22.4, 25.6, 28.8, 32, .2, 38.4, 41.6, 44.8, 48, 51.2, 54.4, 57.6, 60.8 and 64. Boundaries were placed at locations where the accepted concentration value never rises above 10^{-5} during the course of the longest modeling period of 64, so as not to force a concentration value of zero at a place that is not supposed to be within 10^{-5} of zero. All of the modeling results were found to be overlapping well with the analytical solution, which is indicative of an accurate simulation. The fully implicit scheme is the most accurate of the three dispersion models at $\Delta x = 2^{-6}$; however, at larger step sizes, the Crank-Nicolson scheme ($\alpha = 0.5$) was found to be the most accurate dispersion model, whereas the fully implicit scheme ($\alpha = 1$) was the least accurate model at these larger step sizes.

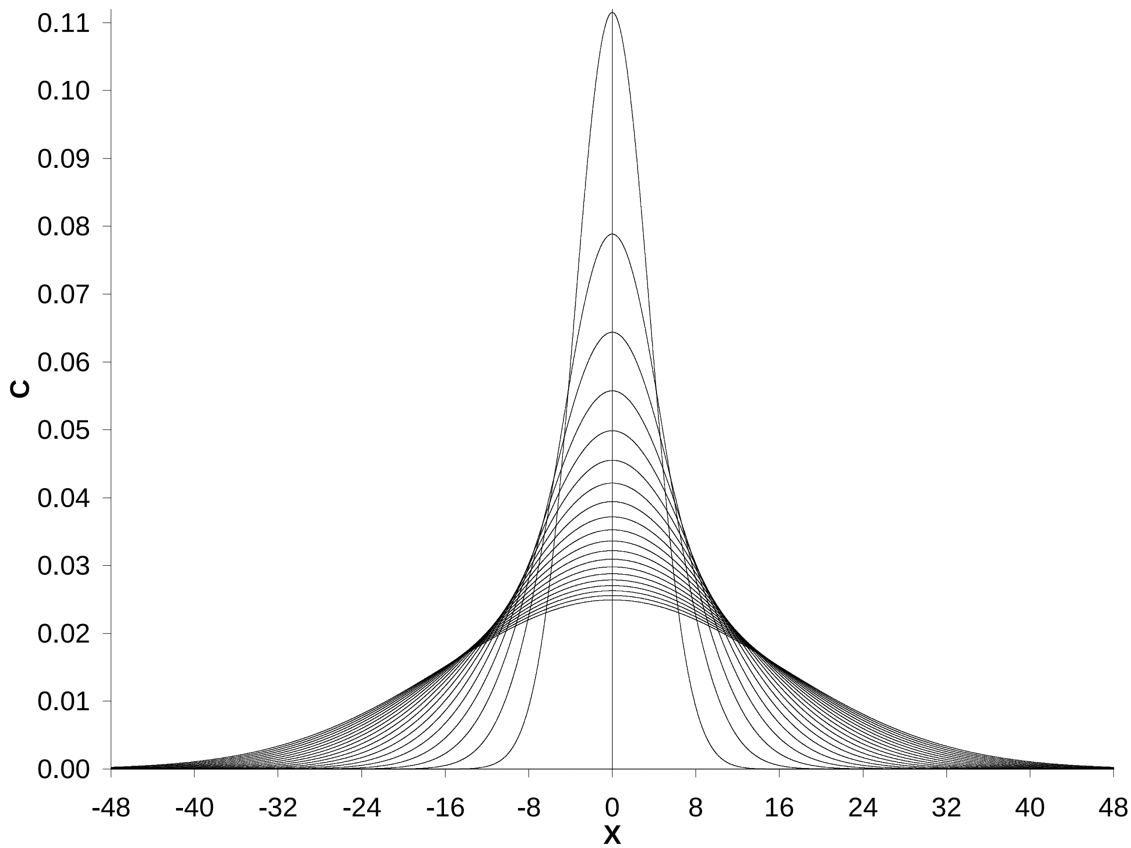

Figure 3.2: Test results for fully implicit scheme dispersion ($\alpha = 1$) using $\Delta x = 2^{-6}$ (modeled results are overlapping the analytical solution)

Figure 3.3 shows the test results for the case of fully implicit scheme advection (*model* = 5), fully explicit scheme dispersion ($\alpha = 0$) and fully explicit scheme decay ($\beta = 0$) using the same spatial step size of $\Delta x = 2^{-6}$. The results were compared against the analytical solution using the same time spans as before, specifically: 0, 3.2, 6.4, 9.6, 12.8, 16, 19.2, 22.4, 25.6, 28.8, 32, 35.2, 38.4, 41.6, 44.8, 48, 51.2, 54.4, 57.6, 60.8 and 64. Just like the dispersion model, boundaries were placed at locations where the accepted concentration value never rises above 10^{-5} during the course of the longest modeling period of 64, so as not to force a concentration value of zero at a place that is not supposed to be within 10^{-5}

of zero. The difference between the modeled results and the analytical solution is so small that they are virtually one in the same. The fully implicit scheme and Fromm's scheme were the first and second most accurate advection models, respectively; whereas, the generalized box explicit scheme, backward (upwind) differences, McCormack's scheme and Lax-Wendroff scheme were among the least accurate of the eight advection models.

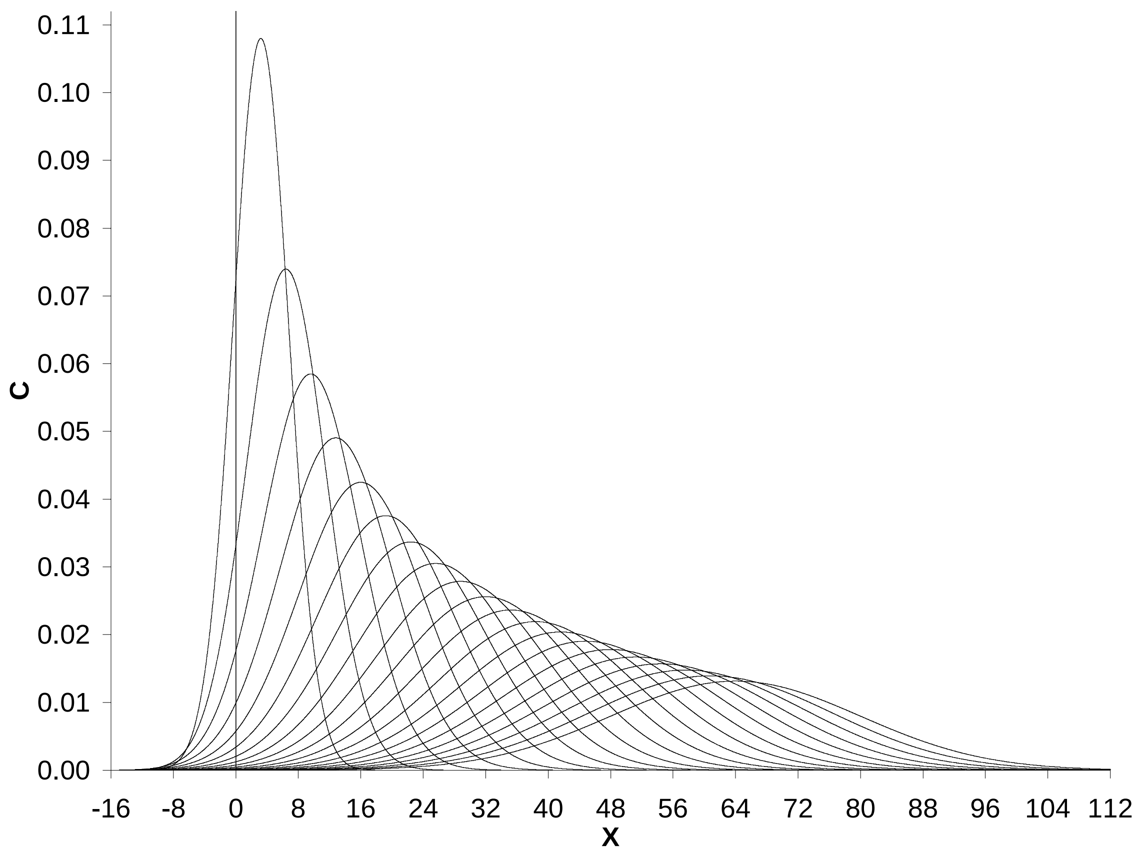

Figure 3.3: Test results for fully implicit scheme advection (*model* = 5), fully explicit scheme dispersion ($\alpha = 0$) and fully explicit scheme decay ($\beta = 0$) using $\Delta x = 2^{-6}$ (modeled results are overlapping the analytical solution)

The combination of fully implicit scheme advection (*model* = 5), Crank-Nicolson scheme dispersion ($\alpha = 0.5$) and fully explicit scheme decay ($\beta = 0$) remains more accurate at larger spatial and temporal step sizes than the other model combinations do and, therefore, will tend to satisfy accuracy and stability requirements within fewer computations.

Figure 3.4 shows the test results for the Neumann boundary condition case using fully explicit scheme dispersion ($\alpha = 0$) and a spatial step size of $\Delta x = 0.9/2^9$. The results were compared against the analytical solution at the following time spans: 0, 0.15, 0.3, 0.45, 0.6, 0.75, 0.9, 1.05, 1.2, 1.35, 1.5, 1.65, 1.8, 1.95, 2.1, 2.25, 2.4, 2.55, 2.7, 2.85 and 3. Again, there is such a small difference between the model results and the analytical solution that they are practically the same, indicating a high level of accuracy. Fully explicit scheme dispersion ($\alpha = 0$) is the only model that gave accurate solutions for this Neumann boundary condition case; whereas, fully implicit ($\alpha = 1$) and Crank-Nicolson ($\alpha = 0.5$) scheme dispersion did not model this case correctly.

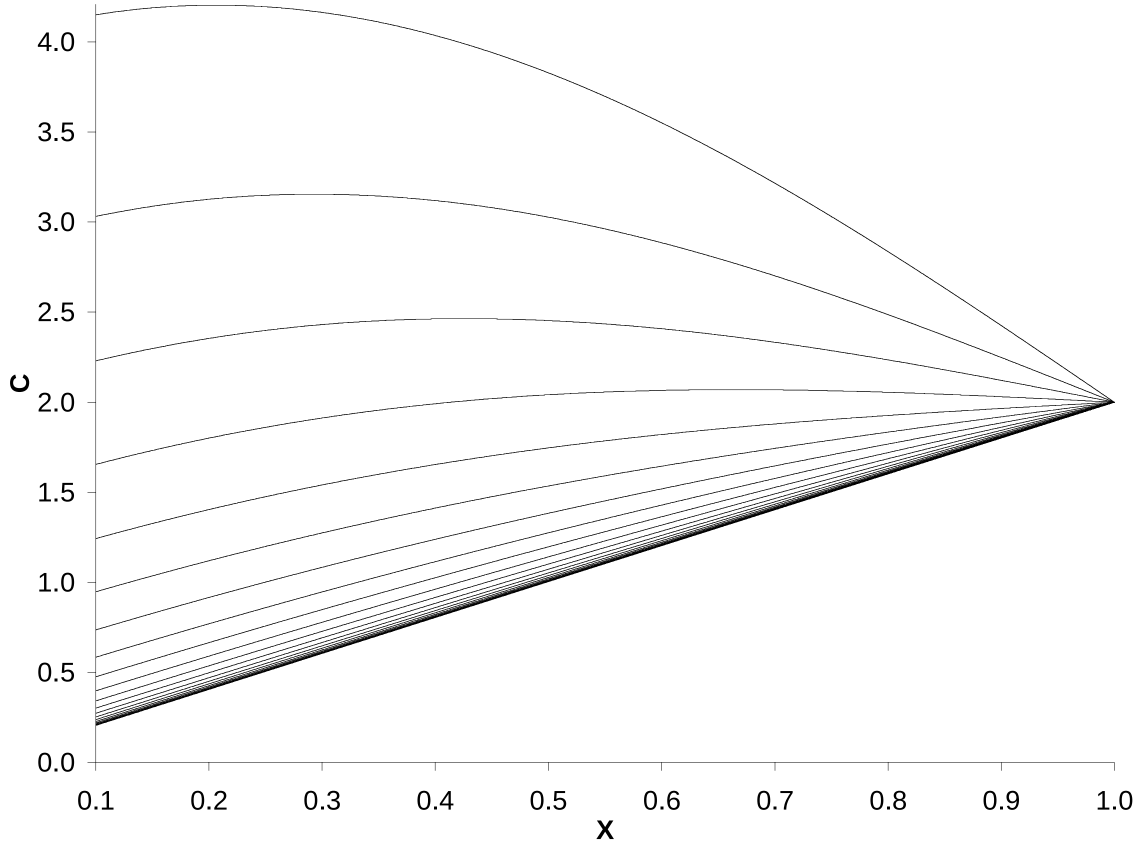

Figure 3.4: Test results for the Neumann boundary condition case using fully explicit scheme dispersion ($\alpha = 0$) and $\Delta x = 0.9/2^9$ (modeled results are overlapping the analytical solution)

3.5: Concluding Remarks on the 1-D A-D-R Model

The one-dimensional advection-dispersion-reaction equation with constant velocity, dispersivity and decay rate parameters was approximated using different combinations of finite-differencing schemes for advection, dispersion and reactions, where any advection model may be combined with any dispersion model and any reaction model to approximate the A-D-R equation. The accuracy and stability tests conclude that fully implicit scheme advection (*model* = 5) combined with fully explicit scheme dispersion (α

= 0) and fully explicit scheme decay (β = 0) would likely satisfy accuracy and stability within the fewest number of computations because this model combination gives more accurate results at larger spatial and temporal step sizes than the other model combinations do, therefore, making this model combination the best choice for simulating *Bacteroidales* concentrations. This 1-D model can be applied to river reaches to model *Bacteroidales* concentrations as they travel within a riverine system; however, it does not account for any velocity variance that may occur along river reaches. Simulations like these can be calibrated with available measurements in order to determine appropriate modeling parameters such as dispersivity and decay rate constants.

Chapter 4: Semi-Implicit Three-Dimensional Flow Modeling

4.1: Introduction to the S-I 3-D Flow Model

Doctor Smith (1997) authored a semi-implicit, three-dimensional, finite-differencing model for estuarine circulation in the FORTRAN 90 programming language. This program, commonly known as Si3D, was the topic of his Ph.D. dissertation. He has implemented the program to simulate circulation in the San Francisco Bay and Estuary from the ocean to the delta. The Si3D program simulates estuarine flows within a three-dimensional grid which is horizontally resolved by squares and vertically resolved by layers. A bathymetry file tells the program which cells are open to flows and which ones are not. An initial salinity condition is needed, and boundary files are used to indicate flow rate, water surface elevation and salinity, if necessary, in regular time increments at each open boundary of the model perimeter. Each vertical layer is set to the same thickness, except for the bottom layer, which defines the local bathymetry, and the top layer, which adjusts with the changing water surface elevation. All modeling parameters and output specifications are given in the general input file.

According to Smith (1997), the shallow-water flows of an estuary can essentially be considered horizontal and, therefore, vertical velocities and accelerations are negligible compared to gravity. As a result of this assumption, only the pressure and gravity terms are retained in the *z*-momentum equation, reducing it to the hydrostatic pressure equation.

The Coriolis terms in the horizontal momentum equations involving vertical velocity w can also be neglected. By incorporating these assumptions, the continuity, *x*-momentum, *y*-momentum, *z*-momentum and salt transport equations become the following five equations, respectively:

$$\frac{\partial u}{\partial x}+\frac{\partial v}{\partial y}+\frac{\partial w}{\partial z}=0 \tag{4.1}$$

$$\frac{\partial u}{\partial t}+\frac{\partial uu}{\partial x}+\frac{\partial uv}{\partial y}+\frac{\partial uw}{\partial z}-fv=-\frac{1}{\rho_0}\frac{\partial p}{\partial x}+\frac{\partial}{\partial x}\left(A_H\frac{\partial u}{\partial x}\right)+\frac{\partial}{\partial y}\left(A_H\frac{\partial u}{\partial y}\right)+\frac{\partial}{\partial z}\left(A_V\frac{\partial u}{\partial z}\right) \tag{4.2}$$

$$\frac{\partial v}{\partial t}+\frac{\partial uv}{\partial x}+\frac{\partial vv}{\partial y}+\frac{\partial vw}{\partial z}+fu=-\frac{1}{\rho_0}\frac{\partial p}{\partial y}+\frac{\partial}{\partial x}\left(A_H\frac{\partial v}{\partial x}\right)+\frac{\partial}{\partial y}\left(A_H\frac{\partial v}{\partial y}\right)+\frac{\partial}{\partial z}\left(A_V\frac{\partial v}{\partial z}\right) \tag{4.3}$$

$$0=-\frac{1}{\rho_0}\frac{\partial p}{\partial z}-\frac{\rho}{\rho_0}g \tag{4.4}$$

$$\frac{\partial s}{\partial t}+\frac{\partial us}{\partial x}+\frac{\partial vs}{\partial y}+\frac{\partial ws}{\partial z}=\frac{\partial}{\partial x}\left(D_H\frac{\partial s}{\partial x}\right)+\frac{\partial}{\partial y}\left(D_H\frac{\partial s}{\partial y}\right)+\frac{\partial}{\partial z}\left(D_V\frac{\partial s}{\partial z}\right) \tag{4.5}$$

where *u*, *v* and *w* are the velocities in the *x*, *y* and *z* directions, respectively, and *f* is the Coriolis parameter. The advective acceleration terms $\partial uu/\partial x$, $\partial uv/\partial y$, $\partial uw/\partial z$, $\partial uv/\partial x$, $\partial vv/\partial y$, and $\partial vw/\partial z$ are written in a conservative or divergence form.

By substituting in baroclinic terms for the pressure gradient terms in the *x*- and *y*-momentum equations, assuming $\rho_s = \rho_0$ to the same order of approximation as the Boussinesq approximation, we get a form that applies to estuarine tidal flows that are influenced by density variations.

$$\frac{\partial u}{\partial t} + \frac{\partial uu}{\partial x} + \frac{\partial uv}{\partial y} + \frac{\partial uw}{\partial z} - fv =$$

$$-g\frac{\partial \zeta}{\partial x} - g\frac{1}{\rho_0}\int_z^{\zeta} \frac{\partial \rho}{\partial x} dz' + \frac{\partial}{\partial x}\left(A_H \frac{\partial u}{\partial x}\right) + \frac{\partial}{\partial y}\left(A_H \frac{\partial u}{\partial y}\right) + \frac{\partial}{\partial z}\left(A_V \frac{\partial u}{\partial z}\right) \tag{4.6}$$

$$\frac{\partial v}{\partial t} + \frac{\partial uv}{\partial x} + \frac{\partial vv}{\partial y} + \frac{\partial vw}{\partial z} + fu =$$

$$-g\frac{\partial \zeta}{\partial y} - g\frac{1}{\rho_0}\int_z^{\zeta} \frac{\partial \rho}{\partial x} dz' + \frac{\partial}{\partial x}\left(A_H \frac{\partial v}{\partial x}\right) + \frac{\partial}{\partial y}\left(A_H \frac{\partial v}{\partial y}\right) + \frac{\partial}{\partial z}\left(A_V \frac{\partial v}{\partial z}\right) \tag{4.7}$$

The layer-averaged form of the Si3D governing equations is as follows.

Continuity equations:

$$\frac{\partial \zeta}{\partial t} + \frac{\partial}{\partial x}\left(\sum_{k=1}^{km} U_k\right) + \frac{\partial}{\partial y}\left(\sum_{k=1}^{km} V_k\right) = 0 \tag{4.8}$$

$$\left(w\right)\Big|_{k+½}^{k-½} = -\frac{\partial U_k}{\partial x} - \frac{\partial V_k}{\partial y} \quad k = 2, 3, \ldots, km \tag{4.9}$$

Momentum equations:

$$\frac{\partial U_k}{\partial t}+\frac{\partial (Uu)_k}{\partial x}+\frac{\partial (Vu)_k}{\partial y}+(uw)\Big|_{k+½}^{k-½}-fV_k+\frac{h_k}{\rho_k}g\rho_1\frac{\partial \zeta}{\partial x}= \tag{4.10}$$

$$-\frac{h_k}{\rho_k}\left[\frac{gh_1}{2}\frac{\partial \rho_1}{\partial x}+\sum_{m=2}^{k}\left(\frac{gh_{m-1}}{2}\frac{\partial \rho_{m-1}}{\partial x}+\frac{gh_m}{2}\frac{\partial \rho_m}{\partial x}\right)\right]+\frac{\partial}{\partial x}\left(A_H h\frac{\partial u}{\partial x}\right)_k+\frac{\partial}{\partial y}\left(A_H h\frac{\partial u}{\partial y}\right)_k+\left(\frac{\tau_{xz}}{\rho}\right)\Big|_{k+½}^{k-½}$$

$$\frac{\partial V_k}{\partial t}+\frac{\partial (Uv)_k}{\partial x}+\frac{\partial (Vv)_k}{\partial y}+(vw)\Big|_{k+½}^{k-½}+fU_k+\frac{h_k}{\rho_k}g\rho_1\frac{\partial \zeta}{\partial y}= \tag{4.11}$$

$$-\frac{h_k}{\rho_k}\left[\frac{gh_1}{2}\frac{\partial \rho_1}{\partial y}+\sum_{m=2}^{k}\left(\frac{gh_{m-1}}{2}\frac{\partial \rho_{m-1}}{\partial y}+\frac{gh_m}{2}\frac{\partial \rho_m}{\partial y}\right)\right]+\frac{\partial}{\partial x}\left(A_H h\frac{\partial v}{\partial x}\right)_k+\frac{\partial}{\partial y}\left(A_H h\frac{\partial v}{\partial y}\right)_k+\left(\frac{\tau_{yz}}{\rho}\right)\Big|_{k+½}^{k-½}$$

Salt transport equation:

$$\frac{\partial (hs)_k}{\partial t}+\frac{\partial (uhs)_k}{\partial x}+\frac{\partial (vhs)_k}{\partial y}+(ws)\Big|_{k+½}^{k-½}=\frac{\partial}{\partial x}\left(D_H h\frac{\partial s}{\partial x}\right)_k+\frac{\partial}{\partial y}\left(D_H h\frac{\partial s}{\partial y}\right)_k+\left(\frac{J_z}{\rho}\right)\Big|_{k+½}^{k-½} \tag{4.12}$$

The notation $(\ )\Big|_{k+½}^{k-½}$ represents the difference between interface values for a particular layer. Layer-averaged density ρ_k has been substituted for ρ_0 in the denominator of the pressure, vertical stress and vertical salt flux terms. This substitution reduces any error caused by the Boussinesq approximation. Except as noted in Equation 4.9, these governing equations apply to all layers. The bottom and free surface boundary conditions are satisfied by defining $w_{km+½} = 0$, $(uw)_{½} = (uw)_{km+½} = 0$, $(vw)_{½} = (vw)_{km+½} = 0$, $(\tau_{xz},\ \tau_{yz})_{½}$

$= (\tau_{xs}, \tau_{ys}), (\tau_{xz}, \tau_{yz})_{km+½} = (\tau_{xb}, \tau_{yb}), (ws)_{½} = (ws)_{km+½} = 0$ and $(J_z)_{½} = (J_z)_{km+½} = 0$. The summation term in Equations 4.10 and 4.11 is omitted for a surface layer ($k = 1$). These five three-dimensional governing equations are discretized using semi-implicit leapfrog and semi-implicit trapezoidal finite-differencing schemes for use in the Si3D model.

4.2: The Si3D Input File and Dictionary of Terminology

The Si3D input file specifies all necessary run parameters, including flow conditioning parameters. This file specifies which locations to produce a time series output at. It indicates the locations of all open boundaries and whether flow rate, water surface elevation and salinity will be assumed constant or require time-series data from external files. The Si3D input file also specifies how many thin-wall barriers and single dry cells are in the barrier locations file as well as the name for the salinity initial condition file. A sample Si3D input file that was used for a one-day test run is contained in Appendix C.

The Si3D dictionary of terminology is a list of terms and variables used in the Si3D program along with their corresponding definitions. This dictionary is printed in Appendix D and may be used as a general reference to better understand the terminology that is used in the program. Many of these terms are specifically found in the input file as well as being used in the Si3D source code.

4.3: Coarsening Bathymetric Data for Input into the Si3D Program

The National Ocean Service (NOS), a division of the National Oceanic and Atmospheric Administration (NOAA), has bathymetric data for seventy of the approximately 130 estuaries located within the forty-eight conterminous United States stored online at their Estuarine Bathymetry Web site, http://estuarinebathymetry.noaa.gov/. Bathymetric elevations found on this site are referenced to the local tidal datum which is typically mean lower-low water (MLLW) averaged over a nineteen year tidal epoch, according to the Estuarine Bathymetry Web site. The bathymetric data for each one of these different estuaries is stored as a USGS DEM, a self-contained set of 1024-byte ASCII-encoded blocks of text representing a raster-based digital elevation model developed by the United States Geological Survey. These DEMs are single files with a square grid of elevation data at thirty-meter resolution, i.e., thirty meters between elevation measurements, corresponding to about one arc second of the Earth's surface. Elevation values are positive above the tidal datum and, therefore, negative below the datum.

Data for the San Francisco Bay is stored in their group of Pacific Coast Estuaries under filing number P090, where "P" represents Pacific Coast and "090" represents a relative position along this coast. The bathymetry for this estuary was derived from thirty surveys containing 417,452 soundings having an average separation of fifty-three meters, according to the Estuarine Bathymetry Web site. Older, less accurate, overlapping surveys were either partially or entirely omitted.

The DEM is easily transcribed into a list of *x-y-z* triples using a program such as MicroDEM, a freeware microcomputer mapping program written by Professor Guth of the Oceanography Department at the United States Naval Academy. An *x-y-z* triple is a line of ASCII-encoded text containing three numbers, a UTM easting value *x*, a UTM northing value *y* and an elevation value *z*, each separated by white space. UTM represents the Universal Transverse Mercator coordinate system, a grid-based method of specifying locations on the surface of the Earth.

I developed a FORTRAN 77 program to read this list of *x-y-z* triples for the San Francisco Bay, fill in any missing elevation data, increase the cell-grid spacing (e.g., transform the original thirty-meter grid to 60, 90, 120 etc. meters) and output the data as a new list of *x-y-z* triples or as an Si3D bathymetry file.

The program automatically interpolates to fill in single elevation values that are missing from the DEM. If a particular cell is missing its elevation data, the program will interpolate across the eight surrounding or bordering cells, providing that all eight of the bordering cells have elevation data. The following interpolation scheme is used based upon the distances between the eight bordering cells (N, NE, E, SE, S, SW, W and NW) and the center cell. The bordering cells are multiplied by a weighting factor which depends on whether they are thirty meters (N, E, S and W cells) or forty-two meters (NE, SE, SW and NW cells) from the center cell. This scheme allows for the closer cells to have more influence than the ones that are farther away, as the program works to fill in the missing elevation values.

$$\frac{\sqrt{2}}{1+\sqrt{2}}(\text{avg. of N, E, S, W cells}) + \frac{1}{1+\sqrt{2}}(\text{avg. of NE, SE, SW, NW cells}) \tag{4.13}$$

This program also searches the entire list of *x*-*y*-*z* triples for larger groups of missing cells. The program user may specify the search-box radius and the maximum number of empty cells within this box to be considered a group of missing cell data. For example, a search-box radius of one means the program will search groups of nine cells (the center cell plus the eight bordering cells) and a search-box radius of two means the program will search groups of twenty-five cells (the center cell, the eight bordering cells, plus the sixteen cells which border that group of nine cells). The program counts the number of empty cells within the search box and, if it does not exceed the specified maximum empty cell count, it records the location of this missing group of cells in a separate file. The search-box radius and maximum empty cell count values may be refined to reduce the number of false positives and negatives.

This list of empty cell groups is used to assist the user in a manual search for all the missing cell groups within the list of *x*-*y*-*z* triples and manually replace them with values according to the same interpolation scheme which the program uses for single missing cells. This manual search helps to ensure that all missing cell groups are found and filled in and that no intentionally empty cells are accidentally filled.

The program can now read the newly filled in list of *x*-*y*-*z* triples and increase the cell grid spacing according to the specified coarsening factor, a positive integer which is the square root of the number of cells that are merged. For example, “1” preserves the original cell grid spacing (e.g., thirty meters); “2” doubles the cell grid spacing by merging square blocks of four cells; “3” triples the cell grid spacing by merging square blocks of nine cells, and “4” quadruples the cell grid spacing by merging square blocks of sixteen cells. The new elevations and UTM easting and northing values for the coarsened cell grids are simply the arithmetic means of the respective groups of values being merged. This coarsened DEM is outputted both as a list of *x*-*y*-*z* triples and as an Si3D bathymetry file.

The Si3D bathymetry file is an ASCII-encoded text file in a raster format with the elevation values arranged the way you would see them on a map with north at the top. The elevation data is only eighteen columns wide, so in order to accommodate this constraint, the second group of eighteen columns is concatenated below the first group, etc. The Si3D bathymetry file can use the same datum as NOS’s DEM files, i.e., mean lower-low water (MLLW); however, elevations are in decimeters, and positive elevation values in the Si3D file are below the tidal datum; whereas, values above the tidal datum are given a value of -90, to indicate a land point. Once the bathymetric data is presented in this format it can be further edited and refined by the USGS Gr Graphing Application written by John Donovan.

Appendix E contains the FORTRAN 77 source code for the program which was written and used to coarsen the San Francisco Bay DEM file from the National Ocean Service’s Estuarine Bathymetry Web site. The two figures that follow the source code show the effect which increased cell grid spacing has on the resolution of NOS’s original San

Francisco Bay DEM. Figure 4.1 shows the digital elevation model at its original thirty-meter resolution with all missing elevation data filled in; whereas, Figure 4.2 shows this same DEM after its cell-grid spacing has been increased to 240 meters.

Figure 4.1: San Francisco Bay DEM at its original thirty-meter resolution

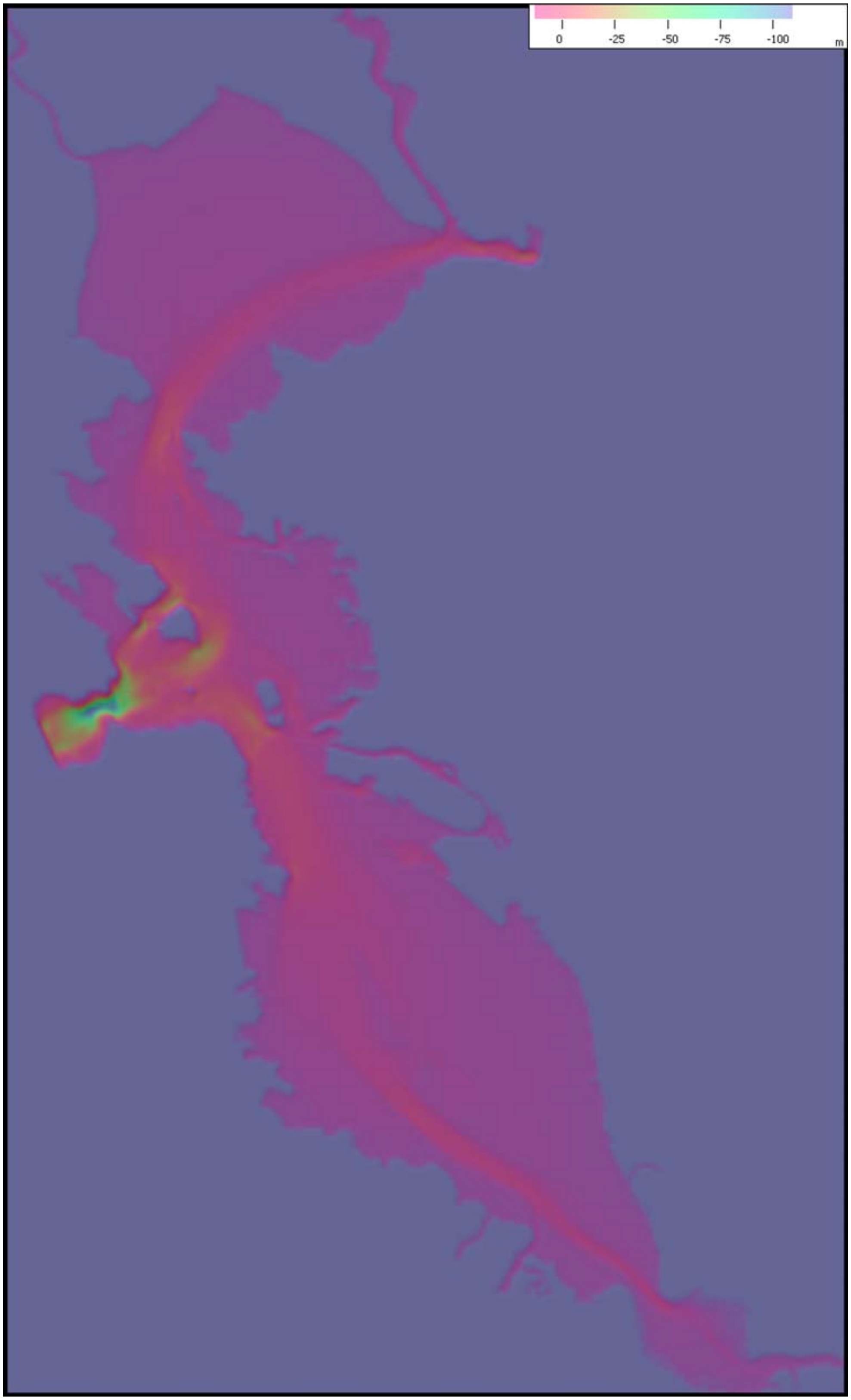

Figure 4.2: San Francisco Bay DEM with its cell-grid spacing increased to 240 meters

4.4: Results of the 1000-Meter San Francisco Bay 1-Day Test Run

The sample Si3D input file in Appendix C was used to execute a one thousand-meter San Francisco Bay model one-day test run. *ipxml* will be set to twelve for this particular simulation. The parameter *ipxml* specifies the number of temporal steps between outputting the current flow or velocity data for the entire estuary. Each temporal step is five minutes long in this particular model, so setting *ipxml* equal to twelve means that flow data for the entire system will be reported at hourly intervals. This simulation is just long enough to begin the cyclic tidal action of entering and exiting the estuary as it floods and ebbs. Longer simulations are necessary to begin calibrating the model with observed stage data within the estuary; however, for demonstrative purposes this model is sufficient enough to give reasonable circulation data for the San Francisco Bay and Estuary. In addition, the results of this run were used to select appropriate locations to perform field sampling of *Bacteroidales*, shown in Figure 1.1.

Figure 4.3 is a depiction of the 1000-meter bathymetric model of the San Francisco Bay which was used in this Si3D simulation. One thousand meters is much coarser than the thirty or the 240-meter bathymetric models shown in Figures 4.1 and 4.2; therefore, many of the smaller features that appeared in these finer grids cannot be resolved at the 1000-meter level. These smaller features are represented by thin-wall barriers and single dry cells which can be seen as brown lines and blocks, respectively, within the extents of the bathymetric model found in Figure 4.3. Also displayed along the edges of this figure are the *x*- and *y*-direction cell numbers, as well as all the water depths given in decimeters and referenced to a datum of mean lower-low water.

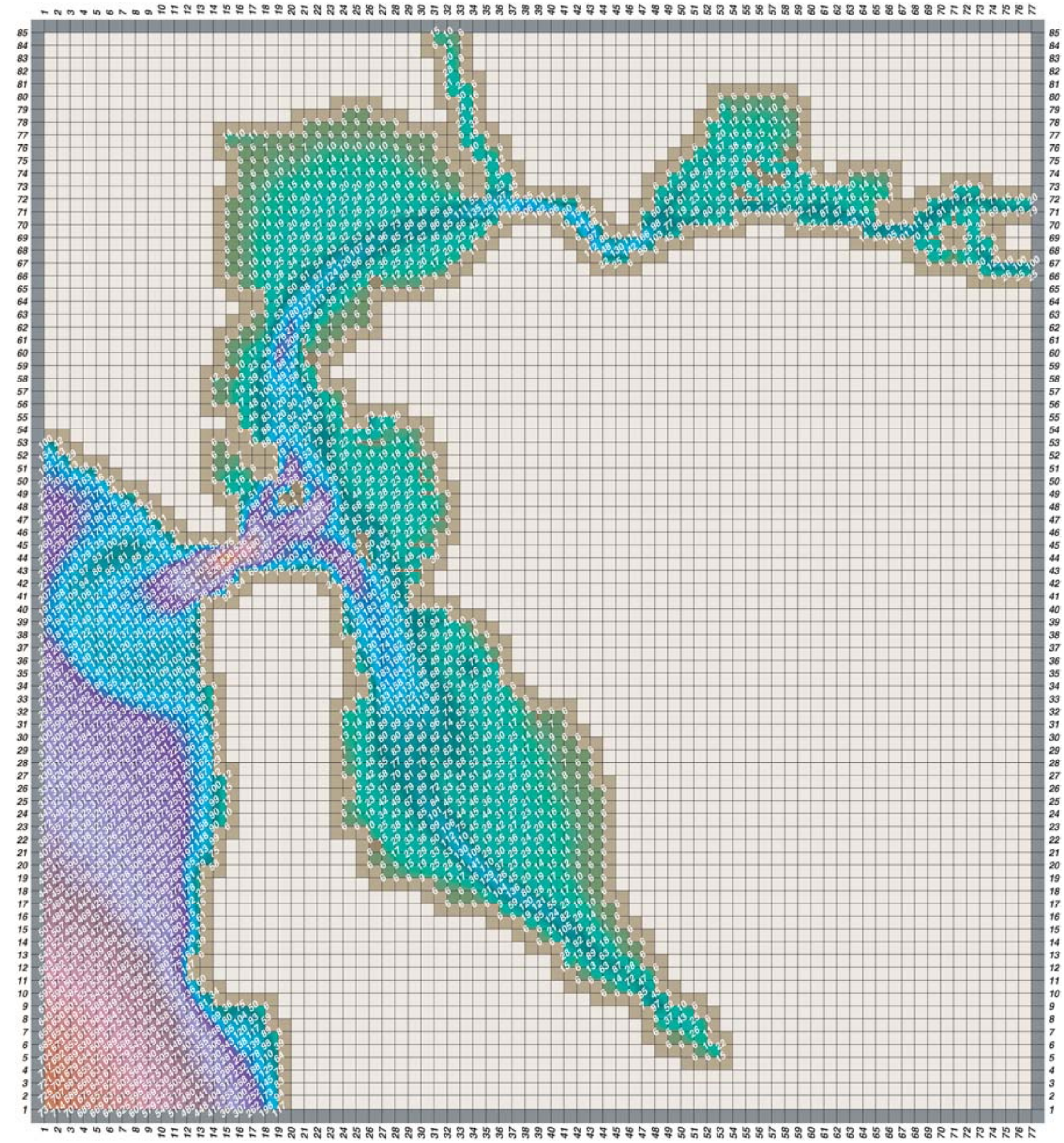

Figure 4.3: One thousand-meter bathymetric model of the San Francisco Bay, including coordinates, water depths in decimeters below MLLW, thin-wall barriers and single dry cells

The hourly flow data output contains all necessary information for displaying velocity fields and profiles. The velocity field information for the free surface can be found in the flow data output file, and with a simple algorithm one can isolate and plot the data for the velocity vectors at the top layer. One such algorithm was implemented in MATLAB by Laura DiPalermo, a Ph.D. student in Environmental Fluid Dynamics here at the University of California, Davis. When applied to the flow data output in this simulation, a velocity field diagram was created for each hour of the twenty-four-hour modeling period. The next four figures show the free surface velocity field during times when the main section of the San Francisco Bay is at high slack tide (hour 13), ebb tide (hour 16), low slack tide (hour 20) and flood tide (hour 23), respectively. Vectors showing the horizontal velocity are plotted at each cell location, and the *x*- and *y*-direction cell numbers are displayed along the edges of these figures.

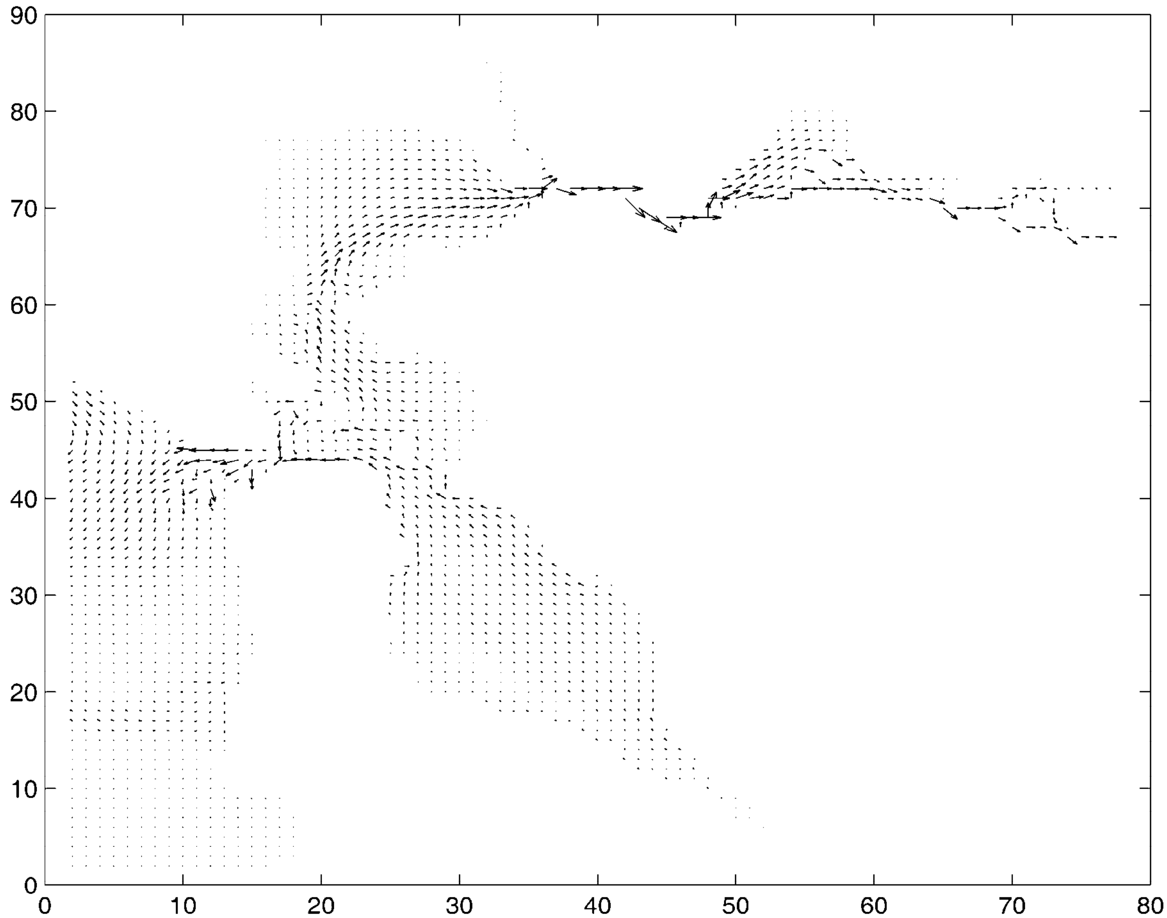

Figure 4.4: Velocity field at the free surface during a high slack tide in San Francisco Bay (hour 13)

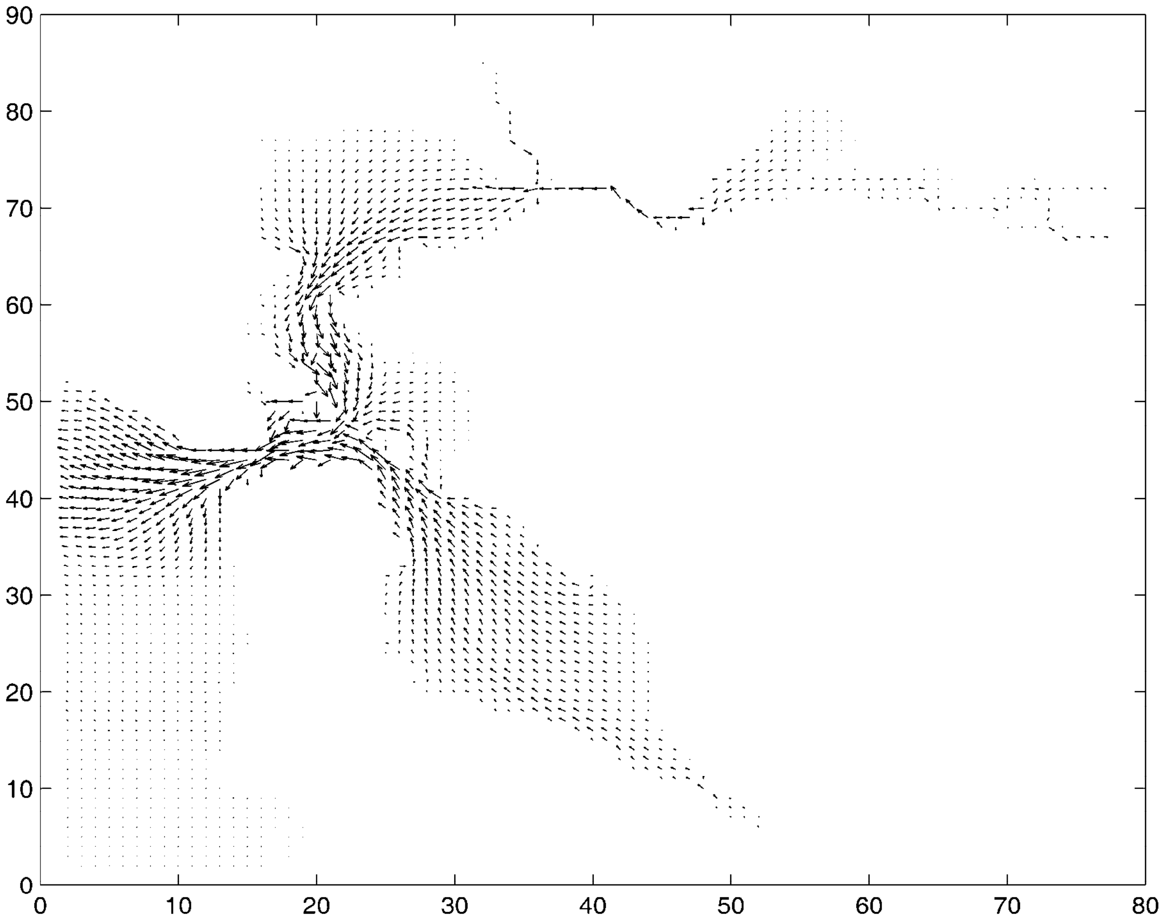

Figure 4.5: Velocity field at the free surface during an ebb tide in San Francisco Bay (hour 16)

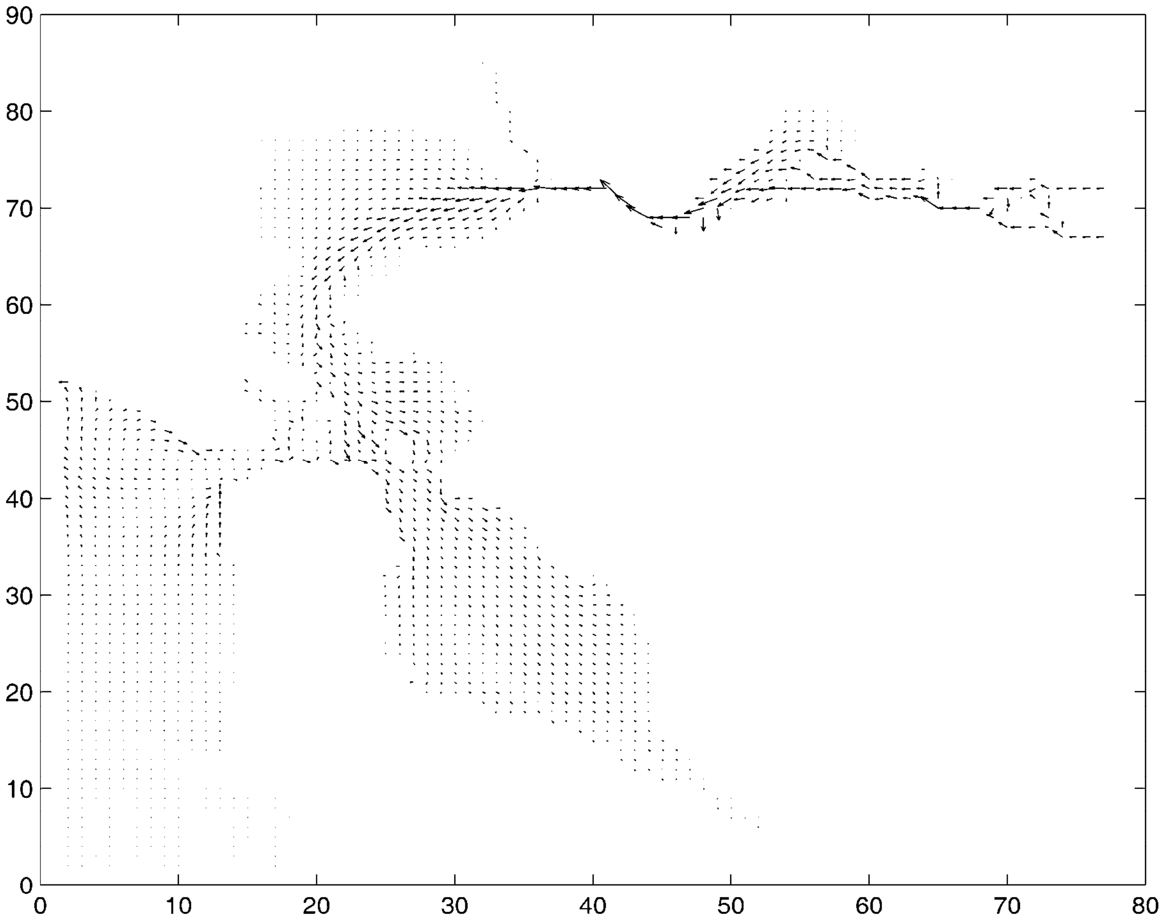

Figure 4.6: Velocity field at the free surface during a low slack tide in San Francisco Bay (hour 20)

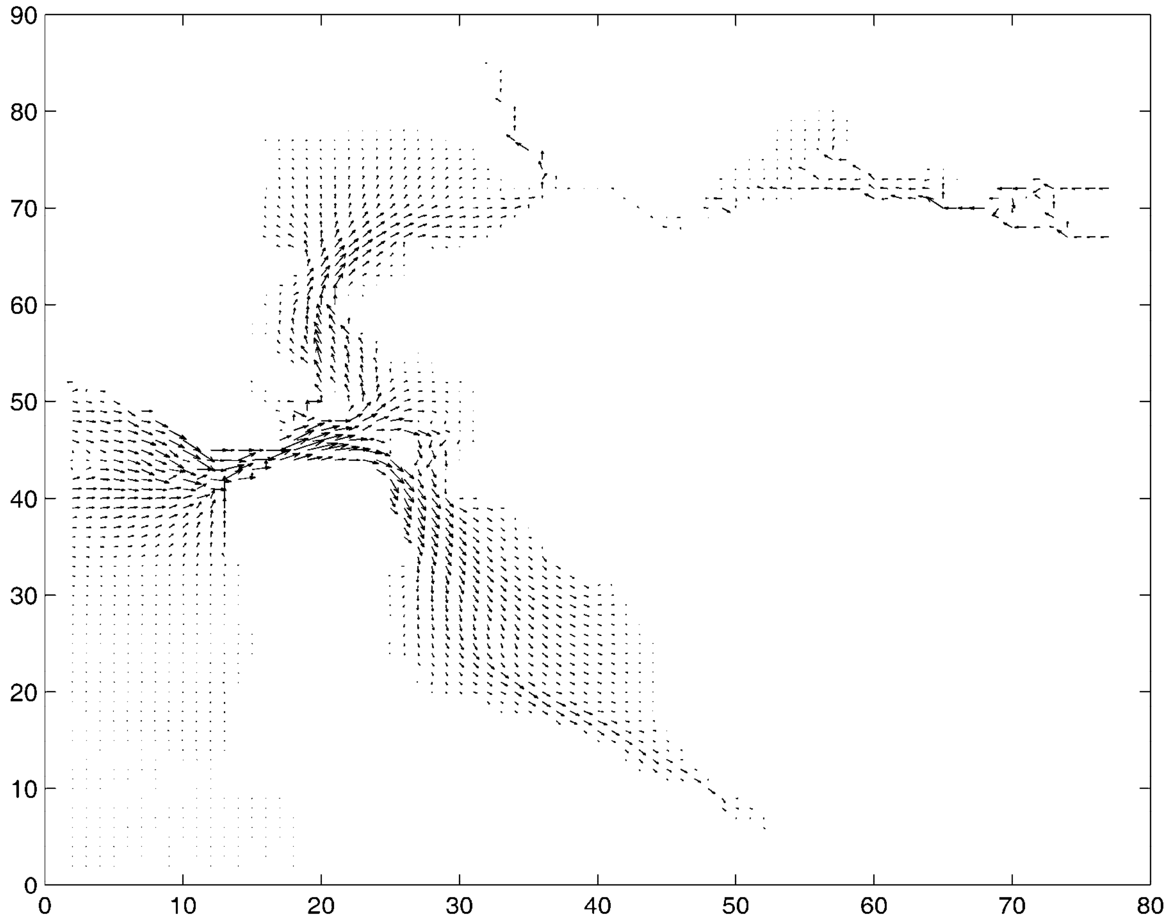

Figure 4.7: Velocity field at the free surface during a flood tide in San Francisco Bay (hour 23)

By setting *ivpv* equal to one, the Si3D program writes time-series output data formatted for the USGS Velocity Profile Viewer written by John Donovan. This data provides horizontal velocity vectors for each layer modeled at the nodes specified in the Si3D input file. For this test run, nodes (34, 71) and (15, 44) were specified according to the Si3D input file in Appendix C. These nodes correspond to the Carquinez Strait and the Golden Gate, respectively. The following eight figures show velocity profiles for these two locations during the same four times that were used in the velocity field diagrams. In these profiles, horizontal velocity is plotted for each vertical layer of the model. Water generally flows in the same direction at the Carquinez Strait and the Golden Gate during flooding and ebbing; however, water at these points will flow in opposing directions during slack tides. The Golden Gate is much deeper than the Carquinez Strait, and therefore, there are more vertical layers used to model flow at that location.

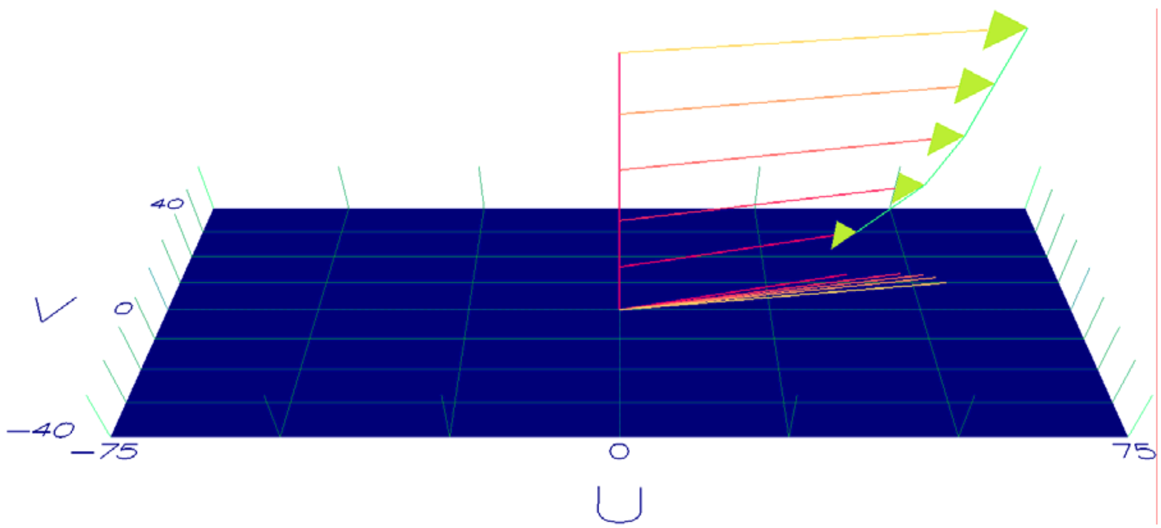

Figure 4.8: Velocity profile at the Carquinez Strait, node (34, 71), during a high slack tide in San Francisco Bay (hour 13)

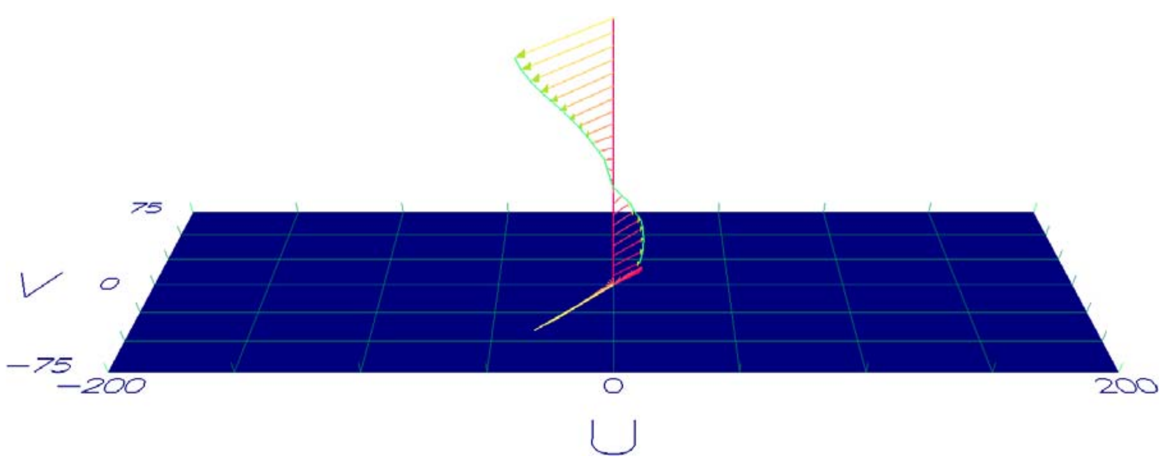

Figure 4.9: Velocity profile at the Golden Gate, node (15, 44), during a high slack tide in San Francisco Bay (hour 13)

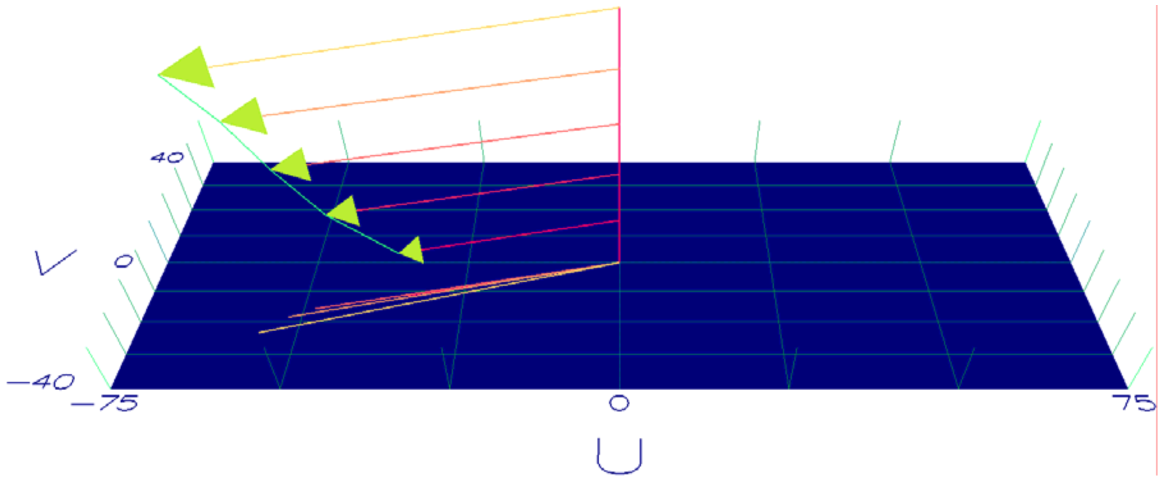

Figure 4.10: Velocity profile at the Carquinez Strait, node (34, 71), during an ebb tide in San Francisco Bay (hour 16)

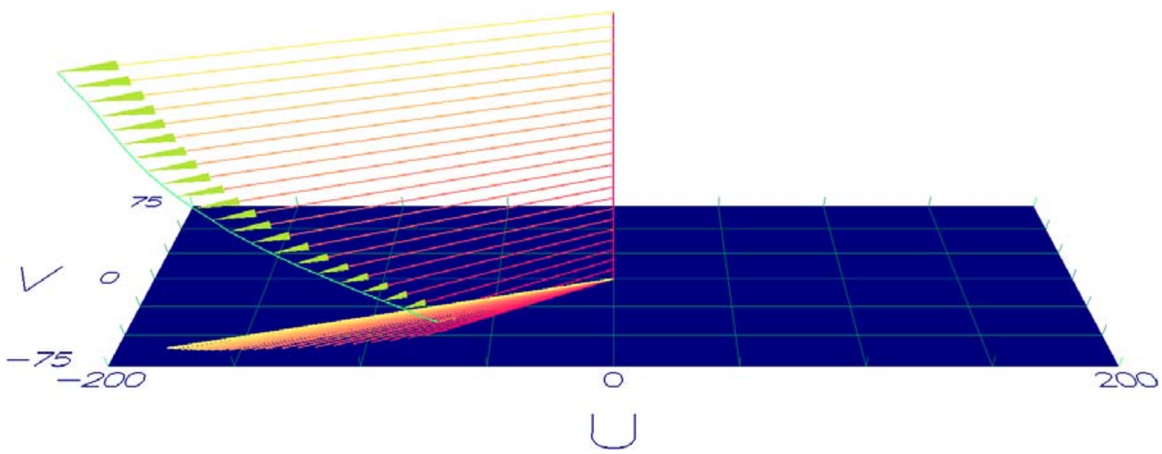

Figure 4.11: Velocity profile at the Golden Gate, node (15, 44), during an ebb tide in San Francisco Bay (hour 16)

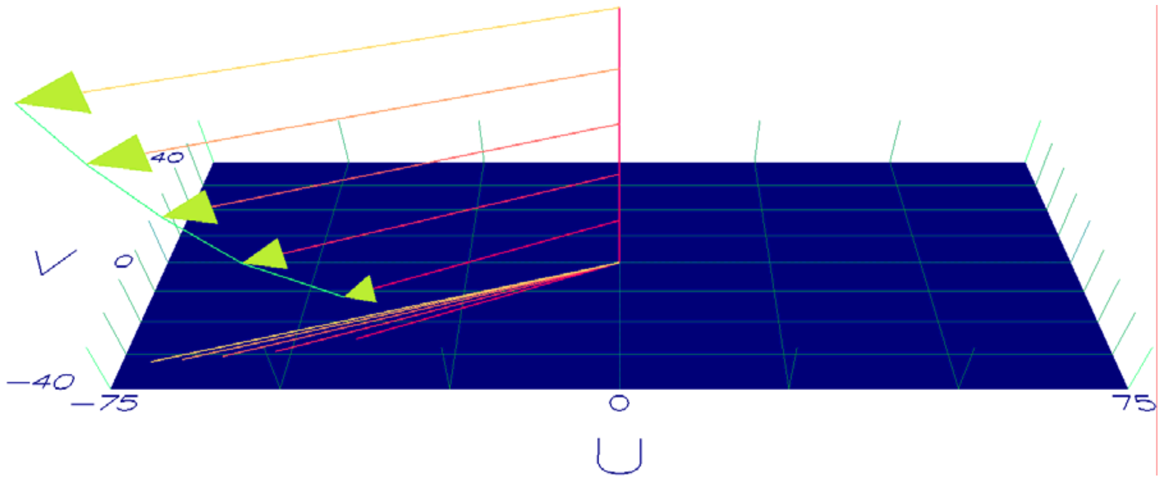

Figure 4.12: Velocity profile at the Carquinez Strait, node (34, 71), during a low slack tide in San Francisco Bay (hour 20)

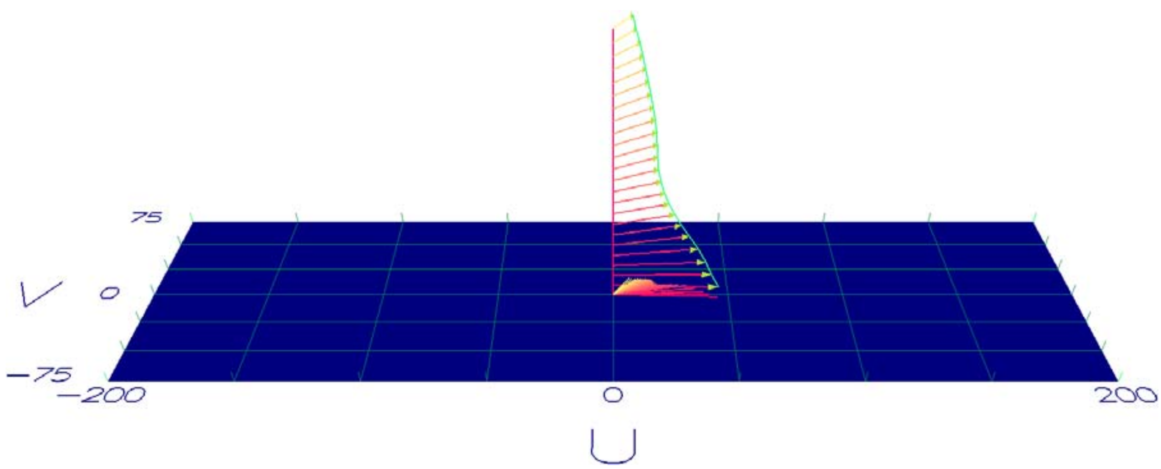

Figure 4.13: Velocity profile at the Golden Gate, node (15, 44), during a low slack tide in San Francisco Bay (hour 20)

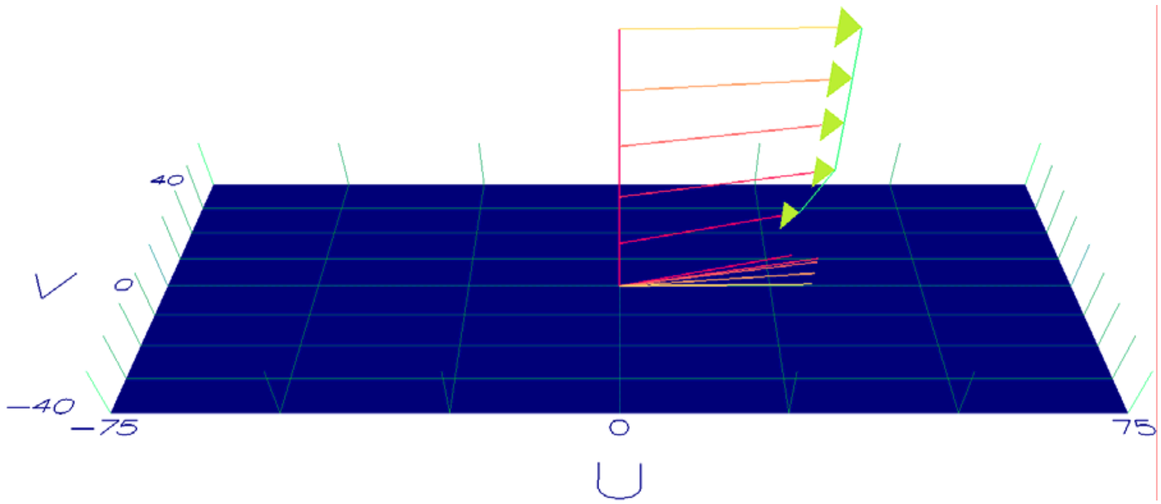

Figure 4.14: Velocity profile at the Carquinez Strait, node (34, 71), during a flood tide in San Francisco Bay (hour 23)

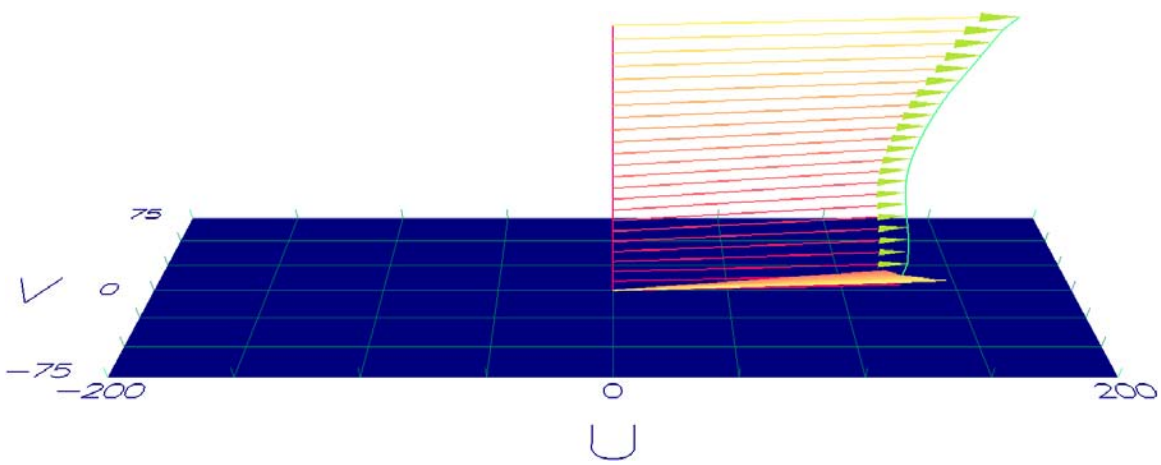

Figure 4.15: Velocity profile at the Golden Gate, node (15, 44), during a flood tide in San Francisco Bay (hour 23)

Flow information accompanied with particle tracking, diffusion and decay modeling is necessary to successfully model *Bacteroidales* concentrations within estuaries like the San Pablo Bay. Such a model can be calibrated against existing *Bacteroidales* measurements to successfully predict the transport and fate of these bacteria.

Conclusion

Modeling *Bacteroidales* concentrations within an estuarine environment is indeed a complex process. It involves knowing where individual bacterium particles are traveling within a system, plus the diffusion and decay of these bacteria needs to be accounted for. *Bacteroidales* have recently come into use as an indicator for the presence of pathogens and may be a better predictor of these disease causing agents than traditional *E. coli* counts (Shanks et al., 2006). *Bacteroidales* measurements, besides the historical record that they provide, are the basis for judging the accuracy of the model and are also needed for its calibration. A well calibrated model can accurately simulate the transport and fate of these bacteria and is useful for predicting their concentrations. Such information can provide the necessary insight that is needed to determine allowable total maximum daily loads, TMDLs, for meeting local water quality standards.

For a good model of estuarine circulation, reasonable initial conditions as well as boundary data for flow rate, water surface elevation and salinity are needed to accurately determine the circulation of water within the estuary. This information needs to be obtained at a high enough frequency to reasonably represent a daily tidal cycle. A good representation of the estuary's bathymetry is also needed. Such representations need to resolve all important features such as straits, channels, islands and shoals. This vital information can be gathered directly from the historical record or can be synthetically created to simulate a hypothetical situation. There are many Internet sources for obtaining flow, stage, salinity and bathymetric data, and an extensive list is contained in Appendix A. A good advection-diffusion-reaction model needs to be incorporated with the flow model to simulate *Bacteroidales* concentration. Initial conditions and boundary data will be needed for the A-D-R model to simulate these bacteria. *Bacteroidales* measurements, however, are difficult to obtain because their collection is quite complex; therefore, model calibration will be limited to the amount of existing *Bacteroidales* measurements that are available. In this case, the existing data may have to be adapted or interpolated. Weather data, specifically rainfall and runoff data, may be used to simulate *Bacteroidales* source release events in order to help predict the concentration of these bacteria.

The methodologies and results of previous *Bacteroidales* studies are contained within the literature. In summary, *Bacteroidales* as well as pathogens originate from the intestine and may come from a variety of sources, both human and animal. A significant runoff event is generally the mechanism that is needed to effectively transport these bacteria from a catchment of land to its neighboring waterway. Whether *Bacteroidales* actually enter a waterway depends upon a variety of factors, including their initial concentration, amount of runoff, the traveling distance needed to get to the nearest waterway and the existence of wetlands or filtration systems. Bacterial concentrations within a catchment can build up over time and be flushed away later by a significant runoff event.

Bacteroidales may adsorb to particles or be transported in suspension while traveling through water. Findings on actual adsorption rates are not consistent; however, most bacteria that are being transported in suspension are moving individually and not in cell masses (Muirhead et al., 2005). *Bacteroidales* markers may be detectable for anywhere from one day to a few weeks, depending upon the conditions; however, the general tendency is that *Bacteroidales* persist longer in colder environments, corresponding to lower decay rates at lower temperatures, verifying the T_{20} equation (Kreader, 1998; Seurinck et al., 2005). Solar radiation also increases their decay rate (Tian et al., 2002). *Bacteroidales* can be a reasonable measure of fecal pathogen loads, assuming they exhibit similar decay rates and exist in concentrations proportional to those of fecal pathogens.

These study findings may be useful for the creation of a three-dimensional advection-diffusion-reaction model that can predict *Bacteroidales* concentration within an estuary at much higher spatial and temporal frequencies than can be reasonably obtained through physical measurements alone.

Bibliography

Bengtsson, G. "Growth and metabolic flexibility in groundwater bacteria." *Microbial Ecology*, 18 (3): 235-248, 1989.

Benham, B. L., Baffaut, C., Zeckoski, R. W., Mankin, K. R., Pachepsky, Y. A., Sadeghi, A. A., Brannan, K. M., Soupir, M. L., Habersack, M. J. "Modeling bacteria fate and transport in watersheds to support TMDLs." *Transactions of the ASABE*, 49 (4): 987-1002, Jul-Aug 2006.

Bicknell, B. R., Imhoff, J. C., Kittle, J. L., Jr., Donigan, A. S., Jr., Johanson, R. C. *Hydrological Simulation Program–FORTRAN: User's Manual for Version 11*. EPA/600/SR-97/080, National Exposure Research Laboratory, USEPA, Research Triangle Park, NC: Aug 1997.

Bradford, S. A., Schijven, J. "Release of *Cryptosporidium* and *Giardia* from dairy calf manure: Impact of solution salinity." *Environmental Science and Technology*, 36 (18): 3916-3923, Sep 15, 2002.

Chick, H. "An investigation of the laws of disinfection." *The Journal of Hygiene*, 8 (1): 92-158, Jan. 1908.

Crane, S. R., Moore, J. A. "Modeling enteric bacterial die-off: A review." *Water, Air and Soil Pollution*, 27 (3-4): 411-439, Feb 1986.

Fletcher, C. A. J. "Boundary and initial conditions." *Computational Techniques for Fluid Dynamics: Fundamental and General Techniques*, Springer Series in Computational Physics, vol. 1, ed. 2, 7.3: 236-241, 1991.

Hagedorn, C., Hansen, D. T., Simonson, G. H. "Survival and movement of fecal indicator bacteria in soil under conditions of saturated flow." *Journal of Environmental Quality*, 7 (1): 55-59, 1978.

Koutitas, C. G. "Numerical solutions. Critical presentation of finite difference schemes." *Mathematical Models in Coastal Engineering*, Pentech Press, London, 3.2: 108-116, 1988.

Kreader, C. A. "Persistence of PCR-detectable *Bacteroides distasonis* from human feces in river water." *Applied and Environmental Microbiology*, 64 (10): 4103-4105, Oct 1998.

Moore, J. A., Smyth, J., Baker, S., Miner, J. R. "Evaluating coliform concentrations in runoff from various animal waste management systems." *Special Report 817*, Agricultural Experiment Station, Oregon State University, Corvallis: 1988.

Muirhead, R. W., Collins, R. P., Bremer, P. J. "Erosion and subsequent transport state of Escherichia coli from cowpats." *Applied and Environmental Microbiology*, 71 (6): 2875-2879, Jun 2005.

Pachepsky, Y. A., Sadeghi, A. M., Bradford, S. A., Shelton, D. R., Guber, A. K., Dao, T. "Transport and fate of manure-borne pathogens: Modeling perspective." *Agricultural Water Management*, 86 (1-2): 81-92, Nov 16, 2006.

Sadeghi, A. M., Arnold, J. G. "A SWAT/microbial sub-model for predicting pathogen loadings in surface and groundwater at watershed and basin scales." *Total Maximum Daily Load (TMDL) Environmental Regulations*, proceedings of the conference at Fort Worth, TX, ASAE Publication 701P0102: 56-63, Mar 11-13, 2002.

San Francisco Estuary Institute. "CISNet San Pablo Bay Study Data." Coastal Intensive Sites Network, URL: http://www.sfei.org/cmr/data/CISNetdata.htm, 2007.

Seurinck, S., Defoirdt, T., Verstraete, W., Siciliano, S. D. "Detection and quantification of the human-specific HF183 Bacteroides 16S rRNA genetic marker with real-time PCR for assessment of human fecal pollution in freshwater." Environmental Microbiology, 7 (2): 249-259, Feb 2005.

Shanks, O. C., Nietch, C., Simonich, M., Younger, M., Reynolds, D., Field, K. G. "Basin-wide analysis of the dynamics of fecal contamination and fecal source identification in Tillamook Bay, Oregon." *Applied and Environmental Microbiology*, 72 (8): 5537-5546, Aug 2006.

Smith, P. E. *A three-dimensional, finite-difference model for estuarine circulation*. Ph.D. Dissertation, Department of Civil and Environmental Engineering, University of California, Davis: 1997.

State of California. "Interactive Map of D-1641 Monitoring Stations." Bay Delta and Tributaries Project, Environmental Monitoring Program, URL: http://bdat.water.ca.gov/emp/Stations/D1641_station_gallery.html, 2006.

Tian, Y. Q., Gong, P., Radke, J. D., Scarborough, J. "Spatial and temporal modeling of microbial contaminants on grazing farmlands." *Journal of Environmental Quality*, 31 (3): 860-869, May-Jun 2002.

U.S. Dept. of Commerce. "Monterey Bay Recent Marine Data." National Oceanic and Atmospheric Administration, National Weather Service, National Data Buoy Center, URL: http://www.ndbc.noaa.gov/maps/Monterey_Bay.shtml, 2007.

Vadas, P. A., Kleinman, P. J. A., Sharpley, A. N. "A simple method to predict dissolved phosphorus in runoff from surface-applied manures." *Journal of Environmental Quality*, 33 (2): 749-756, Mar-Apr 2004.

Walters, S. P., Field, K. G. "Persistence and growth of fecal *Bacteroidales* assessed by bromodeoxyuridine immunocapture." *Applied and Environmental Microbiology*, 72 (7): 4532-4539, Jul 2006.

Appendix A: List of Internet Sources for Model Calibration Data

BDAT: Bay Delta and Tributaries Project: DFG: Fall Midwater Trawl

Parameter: specific conductance, water temperature, water depth, secchi depth
Frequency: monthly
Period: 09/1967 — 12/2002
Location: hundreds of different points in San Pablo Bay
URL: http://bdat.ca.gov/Php/Data_Retrieval/data_retrieval_by_category_Projects.php?category_code=16&category_name=Water+Quality

BDAT: Bay Delta and Tributaries Project: DFG: San Francisco Bay Studies

Parameter: salinity, water temperature, water depth
Frequency: monthly
Period: 01/1980 — 12/2004
Location: hundreds of different points in San Pablo Bay
URL: http://bdat.ca.gov/Php/Data_Retrieval/data_retrieval_by_category_Projects.php?category_code=16&category_name=Water+Quality

BDAT: Bay Delta and Tributaries Project: EMP: Environmental Monitoring Program

Parameter: suspended solids, organic nitrogen, ammonia, nitrite and nitrate, kjeldahl nitrogen, phosphorus, ortho-phosphate, chloride, silica (SiO2), chlorophyll a, pheophytin a, water temp, 1% light depth, specific conductance, turbidity, fluorescence, pH, oxygen, secchi depth, water depth

Frequency: biweekly
Period: 01/08/1975 — 12/16/1975
Location: Suisun Bay near Preston Point (D2)

Frequency: biweekly
Period: 01/07/1975 — 12/12/2006
Location: Sacramento River above Point Sacramento (D4)

Frequency: biweekly
Period: 01/08/1975 — 12/12/2006
Location: Suisun Bay at Bulls Head near Martinez (D6)

Frequency: monthly
Period: 01/08/1975 — 12/11/2006
Location: Grizzly Bay at Dolphin near Suisun Slough (D7)

Frequency: monthly
Period: 01/08/1975 — 12/12/2006
Location: Suisun Bay off Middle Point near Nichols (D8)

Frequency: monthly
Period: 01/08/1975 — 12/18/1995
Location: Honker Bay near Wheeler Point (D9)

Frequency: monthly
Period: 01/08/1975 — 12/13/2006
Location: Sacramento River at Chipps Island (D10)

Frequency: biweekly
Period: 01/07/1975 — 12/18/1995
Location: Sherman Lake near Antioch (D11)

Frequency: monthly
Period: 01/08/1975 — 12/13/2006
Location: San Joaquin River at Antioch Ship Channel (D12)

Frequency: monthly
Period: 01/07/1975 — 12/12/2006
Location: Sacramento River at Emmaton (D22)

Frequency: biweekly
Period: 02/14/1980 — 12/13/2006
Location: near Pinole Point (D41)

Frequency: monthly
Period: 10/21/2003 — 12/13/2006
Location: San Pablo Bay near mouth of Petaluma River (D41A)

Frequency: biweekly
Period: 03/26/1976 — 12/12/1979
Location: San Pablo Bay near Mare Island (D42)

Frequency: biweekly
Period: 02/22/1978 — 10/16/1984
Location: Suisun Slough 300 feet south of Volanti Slough (S42)

Frequency: monthly
Period: 1/26/1996 — 12/11/2006
Location: Montezuma Slough, second bend from mouth (NZ032)

URL: http://bdat.ca.gov/Php/Data_Retrieval/data_retrieval_by_category_preselected_Projects.php?category_code=16&category_name=Water+Quality&project_code=270

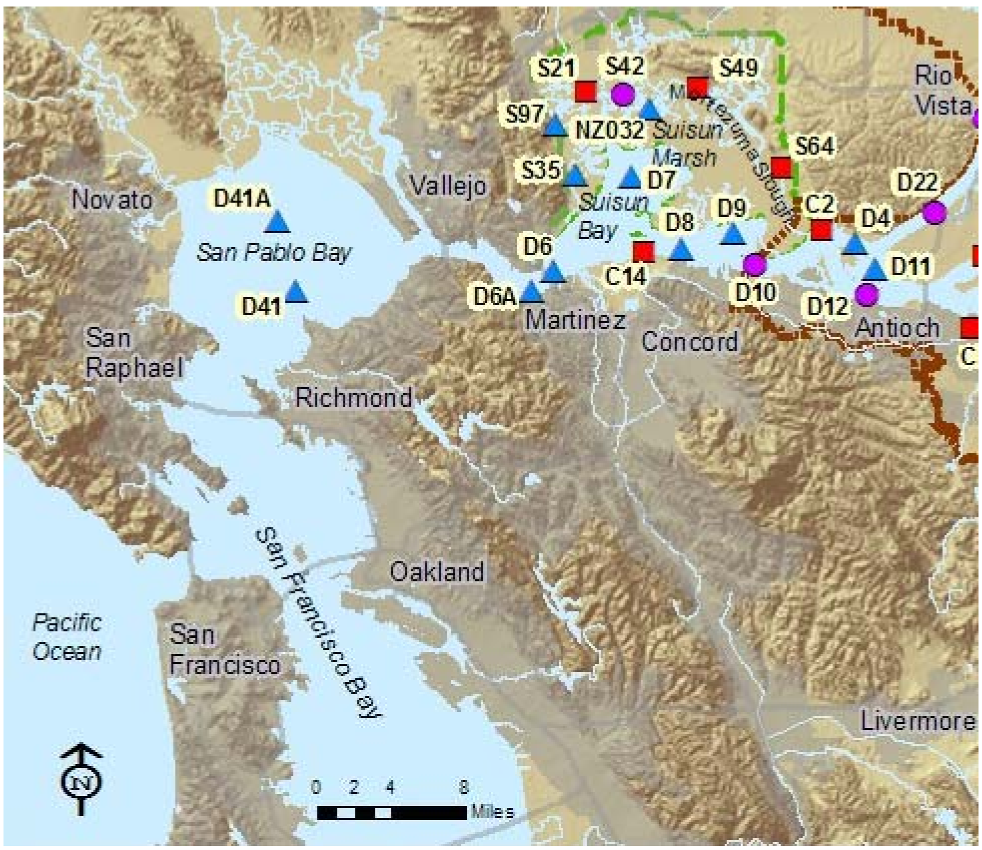

Figure A.1: BDAT-EMP sampling locations (State of California, 2006)

CDEC: California Data Exchange Center

Parameter: river stage
Frequency: hourly
Period: 01/01/1984 — present

Parameter: electrical conductivity
Frequency: hourly
Period: 02/01/1984 — present

Parameter: water temperature
Frequency: hourly
Period: 01/01/1995 — present

Parameter: wind speed, wind direction
Frequency: hourly
Period: 02/01/1995 — present

Parameter: dissolved oxygen
Frequency: hourly
Period: 02/06/2003 — present

Location: San Joaquin River at Antioch (ANH)
URL: http://cdec.water.ca.gov/cgi-progs/staMeta?station_id=ANH

Parameter: electrical conductivity, bottom electrical conductivity, water temperature
Frequency: hourly
Period: 03/01/1999 — present

Location: Antioch (USBR) (ANC)
URL: http://cdec.water.ca.gov/cgi-progs/staMeta?station_id=ANC

Parameter: electrical conductivity
Frequency: hourly
Period: 03/31/1988 — present

Parameter: bottom electrical conductivity, water temperature
Frequency: hourly
Period: 04/05/1999 — present

Location: Pittsburg (PTS)
URL: http://cdec.water.ca.gov/cgi-progs/staMeta?station_id=PTS

Parameter: electrical conductivity
Frequency: hourly
Period: 01/01/1984 — present

Parameter: water temperature, chorophyll
Frequency: hourly
Period: 06/13/1986 — present

Parameter: river stage
Frequency: hourly
Period: 10/01/1987 — present

Parameter: bottom electrical conductivity
Frequency: hourly
Period: 02/01/1995 — present

Location: Sacramento River at Mallard Island (MAL)
URL: http://cdec.water.ca.gov/cgi-progs/staMeta?station_id=MAL

Parameter: electrical conductivity
Frequency: hourly
Period: 03/31/1988 — present

Parameter: bottom electrical conductivity, water temperature
Frequency: hourly
Period: 02/23/1999 — present

Location: Collinsville (CLL)
URL: http://cdec.water.ca.gov/cgi-progs/staMeta?station_id=CLL

Parameter: electrical conductivity
Frequency: hourly
Period: 01/09/1987 — 01/20/1997

Parameter: river stage
Frequency: hourly
Period: 01/01/1987 — present

Location: Roaring River (ROR)
URL: http://cdec.water.ca.gov/cgi-progs/staMeta?station_id=ROR

Parameter: electrical conductivity, river stage, water temperature
Frequency: hourly
Period: 04/21/2005 — present
Location: National Steel (NSL)
URL: http://cdec.water.ca.gov/cgi-progs/staMeta?station_id=NSL

Parameter: atmospheric pressure, electrical conductivity, precipitation, river stage, water temperature, wind speed, wind direction
Frequency: hourly
Period: 01/07/2005 — present
Location: Blacklock (NE1) (BLL)
URL: http://cdec.water.ca.gov/cgi-progs/staMeta?station_id=BLL

Parameter: water temperature
Frequency: hourly
Period: 05/24/2000 — present

Parameter: electrical conductivity, river stage
Frequency: hourly

Period: 11/05/1997 — present
Location: Volanti (VOL)
URL: http://cdec.water.ca.gov/cgi-progs/staMeta?station_id=VOL

Period: 07/01/1994 — present
Location: Sunrise Club (SNC)
URL: http://cdec.water.ca.gov/cgi-progs/staMeta?station_id=SNC

Period: 09/29/1988 — present
Location: Beldon Landing (BDL)
URL: http://cdec.water.ca.gov/cgi-progs/staMeta?station_id=BDL

Parameter: electrical conductivity
Frequency: hourly
Period: 07/01/1994 — 01/23/1998

Parameter: river stage
Frequency: hourly
Period: 07/01/1994 — present

Parameter: electrical conductivity, water temperature
Frequency: hourly
Period: 03/26/2004 — present
Location: Ibis (IBS)
URL: http://cdec.water.ca.gov/cgi-progs/staMeta?station_id=IBS

Parameter: electrical conductivity, water temperature, river stage
Frequency: hourly
Period: 08/15/1994 — present
Location: Goodyear Slough (GYS)
URL: http://cdec.water.ca.gov/cgi-progs/staMeta?station_id=GYS

Parameter: electrical conductivity
Frequency: hourly
Period: 01/01/1997 — present

Parameter: bottom electrical conductivity, water temperature
Frequency: hourly
Period: 04/06/1999 — present
Location: Port Chicago (PCT)
URL: http://cdec.water.ca.gov/cgi-progs/staMeta?station_id=PCT

Parameter: electrical conductivity, bottom electrical conductivity, water temp, river stage
Frequency: hourly
Period: 07/01/1994 — present
Location: Martinez (MRZ)
URL: http://cdec.water.ca.gov/cgi-progs/staMeta?station_id=MRZ

Parameter: precipitation
Frequency: event
Period: 02/25/2004 — present

Location: Rodeo Fire Department (ROF)
URL: http://cdec.water.ca.gov/cgi-progs/staMeta?station_id=ROF

Location: Alhambra Creek (ABA)
URL: http://cdec.water.ca.gov/cgi-progs/staMeta?station_id=ABA

Location: Flood Control Headquarters - Contra Costa County (FCD)
URL: http://cdec.water.ca.gov/cgi-progs/staMeta?station_id=FCD

Location: Orinda Fire Station 3 (ODA)
URL: http://cdec.water.ca.gov/cgi-progs/staMeta?station_id=ODA

Location: Ygnacio Valley Fire (YGF)
URL: http://cdec.water.ca.gov/cgi-progs/staMeta?station_id=YGF

Location: Cummings Peak (CMG)
URL: http://cdec.water.ca.gov/cgi-progs/staMeta?station_id=CMG

Period: 12/11/1997 — present

Location: Petaluma River near Corona Road (CRD)
URL: http://cdec.water.ca.gov/cgi-progs/staMeta?station_id=CRD

Location: Novato Creek (NVC)
URL: http://cdec.water.ca.gov/cgi-progs/staMeta?station_id=NVC

Period: 02/23/1998 — present
Location: Petaluma River at D Street Bridge (PTB)
URL: http://cdec.water.ca.gov/cgi-progs/staMeta?station_id=PTB

Period: 12/01/2000 — present
Location: San Rafael Civic Center (SFC)
URL: http://cdec.water.ca.gov/cgi-progs/staMeta?station_id=SFC

Period: 01/10/2000 — present
Location: Arroyo Corte Madera Mill Valley (ACM)
URL: http://cdec.water.ca.gov/cgi-progs/staMeta?station_id=ACM

Period: 01/22/2005 — present

Location: Richmond City Hall (RHL)
URL: http://cdec.water.ca.gov/cgi-progs/staMeta?station_id=RHL

Location: Bald Peak (BPK)
URL: http://cdec.water.ca.gov/cgi-progs/staMeta?station_id=BPK

Period: 10/25/2005 — present
Location: Rossmoor (RSS)
URL: http://cdec.water.ca.gov/cgi-progs/staMeta?station_id=RSS

Period: 02/25/2004 — present

Location: St. Mary's College (SMC)
URL: http://cdec.water.ca.gov/cgi-progs/staMeta?station_id=SMC

Location: Rocky Ridge (RKY)
URL: http://cdec.water.ca.gov/cgi-progs/staMeta?station_id=RKY

Period: 10/01/1995 — present
Location: San Leandro Bay (SLE)
URL: http://cdec.water.ca.gov/cgi-progs/staMeta?station_id=SLE

Period: 01/06/2000 — present
Location: Palo Alto 3E (PAA)
URL: http://cdec.water.ca.gov/cgi-progs/staMeta?station_id=PAA

Frequency: hourly
Period: 04/19/1999 — present

Location: Crystal Springs Cottage (CSC)
URL: http://cdec.water.ca.gov/cgi-progs/staMeta?station_id=CSC

Location: Pilarcitos Dam (PLD)
URL: http://cdec.water.ca.gov/cgi-progs/staMeta?station_id=PLD

Location: San Andreas Cottage (SNA)
URL: http://cdec.water.ca.gov/cgi-progs/staMeta?station_id=SNA

Parameter: accumulated precipitation, relative humidity, air temperature, wind speed, wind direction, wind peak gust speed, wind peak gust direction
Frequency: hourly

Period: 04/28/1997 — present

Location: Briones (BNE)
URL: http://cdec.water.ca.gov/cgi-progs/staMeta?station_id=BNE

Location: Las Trampas (LTR)
URL: http://cdec.water.ca.gov/cgi-progs/staMeta?station_id=LTR

Period: 12/04/1997 — present
Location: Los Altos Hills (LSA)
URL: http://cdec.water.ca.gov/cgi-progs/staMeta?station_id=LSA

Parameter: accumulated precipitation, air temperature
Frequency: hourly
Period: 11/01/1992 — present

Parameter: relative humidity, wind speed, wind direction, wind peak gust speed, wind peak gust direction
Frequency: hourly
Period: 01/01/1995 — present

Location: Oakland North (ONO)
URL: http://cdec.water.ca.gov/cgi-progs/staMeta?station_id=ONO

Location: Oakland South (OSO)
URL: http://cdec.water.ca.gov/cgi-progs/staMeta?station_id=OSO

CICORE: Center for Integrative Coastal Observation, Research and Education: SFBEAMS: San Francisco Bay Environmental Assessment and Monitoring Station

Parameter: water temperature, conductivity, barometric pressure, transmissivity, photosynthetically active radiation, salinity
Frequency: 6 min

Depth:	1 meter below low low tide
Period:	09/07/2005 — present
URL:	http://sfbeams.sfsu.edu/download_fixed.htm

Depth:	0.5 meters below surface
Period:	05/01/2006 — present
URL:	http://sfbeams.sfsu.edu/download_float.htm

Parameter:	air temp, relative humidity, barometric pressure, photosynthetically active radiation, precipitation, wind speed, wind direction, maximum wind speed
Frequency:	5 min
Height:	2 meters above the pier
Period:	11/08/2003 — present
URL:	http://sfbeams.sfsu.edu/download_met.htm

Parameter:	ammonium, nitrite and nitrate, phosphate, silicate, dissolved inorganic carbon, primary productivity, primary productivity/chlorophyll a
Frequency:	weekly
Depth:	surface water
Period:	04/09/2003 — present
URL:	http://sfbeams.sfsu.edu/download_nut.htm
Location:	37.8915 N, 122.4467 W (SF Bay, Romberg Tiburon Center Pier)

CICORE: Center for Integrative Coastal Observation, Research and Education: San Francisco Bay Water Quality Monitoring Stations: California State University, East Bay

Parameter:	percent fluorescence, battery voltage, chlorophyll, conductivity, depth, dissolved oxygen concentration, dissolved oxygen percent, ORP, percent hydrogen, air pressure, resistivity, salinity, specific conductance, total dissolved solids, water temperature, turbidity
Frequency:	15 min

Period:	07/09/2005 — present
Location:	37.6960 N, 122.1922 W (SF Bay, San Leandro Marina)
URL:	http://www.sci.csueastbay.edu/cicore/san_leandro/SLarchive.csv

Period:	08/10/2005 — present
Location:	37.5068 N, 122.1167 W (SF Bay, Dumbarton Pier)
URL:	http://www.sci.csueastbay.edu/cicore/dumbarton/DBarchive.csv

CIMIS: California Irrigation Management Information System

Parameter:	evapotranspiration, precipitation, solar radiation, vapor pressure, air temperature, relative humidity, dew point, wind speed, wind direction, soil temperature
Frequency:	hourly
Period:	11/18/1985 — present
Location:	Brentwood, #47, E of Brentwood, 37°55’43”N, 121°39’31”W
Period:	07/01/1986 — 01/18/2002
Location:	Novato, #63, NE of Novato, 38°07’17”N, 122°32’34”W
Period:	07/22/1987 — 03/08/2002
Location:	Walnut Creek, #65, NW of Walnut Creek, 37°54’49”N, 122°04’54”W
Period:	06/08/1987 — 11/22/2002
Location:	San Jose, #69, SW of San Jose, 37°19’33”N, 121°57’00”W
Period:	10/31/1990 — 01/24/1994
Location:	Woodside, #96, NW of Woodside, 37°27’11”N, 122°16’49”W
Period:	08/29/1991 — 06/19/2000
Location:	Fremont, #100, SSE of Fremont, 37°31’30”N, 121°58’03”W
Period:	03/11/1993 — present
Location:	Carneros, #109, SW of Napa, 38°13’08”N, 122°21’14”W
Period:	03/28/1995 — present
Location:	Hastings Tract, #122, NW of Rio Vista, 38°16’57”N, 121°47’24”W
Period:	08/18/1994 — present
Location:	Suisun Valley, #123, NE of Cordelia, 38°14’02”N, 122°07’00”W
Period:	10/08/1997 — present
Location:	Twitchell Island, #140, SE of Rio Vista, 38°07’00”N, 121°39’29”W
Period:	08/25/1999 — present
Location:	Petaluma East, #144, NE of Petaluma, 38°16’02”N, 122°36’58”W
Period:	03/25/1999 — present
Location:	Oakland Foothills, #149, NE of Alameda, 37°46’51”N, 122°10’44”W
Period:	10/11/2002 — present
Location:	Point San Pedro, #157, NE of San Rafael, 37°59’30”N, 122°28’12”W

Period: 04/01/2000 — 12/18/2001
Location: Valley of the Moon, #164, NW of Sonoma, 38°18’42”N,122°29’58”W

Period: 04/06/2001 — present
Location: Concord, #170, N of Concord, 38°00’15”N, 122°01’12”W

Period: 02/05/2001 — present
Location: Union City, #171, NW of Union City, 37°35’56”N, 122°03’07”W

Period: 02/27/2002 — present
Location: Moraga, #178, SW of Moraga, 37°50’16”N, 122°08’22”W

Period: 06/01/2003 — present
Location: Black Point, #187, SE of Novato, 38°05’28”N, 122°31’36”W

URL: http://wwwcimis.water.ca.gov/cimis/frontHourlyReport.do

IEP: Interagency Ecological Program: Dayflow Program

Parameter: mean daily flow
Frequency: daily
Period: 10/01/1955 — 09/30/2006
Location: Delta Cross Channel, Georgiana Slough, Jersey Point, Chipps Island
URL: http://iep.water.ca.gov/dayflow/output/index.html

IEP: Interagency Ecological Program: HEC-DSS Time-Series Databases

Parameter: electrical conductivity
Frequency: daily
Period: 01/01/1966 — 12/31/1998

Parameter: bottom electrical conductivity
Frequency: daily
Period: 01/01/1994 — 12/31/1998

Parameter: electrical conductivity
Frequency: hourly
Period: 04/01/1996 — present

Parameter: bottom electrical conductivity
Frequency: hourly
Period: 04/01/1996 — 05/31/2005
Location: Sacramento River at Port Chicago (RSAC064)
URL: http://iep.water.ca.gov/cgi-bin/dss/dss1.pl?station=RSAC064

Parameter: electrical conductivity
Frequency: 15 min
Period: 01/01/1986 — 10/31/2001
Location: Goodyear Slough at Fleet (SLGYR008)
URL: http://iep.water.ca.gov/cgi-bin/dss/dss1.pl?station=SLGYR008

Parameter: electrical conductivity
Frequency: daily
Period: 01/01/1965 — 12/31/1996
Location: Sacramento River at Benicia Bridge (RSAC056)
URL: http://iep.water.ca.gov/cgi-bin/dss/dss1.pl?station=RSAC056

Parameter: stage
Frequency: 15 min
Period: 06/01/1986 — 09/30/2002

Parameter: stage
Frequency: hourly
Period: 06/01/1994 — present

Parameter: air temperature, dissolved oxygen, percent hydrogen
Frequency: hourly
Period: 05/01/1983 — 09/30/2002

Parameter: electrical conductivity
Frequency: hourly
Period: 05/01/1983 — present

Parameter: electrical conductivity, bottom electrical conductivity
Frequency: 15 min
Period: 12/01/1990 — 09/30/2002

Parameter: water temperature
Frequency: hourly
Period: 05/01/1983 — present
Location: Sacramento River at Martinez (RSAC054)
URL: http://iep.water.ca.gov/cgi-bin/dss/dss1.pl?station=RSAC054

Parameter: electrical cond, bottom electrical cond, water temp, bottom water temp, stage
Frequency: 15 min
Period: 10/01/1986 — 01/31/1998
Location: Selby (Wickland Oil Pier) (RSAC045)
URL: http://iep.water.ca.gov/cgi-bin/dss/dss1.pl?station=RSAC045

Parameter: stage
Frequency: 15 min
Period: 06/01/1986 — 09/30/1996
Location: San Pablo Strait at Point San Pablo (RSAC020)
URL: http://iep.water.ca.gov/cgi-bin/dss/dss1.pl?station=RSAC020

Parameter: electrical conductivity, bottom electrical conductivity, water temperature
Frequency: 15 min
Period: 10/01/1990 — 09/30/1996

Parameter: stage
Frequency: hourly
Period: 12/01/1900 — 03/31/2006

Location: Central Bay at Presidio Fort Point (SHWSF001)
URL: http://iep.water.ca.gov/cgi-bin/dss/dss1.pl?station=SHWSF001

Parameter: electrical cond, bottom electrical cond, water temp, bottom water temp
Frequency: 15 min
Period: 12/01/1982 — 09/30/2006
Location: Central Bay at west end of Bay Bridge (SHWSF009)
URL: http://iep.water.ca.gov/cgi-bin/dss/dss1.pl?station=SHWSF009

NERRS: National Estuarine Research Reserve System

Parameter: water temperature, specific conductance, salinity, dissolved oxygen, depth, percent hydrogen, turbidity
Frequency: 15 min
Period: 08/17/2006 — present
Location: China Camp (sfbccwq), Suisun Marsh

Parameter: air temperature, relative humidity, barometric pressure, wind speed, wind direction, precipitation, PAR
Frequency: 15 min
Period: 08/17/2006 — present
Location: Rush Ranch (sfbrrmet), Suisun Marsh

URL: http://cdmo.baruch.sc.edu/QueryPages/csv_export.cfm

NOAA: NDBC: National Data Buoy Center

Parameter: wind direction, wind speed, wind gusts, significant wave height, dominant wave period, average wave period, mean wave direction, barometer, air temperature, water temperature, dew point, visibility, tide

Frequency: 6 min
Period: 04/01/2005 — 06/27/2005

Frequency: hourly
Period: 06/27/2005 — 06/16/2006

Frequency: 6 min
Period: 06/16/2006 — 04/30/2007

Location: Port Chicago (PCOC1)
URL: http://ndbc.noaa.gov/station_history.php?station=pcoc1

Frequency: 6 min
Period: 04/01/2005 — 06/27/2005

Frequency: hourly
Period: 06/27/2005 — 10/13/2005

Location: Richmond (RCMC1)
URL: http://ndbc.noaa.gov/station_history.php?station=rcmc1

Frequency: hourly
Period: 05/01/2006 — 12/27/2006
01/11/2007 — 02/02/2007
02/05/2007 — 04/30/2007
Location: Tiburon Pier (TIBC1)
URL: http://ndbc.noaa.gov/station_history.php?station=tibc1

Frequency: 6 min
Period: 04/01/2005 — 06/27/2005

Frequency: hourly
Period: 06/27/2005 — 08/12/2005
01/25/2006 — 02/15/2006

Frequency: 6 min
Period: 02/15/2006 — 04/19/2006

Frequency: hourly
Period: 04/20/2006 — 06/13/2006

Frequency: 6 min
Period: 06/14/2006 — 04/30/2007

Location: San Francisco (FTPC1)
URL: http://ndbc.noaa.gov/station_history.php?station=ftpc1

Frequency: 6 min
Period: 04/01/2005 — 06/27/2005

Frequency: hourly
Period: 06/27/2005 — 02/15/2006

Frequency: 6 min
Period: 02/15/2006 — 04/30/2007

Location: Alameda (AAMC1)
URL: http://ndbc.noaa.gov/station_history.php?station=aamc1

Frequency: 6 min
Period: 04/01/2005 — 06/27/2005

Frequency: hourly
Period: 06/27/2005 — 06/13/2006

Frequency: 6 min
Period: 06/14/2006 — 04/30/2007

Location: Redwood City (RTYC1)
URL: http://ndbc.noaa.gov/station_history.php?station=rtyc1

Frequency: hourly
Period: 04/01/1981 — 04/30/2007
Location: Bodega Bay: 48 nautical miles NNW of San Francisco (46013)
URL: http://ndbc.noaa.gov/station_history.php?station=46013

Frequency: hourly
Period: 09/08/2004 — 04/30/2007
Location: Point Reyes (46214)
URL: http://ndbc.noaa.gov/station_history.php?station=46214

Frequency: hourly
Period: 04/01/2005 — 05/16/2005

Frequency: 6 min
Period: 03/27/2007 — 04/30/2007

Location: Point Reyes (PRYC1)
URL: http://ndbc.noaa.gov/station_history.php?station=pryc1

Frequency: hourly
Period: 07/08/1982 — 04/30/2007
Location: 18 nautical miles west of San Francisco (46026)
URL: http://ndbc.noaa.gov/station_history.php?station=46026

Frequency: hourly
Period: 11/24/1980 — 04/30/2007
Location: Half Moon Bay: 24 nautical miles SSW of San Francisco (46012)
URL: http://ndbc.noaa.gov/station_history.php?station=46012

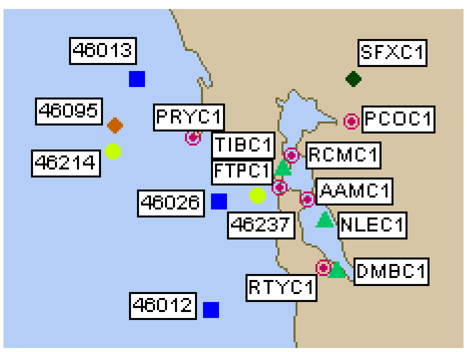

Figure A.2: NOAA-NDBC sampling locations (U.S. Dept. of Commerce, 2007)

NOAA: NGDC: National Geophysical Data Center: MGG: Marine Geology and Geophysics: GEODAS: Geophysical Data System

Parameter: bathymetry
Resolution: 90-meter digital elevation model
Location: US Central Pacific Coast
URL: http://www.ngdc.noaa.gov/mgg/gdas/gd_designagrid.html

NOAA: NOS: National Ocean Service: Estuarine Bathymetry

Parameter: bathymetry
Resolution: 30-meter digital elevation model
Date: 1956, 1971 — 1993
Location: San Francisco Bay, CA (P090)
URL: http://estuarinebathymetry.noaa.gov/pacific.html

NOAA: Tides and Currents

Parameter: wind, water temperature
Frequency: 6 min
Period: 1993 — present

Parameter: air temperature, barometric pressure, water level
Frequency: 6 min
Period: 1996 — present

Parameter: water conductivity
Frequency: hourly
Period: 12/10/1998 — 10/17/2001

Location: San Francisco (9414290)
URL: http://tidesandcurrents.noaa.gov/data_menu.shtml?stn=9414290

Parameter: water level
Frequency: 6 min
Period: 01/01/2005 — 03/30/2005
Location: San Mateo Bridge (9414458)
URL: http://tidesandcurrents.noaa.gov/data_menu.shtml?stn=9414458

Parameter: water temperature
Frequency: hourly
Period: 03/16/1996 — 08/18/1997

Parameter: water level
Frequency: 6 min
Period: 03/15/1996 — 04/05/2005

Location: Dumbarton Bridge (9414509)
URL: http://tidesandcurrents.noaa.gov/data_menu.shtml?stn=9414509

Parameter: wind, air temperature, water temperature, barometric pressure
Frequency: 6 min
Period: 03/26/1996 — present

Parameter: water level
Frequency: 6 min
Period: 08/22/1997 — present

Location: Redwood City (9414523)
URL: http://tidesandcurrents.noaa.gov/data_menu.shtml?stn=9414523

Parameter: water level
Frequency: 6 min
Period: 01/04/2005 — 02/16/2005
Location: San Leandro Marina (9414688)
URL: http://tidesandcurrents.noaa.gov/data_menu.shtml?stn=9414688

Parameter: wind
Frequency: 6 min
Period: 03/04/1994 — present

Parameter: air temperature
Frequency: 6 min
Period: 02/09/1996 — present

Parameter: water temperature
Frequency: 6 min
Period: 04/02/1985 — present

Parameter: barometric pressure
Frequency: 6 min
Period: 02/09/1996 — present

Parameter: water conductivity
Frequency: 6 min
Period: 12/08/1998 — present

Parameter: water level
Frequency: 6 min
Period: 01/01/1996 — present

Location: Alameda (9414750)
URL: http://tidesandcurrents.noaa.gov/data_menu.shtml?stn=9414750

Parameter: water level
Frequency: 6 min
Period: 04/27/1999 — 04/30/2000
Location: GPS Buoy, San Francisco Bay (9414796)
URL: http://tidesandcurrents.noaa.gov/data_menu.shtml?stn=9414796

Parameter: water level
Frequency: 6 min
Period: 04/01/2004 — 07/31/2005
Location: Bradmoor Island (9414811)
URL: http://tidesandcurrents.noaa.gov/data_menu.shtml?stn=9414811

Parameter: water temperature
Frequency: hourly
Period: 09/05/1995 — 06/30/2006

Parameter: wind, air temperature, barometric pressure
Frequency: hourly
Period: 02/10/1996 — 06/30/2006

Parameter: water conductivity
Frequency: 6 min
Period: 12/11/1998 — 02/13/2004

Parameter: water level
Frequency: 6 min
Period: 01/01/1996 — present

Location: Richmond (9414863)
URL: http://tidesandcurrents.noaa.gov/data_menu.shtml?stn=9414863

Parameter: wind
Frequency: 6 min
Period: 03/04/1994 — present

Parameter: air temperature, barometric pressure
Frequency: 6 min
Period: 1992 — present

Parameter: water temperature
Frequency: 6 min
Period: 09/12/1993 — present

Parameter: water conductivity
Frequency: 6 min
Period: 06/03/1998 — 09/25/2003

Parameter: water level
Frequency: 6 min
Period: 01/01/1996 — present

Location: Port Chicago (9415144)
URL: http://tidesandcurrents.noaa.gov/data_menu.shtml?stn=9415144

SFEI: San Francisco Estuary Institute: CISNet: Coastal Intensive Sites Network: San Pablo Bay Data

Parameter: dissolved and total trace element concentrations in water
Frequency: monthly
Period: 07/19/1999 — 03/08/2001

Parameter: trace element concentrations in sediment
dissolved PAH, PCB, OC pesticide, OP pesticide concentrations in water
Frequency: monthly
Period: 03/15/2000 — 03/08/2001

Parameter: particulate PAH, PCB, OC pesticide, OP pesticide concentrations in water
Frequency: monthly
Period: 10/18/2000 — 03/08/2001

Location: Petaluma River-Upper, Napa River-Upper, Napa River-Lower, Canvas Back Duck Club-Napa/Sonoma Marsh, Dutchman Slough-Napa/Sonoma Marsh, Hudeman Slough-Napa/Sonoma Marsh, Sonoma Creek Slough-Napa/Sonoma Marsh, Sonoma Creek Mouth-San Pablo Bay, Davis Point-San Pablo Bay, Radar-San Pablo Bay, Marker 9-San Pablo Bay, Marker 19-San Pablo Bay

Parameter: PAH, PCB, OC pesticide, OP pesticide concentrations in sediment
Frequency: monthly
Period: 07/17/2000 — 03/08/2001
Location: Petaluma River-Upper, Napa River-Upper, Napa River-Lower, Canvas Back Duck Club-Napa/Sonoma Marsh, Sonoma Creek Slough-Napa/Sonoma Marsh, Marker 19-San Pablo Bay

URL: http://www.sfei.org/cmr/data/CISNetdata.htm

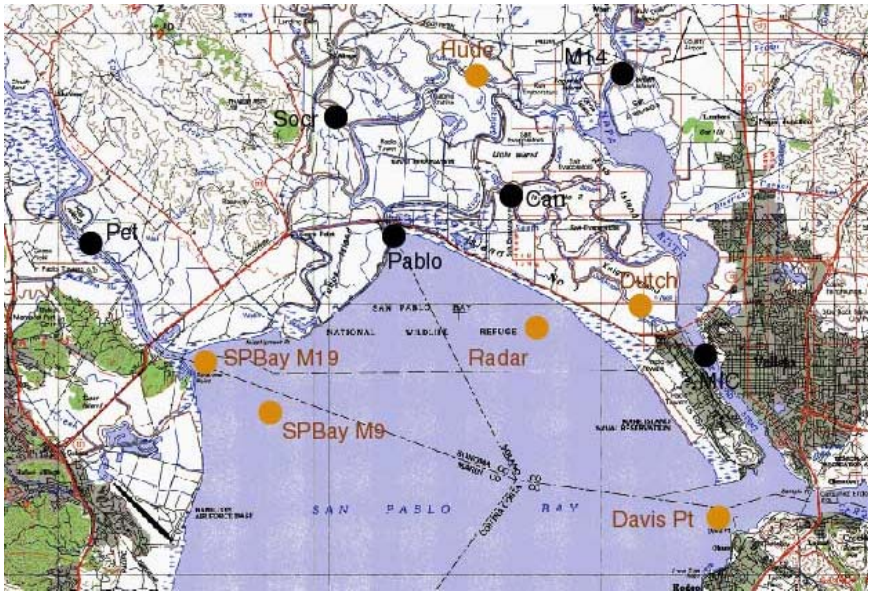

Figure A.3: SFEI-CISNet sampling locations (San Francisco Estuary Institute, 2007)

USGS: SFBAY: San Francisco Bay and Delta: Suisun Bay and Delta Bathymetry

Parameter: bathymetry
Resolution: 10-meter digital elevation model
Location: Suisun Bay and Delta
URL: http://sfbay.wr.usgs.gov/sediment/delta/downloads.html

Appendix B: FORTRAN 77 Program for 1-D A-D-R Finite-Difference Models

```
C COND   CONDITION:   1=REVERSE HEAVISIDE STEP FUNCTION    2=DIRAC DELTA
C                                         3=NEUMANN BOUNDARY CONDITION
C PROFILE 1=(TRUE)CONCENTRATION PROFILE 0=(FALSE)ROOT MEAN SQUARED ERROR
C MODEL  1=BACKWARD   2=LAX DISSIPATIVE    3=LAX-WENDROFF    4=LEAP-FROG
C        5=FULLY IMPLICIT 6=MCCORMACK 7=FROMM 8=GENERALIZED BOX EXPLICIT
C THETA  WEIGHTING FACTOR FOR ADVECTION MODELS 2 AND 8:      0 THROUGH 1
C ALPHA  FOR DISPERSION TERM: 0=EXPLICIT  1=IMPLICIT  0.5=CRANK-NICOLSON
C BETA   FOR REACTION TERM:   0=EXPLICIT  1=IMPLICIT  0.5=AVERAGE  EX/IM
C        U=VELOCITY          D=DISPERSIVITY          LAMBDA=DIE-OFF RATE
C        LBOUND=LEFT BOUNDARY RBOUND=RIGHT BOUNDARY FOR CONDITIONS 1 & 2
C        NUMI=NUMBER OF SPATIAL STEPS      NUMN=NUMBER OF TEMPORAL STEPS
C        LOCI=START LOCATION OF UNIT IMPULSE  OR HEAVISIDE STEP FUNCTION
C
C DATA TYPES
C
      DIMENSION CO(999999),C(999999),CN(999999),BB(999999),DD(999999)
      INTEGER COND,PROFILE,FIRSTI,RBOUND
      REAL*8 CO,C,CN,AA,BB,CC,DD,THETA,ALPHA,BETA,U,D,LAMBDA,T,DX,DT,PI,
     &     SS
      PI=3.14159265358979D0
C
C INPUTS
C
      COND=1
      PROFILE=1
      U=1
      D=0
      LAMBDA=0
      LBOUND=100
      RBOUND=100
      T=32
      MODEL=5
      THETA=0
      ALPHA=0
      BETA=0
      DX=1
C
C END INPUTS
C
      SS=0
C
C DT SIZE CALCULATION
C
      IF(0.8D0*DX/U.LT.0.4D0*DX*DX/D)THEN
      DT=0.8D0*DX/U
      ELSE
      DT=0.4D0*DX*DX/D
      ENDIF
C
C SPATIAL AND TEMPORAL STEP ARRAY PARAMETERS
C
      IF(COND.EQ.1.OR.COND.EQ.2)THEN
```

```
      FIRSTI=3
      NUMI=(LBOUND+RBOUND)/DX+2.5
      LOCI=LBOUND/DX+2.5
      ELSE
      FIRSTI=2
      NUMI=0.9D0/DX+2.5
      ENDIF
      NUMN=T/DT+0.5
C
C BEGIN INITIAL CONDITION LOOP
C
      DO I=1,NUMI
      CO(I)=0
      C(I)=0
      CN(I)=0
C
C REVERSE HEAVISIDE STEP FUNCTION
C
      IF(COND.EQ.1)THEN
      IF(I.LE.LOCI)THEN
      C(I)=1
      ELSE
      C(I)=0
      ENDIF
C
C DIRAC DELTA
C
      ELSEIF(COND.EQ.2)THEN
      IF(I.EQ.LOCI)THEN
      C(I)=1/DX
      ELSE
      C(I)=0
      ENDIF
C
C NEUMANN
C
      ELSE
      C(I)=2*((I-2)*DX+0.1D0)+4*COS(0.5*PI*((I-2)*DX+0.1D0))
      ENDIF
C
      CO(I)=C(I)
C
C END INITIAL CONDITION LOOP
C
      ENDDO
C
C AA AND CC COEFFICIENTS FOR IMPLICIT MODELS
C
      AA=0
      CC=0
      IF(MODEL.EQ.5)THEN
      AA=-U/4/DX-ALPHA*D/DX/DX
      CC=U/4/DX-ALPHA*D/DX/DX
C
      ELSEIF(MODEL.EQ.8)THEN
      AA=THETA/DT-U/2/DX-ALPHA*D/DX/DX
      CC=-ALPHA*D/DX/DX
C
      ELSEIF(ALPHA.NE.0.OR.BETA.NE.0)THEN
      AA=-ALPHA*D/DX/DX
```

```
      CC=AA
C
C END AA AND CC COEFFICIENTS FOR IMPLICIT MODELS
C
      ENDIF
C
C BEGIN TEMPORAL LOOP
C
      DO N=1,NUMN
C
C NEUMANN BOUNDARY CONDITION
C
      IF(COND.EQ.3)THEN
      C(1)=C(3)-2*DX*(2-2*PI*SIN(0.05D0*PI)*EXP(-D*(N-1)*DT*PI*PI/4))
      C(NUMI)=2
C
C END NEUMANN BOUNDARY CONDITION
C
      ENDIF
C
C BEGIN SPATIAL LOOP
C
      DO I=FIRSTI,NUMI-1
C
C BB(I) AND DD(I) COEFFICIENTS FOR IMPLICIT MODELS
C
      IF(MODEL.EQ.5)THEN
      BB(I)=1/DT+2*ALPHA*D/DX/DX
      DD(I)=C(I)/DT-U/4/DX*(C(I+1)-C(I-1))+(1-ALPHA)*D/DX/DX*(C(I+1)-2*C
     &     (I)+C(I-1))-LAMBDA*((1-BETA)*C(I)+BETA*CN(I))
C
      ELSEIF(MODEL.EQ.8)THEN
      BB(I)=(1-THETA)/DT+U/2/DX+2*ALPHA*D/DX/DX
      DD(I)=(1-THETA)*C(I)/DT+THETA*C(I-1)/DT-U/2/DX*(C(I)-C(I-1))+(1-AL
     &     PHA)*D/DX/DX*(C(I+1)-2*C(I)+C(I-1))-LAMBDA*((1-BETA)*C(I)+BET
     &     A*CN(I))
C
      ELSEIF(ALPHA.NE.0.OR.BETA.NE.0)THEN
C
      IF(MODEL.EQ.2)THEN
      BB(I)=THETA/DT+2*ALPHA*D/DX/DX
      DD(I)=(1-THETA)*(C(I+1)+C(I-1))/2/DT-U/2/DX*(C(I+1)-C(I-1))+(1-ALP
     &     HA)*D/DX/DX*(C(I+1)-2*C(I)+C(I-1))-LAMBDA*((1-BETA)*C(I)+BETA
     &     *CN(I))
C
      ELSEIF(MODEL.EQ.4)THEN
      BB(I)=0.5/DT+2*ALPHA*D/DX/DX
      DD(I)=CO(I)/2/DT-U/2/DX*(C(I+1)-C(I-1))+(1-ALPHA)*D/DX/DX*(C(I+1)-
     &     2*C(I)+C(I-1))-LAMBDA*((1-BETA)*C(I)+BETA*CN(I))
C
      ELSE
      BB(I)=1/DT+2*ALPHA*D/DX/DX
      IF(MODEL.EQ.1)DD(I)=C(I)/DT-U/DX*(C(I)-C(I-1))+(1-ALPHA)*D/DX/DX*(
     &     C(I+1)-2*C(I)+C(I-1))-LAMBDA*((1-BETA)*C(I)+BETA*CN(I))
      IF(MODEL.EQ.3)DD(I)=C(I)/DT-U/2/DX*(C(I+1)-C(I-1))+(U*U*DT/DX/DX+(
     &     1-ALPHA)*D/DX/DX)*(C(I+1)-2*C(I)+C(I-1))-LAMBDA*((1-BETA)*C(I
     &     )+BETA*CN(I))
      IF(MODEL.EQ.6)DD(I)=C(I)/DT-U/2/DX*(C(I+1)+C(I)-2*C(I-1))+(U*U*DT/
     &     DX/DX+(1-ALPHA)*D/DX/DX)*(C(I+1)-2*C(I)+C(I-1))-LAMBDA*((1-BE
     &     TA)*C(I)+BETA*CN(I))
```

```
      IF(MODEL.EQ.7)DD(I)=C(I)/DT-U/4/DX*(C(I+1)-C(I-1)+C(I)-C(I-2))+(U*
     &     U*DT/4/DX/DX+(1-ALPHA)*D/DX/DX)*(C(I+1)-2*C(I)+C(I-1))+(U*U*D
     &     T-2*U*DX)/4/DX/DX*(C(I-2)-2*C(I-1)+C(I))-LAMBDA*((1-BETA)*C(I
     &     )+BETA*CN(I))
C
C END BB(I) AND DD(I) COEFFICIENTS FOR IMPLICIT MODELS
C
      ENDIF
C
C CN(I) FOR EXPLICIT MODELS
C
      ELSE
      IF(MODEL.EQ.1)CN(I)=C(I)-U*DT/DX*(C(I)-C(I-1))+D*DT/DX/DX*(C(I+1)-
     &     2*C(I)+C(I-1))-DT*LAMBDA*C(I)
      IF(MODEL.EQ.2)CN(I)=(1/THETA-1)/2*(C(I+1)+C(I-1))-U*DT/2/THETA/DX*
     &     (C(I+1)-C(I-1))+D*DT/THETA/DX/DX*(C(I+1)-2*C(I)+C(I-1))-DT/TH
     &     ETA*LAMBDA*C(I)
      IF(MODEL.EQ.3)CN(I)=C(I)-U*DT/2/DX*(C(I+1)-C(I-1))+(U*U*DT*DT/DX/D
     &     X+D*DT/DX/DX)*(C(I+1)-2*C(I)+C(I-1))-DT*LAMBDA*C(I)
      IF(MODEL.EQ.4)CN(I)=CO(I)-U*DT/DX*(C(I+1)-C(I-1))+D*2*DT/DX/DX*(C(
     &     I+1)-2*C(I)+C(I-1))-2*DT*LAMBDA*C(I)
      IF(MODEL.EQ.6)CN(I)=C(I)-U*DT/2/DX*(C(I+1)+C(I)-2*C(I-1))+(U*U*DT*
     &     DT/DX/DX+D*DT/DX/DX)*(C(I+1)-2*C(I)+C(I-1))-DT*LAMBDA*C(I)
      IF(MODEL.EQ.7)CN(I)=C(I)-U*DT/4/DX*(C(I+1)-C(I-1)+C(I)-C(I-2))+(U*
     &     U*DT*DT/4/DX/DX+D*DT/DX/DX)*(C(I+1)-2*C(I)+C(I-1))+(U*U*DT*DT
     &     -2*U*DT*DX)/4/DX/DX*(C(I-2)-2*C(I-1)+C(I))-DT*LAMBDA*C(I)
C
C END CN(I) FOR EXPLICIT MODELS
C
      ENDIF
C
C END SPATIAL LOOP
C
      ENDDO
C
C THOMAS ALGORITHM TO FIND CN(I) FOR IMPLICIT MODELS
C
      IF(MODEL.EQ.5.OR.MODEL.EQ.8.OR.ALPHA.NE.0.OR.BETA.NE.0)THEN
      DO I=FIRSTI+1,NUMI-1
      BB(I)=BB(I)-AA*CC/BB(I-1)
      DD(I)=DD(I)-AA*DD(I-1)/BB(I-1)
      ENDDO
C
      CN(NUMI-1)=DD(NUMI-1)/BB(NUMI-1)
      DO I=NUMI-2,FIRSTI,-1
      CN(I)=(DD(I)-CC*CN(I+1))/BB(I)
      ENDDO
C
C END THOMAS ALGORITHM TO FIND CN(I) FOR IMPLICIT MODELS
C
      ENDIF
C
C REPLACEMENT LOOP
C
      DO I=FIRSTI,NUMI-1
      CO(I)=0
      CO(I)=C(I)
      C(I)=0
      C(I)=CN(I)
      CN(I)=0
```

```
      BB(I)=0
      DD(I)=0
C
C END REPLACEMENT LOOP
C
      ENDDO
C
C END TEMPORAL LOOP
C
      ENDDO
C
C BEGIN CONCENTRATION PROFILE AND SUM OF SQUARES
C
      DO I=2,NUMI
C
C CONCENTRATION PROFILE FOR DIRAC DELTA AND REVERSE HEAVISIDE FUNCTION
C
      IF(PROFILE.EQ.1.AND.COND.NE.3)WRITE(*,*)(I-LOCI)*DX,C(I)
C
C SUM OF SQUARES FOR DIRAC DELTA AND REVERSE HEAVISIDE STEP FUNCTION
C
      IF(PROFILE.EQ.0.AND.COND.NE.3)SS=SS+(C(I)-EXP(-LAMBDA*T-((I-LOCI)*
     &     DX-U*T)**2/4/D/T)/SQRT(4*PI*D*T))**2
C
C CONCENTRATION PROFILE FOR NEUMANN BOUNDARY CONDITION
C
      IF(PROFILE.EQ.1.AND.COND.EQ.3)WRITE(*,*)(I-2)*DX+0.1D0,C(I)
C
C SUM OF SQUARES FOR NEUMANN BOUNDARY CONDITION
C
      IF(PROFILE.EQ.0.AND.COND.EQ.3)SS=SS+(C(I)-2*((I-2)*DX+0.1D0)+4*COS
     &     (0.5*PI*((I-2)*DX+0.1D0))*EXP(-D*T*PI*PI/4))**2
C
C END CONCENTRATION PROFILE AND SUM OF SQUARES
C
      ENDDO
C
C ROOT MEAN SQUARED ERROR
C
      IF(PROFILE.EQ.0)WRITE(*,*)SQRT(SS/(NUMI-1))
      END
```

Appendix C: Sample Si3D Input File

```
1000-m San Francisco Bay model (1-day test run setup)
Start date:  yr= 1997, mon= 12, day= 1, ihr= 0000, Julian day= -30.0
#1 RUN PARAMETERS
 xl=       76000., yl=      84000., zl=      72.925, tl=      86400.,
 idt=          300, idx=       1000, idy=       1000, idz=          2,
 iexplt=         1, ivde=         1, itrap=        1, niter=        5,
 ismooth=        0, ilin=         0, ihomo=        1, dzmin=     0.19,
 iturb=          3, az0=     2.5E-2, dz0=     2.5E-2, az00=    1.0E-3,
 a1=          10.0, b1=        -0.5, a2=        3.33, b2=        -1.5,
 ax0=         1.E1, ay0=       1.E1, datadj=     1.0, iseich=       0,
 cd=         0.003, cw=     1.4E-3, wa=          0.0, phi=        90.,
 f=         0.0001, amp        0.25, cstar=      0.5, t0=         17.,
 alp=          0.9, beta=      0.10, theta=      1.0, idbg=         0,
 iadv=           1, ihd=          1, ibc=          1, isal=         1,
 ipt=            6, ipx=          0, ipc=          0, iextrp=       0,
 tramp=    54000., istd=          1, igs=          0, ivpv=         0,
 iupwind=        0, ioutg=        1, chi=        1.0, ipv=          0,
 ipsal=          0, ipxml=        0, itspf=        0
#2 NODES WHERE TIME SERIES OUTPUT IS DESIRED
 nnodes=         2
 inodes=    15  19
 jnodes=    44  58
#3 OPEN BOUNDARIES (At all open boundaries wse is specified as time series)
 nopen=          3
 sfile=   wse.txt, qfile=  flw.txt, hcfile= hcn.txt, salfile=sal.txt
 iside=          1, itype=        1, idata=        1, isaldata=     3
 wse=          0.0, sal=       33.5, idtwse=    900., idtsal=    900.
 isbc=           2, jsbc=         2, iebc=         2, jebc=        53
 iside=          3, itype=        1, idata=        1, isaldata=     1
 wse=          0.0, sal=        0.8, idtwse=    900., idtsal=    900.
 isbc=          77, jsbc=        72, iebc=        77, jebc=        72
 iside=          3, itype=        1, idata=        1, isaldata=     1
 wse=          0.0, sal=        0.8, idtwse=    900., idtsal=    900.
 isbc=          77, jsbc=        67, iebc=        77, jebc=        67
#4 INTERIOR THIN-WALL BARRIERS AND SINGLE DRY CELLS
 nbarru=         5, nbarrv=      14, ndrycl=      14
 barrier_file= barr1000.txt
#5 SALINITY INITIAL CONDITION
 sal_ic_file= salic.txt
```

Appendix D: Dictionary of Terminology Used in Si3D

iyr	Start year of the simulation (4 digit integer)
imon	Start month of the simulation (2 digit integer)
iday	Start day of the simulation (2 digit integer)
ihr	Start time of the simulation in hours from the beginning of 'iday' multiplied by 100 and rounded to the nearest integer (4 digit integer) (Note: If the start time is at the beginning of a day then ihr = 0.)
xl	Length of basin in x-direction (meters)
yl	Length of basin in y-direction (meters)
zl	Maximum depth of basin measured from mean water surface (meters) (Note: Mean water surface is used as datum for z-coordinates)
tl	Total duration of simulation (seconds)
idt	Temporal step (seconds)
nts	Number of temporal steps in simulation
idx	Grid spacing in x-direction (meters)
idy	Grid spacing in y-direction (meters)
idz	Thickness of vertical layers (meters) (For 2-D computations set idz > zl)
iexplt	If iexplt = 0 use explicit algorithm for continuity eg and pressure term in momentum eq, otherwise use semi-implicit algorithm (Note: When iexplt = 0 use also theta = 0.0).
ivde	If ivde = 0 the vertical diffusion terms will be treated explicitly, otherwise implicitly (Note: When vertical diffusion is done explicitly, it is finite-differenced at the 'n-1' time level. At the 'n' time level it was unstable. At the present time, I evaluate the eddy viscosity at the 'n' time level.)
itrap	Parameter indicating whether the trapezoidal step is used following the leapfrog step If itrap = 0: Trapezoidal step not used If itrap = 1: Trapezoidal step used every temporal step If itrap = 2: Trapezoidal step used every 2nd temporal step If itrap = 3: Trapezoidal step used every 3rd temporal step If itrap = 4: Trapezoidal step used every 4th temporal step, etc.
niter	Number of iterations of the trapezoidal step used each temporal step (assumes itrap = 1)
ismooth	Parameter indicating whether smoothing is done after the leapfrog step If ismooth = 0: No smoothing If ismooth = 1: Smooth velocity If ismooth = 2: Smooth salinity If ismooth = 3: Smooth velocity and salinity If ismooth = 4: Smooth zeta and velocity If ismooth = 5: Smooth zeta, velocity, and salinity

ilin	Parameter indicating whether the total water depth is linearized by not adjusting the surface layer thickness by zeta. (yes = 1, no = 0)
ihomo	Parameter indicating whether the density (and salinity) are homogeneous [Note: The nonhomogeneous seiching problem uses a linear vertical density gradient of 0.035 $kg/m^3/cm$ (= 3.5 $kg/m^3/m$).] (0 = homogeneous, 1 = nonhomogeneous)
dzmin	The minimum thickness allowed for the bottom layer must be greater than dzmin (usually dzmin = 0.09 or 0.19 meters)
iturb	Parameter defining choices for turbulence model If iturb = 0: Eddy coefficients are constants defined by az0 and dz0 in subroutine ‘turb’ If iturb = 1: Eddy coefficients vary with time and are distributed parabolically in the vertical based on the friction velocity in subroutine ‘turb’ If iturb = 2: Eddy coefficients are determined with a mixing length model and adjusted for stratification using Munk-Anderson type damping functions in subroutine ‘turb’
az0	Constant eddy viscosity used when iturb = 0 (m^2/s)
dz0	Constant eddy diffusivity used when iturb = 0 (m^2/s)
az00	Minimum eddy viscosity allowed when using turbulence model iturb = 1 (m^2/s)
a1,b1 a2,b2	Munk-Anderson coefficients used with mixing length turbulence model (iturb = 2)
ax0	X-direction horizontal eddy viscosity (= 1 m^2/s; reasonable range is 0.1 to 10 m^2/s)
ay0	Y-direction horizontal eddy viscosity (= 1 m^2/s or 10^4 cm^2/s)
datadj	Adjustment to the datum used for the bathymetry (meters). This value is added to every depth value read from the bathymetry file. (For SF Bay use datadj = 1.0 meters to approximately adjust the datum from MLLW to NGVD.)
iseich	Parameter indicating whether the seiching problem is being solved or not. When the seiching problem is being solved, “amp” must be defined and the initial water surface elevations for the seiche are computed in SUB init. When the seiching problem is not solved, all initial water surface elevations are taken as zero. (0 = not seiching problem, 1 = seiching problem.)
cd	Drag coefficient for bottom friction (dimensionless)
cw	Drag coefficient for wind shear (dimensionless)
wa	Wind speed at 10 m level (m/sec)
phi	Angle between y-axis and wind (measured clockwise in degrees)
f	Coriolis parameter (usually F = 0.0001)
amp	Initial amplitude of seiche (meters)
cstar	Nondimensional calibration coefficient for the turbulence model when iturb = 1 (normally cstar = 1).
t0	Constant value of temperature used in simulation (in degrees centigrade) (Usually, t0 = 17.0).

alp — Weighting parameter for diffusive finite-difference scheme used only on the first temporal step of the model to get the simulation going. (alp = 1 is FTCS scheme; alp = 0 is pure diffusive scheme.)

beta — Smoothing coefficient for the leapfrog step when ismooth ≥ 1 (beta = 0.05 is recommended. Values as high as 1.0 can be used.)

theta — Weighting parameter on water surface slope term.
If theta = 1.0: Implicit
If theta = 0.0: Explicit

idbg — Parameter indicating the level of debugging. If idbg = 0, there will be no debugging. If idbg = 1, print statements will output to the screen the subprograms that are entered and exited in the main program. If idbg = 2, then a debugging file (tfxx_xx.dbg) is created. The file contains output from the matmom subroutine for the first node where time series output is requested (inode(1), jnode(1)).

iadv — Parameter indicating whether the advection terms are included in the simulation (yes = 1, no = 0)

ihd — Parameter indicating whether the horizontal diffusion terms are included in the simulation (yes = 1, no = 0)

ibc — Parameter indicating whether the baroclinic term is included in the simulation (yes = 1, no = 0) (Note: If the density field is constant it is helpful to define ibc = 0 so as to be certain that truncation errors do not enter the computation)

isal — Parameter indicating whether the salt transport equation is solved (yes = 1, no = 0)

ipt — Number of temporal steps between output to timefiles

ipx — Number of temporal steps between output to spacefiles (if ipx = 0, there will be no output)

ipc — Number of temporal steps between output to file for checking conservation of mass. This is presently only useful for the seiching test problem. (If ipc = 0, there will be no output)(The output file is called 'si3d_cons.txt')

iextrp — Parameter indicating the extrapolation method to be used in SUBROUTINE openbc1 for the estimation of zeta along the row or column of cells immediately outside any open boundaries.
If iextrp = 0: Assume zero slope in zeta across boundary (0^{th}-order extrapolation)
If iextrp = 1: Use linear extrapolation
If iextrp = 2: Use quadratic extrapolation

tramp — Time over which the model forcing functions are ramped from zero to their full values (in seconds from the start of the simulation). Use tramp = -1 for no ramping. (Note: Presently ramping is only available for flow and water surface elevation forcing at open boundaries, not salinity.)

istd — Parameter indicating whether timefiles are output in standard si3d format (yes = 1, no = 0)

igs — Parameter indicating whether timefiles are output in 'gs' format (yes = 1, no = 0) (Note: 'gs' files are in the format for reading into the Gr post-processing program. See URL: http://ca.water.usgs.gov/program/sfbay/gr/ for more information on the Gr program.)

ivpv Parameter indicating whether timefiles are output in the format for the Velocity Profile Viewer (VPV) program (yes = 1, no = 0). (For a copy of the VPV source code, visit http://ca.water.usgs.gov/program/sfbay/vpv/)

iupwind Parameter indicating whether upwind or centered differencing is used for the horizontal advection of momentum and salinity.
If iupwind = 0: Use centered differencing (for mom and salinity)
If iupwind = 1: Use upwind differencing (for mom and salinity)
If iupwind = 2: Use upwind differencing for momentum only
If iupwind = 3: Use upwind differencing for salinity only
(Note: When upwind differencing is used on the momentum advection terms, a Courant number temporal step limitation based on the advection velocity applies to the hydrodynamic eqs.)

ioutg Parameter indicating whether to output a bathymetry file useful for graphics and particle tracking (yes = 1, no = 0). The bathymetry file is called either si3d_bathy.txt or si3d_bathy.xml. A parameter (ixml) determines whether the .txt or .xml formats are used for the file. (Presently, the parameter ixml is hardwired in SUB outg.)

chi Weighting parameter used on the term in the salt transport equation for computing vertical advection of salt
If chi = 1.0: implicit vertical advection
If chi = 0.0: explicit vertical advection

ipv Number of temporal steps between output to the xy_vec.txt file.
If ipv = 0, no output is written. The xy_vec.txt file is formatted in the first (May 2001) file format used by the Gr application to animate velocity fields for one layer. The velocities are saved at the center of each grid cell as speed and direction.

ipsal Number of temporal steps between output to the xy_sal.txt file.
If ipsal = 0, no output is written. The xy_sal.txt file is formatted in the first (July 2001) file format used by the Gr application to animate salinity fields for one layer. The salinities are saved at the center of each grid cell.

ipxml Number of temporal steps between output to the spacefile.xml file. This is the xml file that is used for post-processing (particle-tracking and animation) of model results with the Gr application. It is essentially a header file for the two sequential binary output files (called spacefile3d.bin and spacefile2d.bin) that contain the actual 3D and 2D data from all the spatial nodes of the solution at snapshots in time. The '3d' .bin file contains the 3-D variables and the '2d' .bin file contains the 2-D variables. The time interval at which data is output to the .bin files is also controlled by ipxml.
If ipxml = 0, no output is written to either the spacefile.xml or the .bin files. The spacefile.xml file is written in subroutine "outs_xml". The two binary files are written in subroutine "outs_bin".

itspf Time in seconds in which first output is going to be written to the binary files. This only has meaning if ipxml > 0. The value for itspf must be

	evenly divisible by 3600 seconds (1 hour) so that it specifies a time that corresponds to the beginning of an hour.
nnodes	Number of nodes where a timefile is desired (if nnodes = 0, no timefiles are created)
inode	Array containing x-axis node numbers for locations where timefiles are to be output
jnode	Array containing y-axis node numbers for locations where timefiles are to be output
nopen	Number of open boundaries
sfile	Boundary condition file for water surface elevation (wse.txt)
qfile	(flw.txt)
hcfile	(hcn.txt)
salfile	Filename containing a time series of salinity to use on open boundaries with isaldata = 1 (sal.txt)
iside	1-west; 2-north; 3-east; 4-south
itype	1-wse; 2-discharge
idata	1-time series; 2-harmonic constants; 3-constant value
isaldata	1-time series; 2-harmonic constants; 3-constant value
wse	Constant water surface elevation (m) used on open boundary if itype = 1 and idata = 3
flw	Constant discharge (m^3/s) used on open boundary if itype = 2 and idata = 3
sal	Constant salinity (psu) used on open boundary if isaldata = 3
idtwse	Time interval in seconds between data values in the bc file for wse
idtsal	Time interval in seconds between data values in the bc file for salinity
idtflw	Time interval in seconds between data values in the bc file for flow
isbc	x-direction cell number for the start of the boundary condition
jsbc	y-direction cell number for the start of the boundary condition
iebc	x-direction cell number for the end of the boundary condition
jebc	y-direction cell number for the end of the boundary condition
nbarru	Number of interior thin-wall barriers to u-direction flow
nbarrv	Number of interior thin-wall barriers to v-direction flow
ndrycl	Number of single dry cells
barrier_file	Filename containing the list of node numbers with interior thin-wall barriers and single dry cells (barr1000.txt)
sal_ic_file	Filename containing salinity initial condition (salic.txt)
sal0	Initial value of salinity assigned to all nodes in homogeneous problems or to the surface layer only in the non-homogeneous seiching problem (in practical salinity units or ppt) (= 20 psu for homogeneous problem and = 0 psu for non-homogeneous problem)
g	Acceleration due to gravity (= 9.807 m/sec^2)
i1	x-direction node number of first wet node after west boundary (= 2 in this program; later it will be converted to an array.)
im	x-direction node number of last wet node at east boundary (Note: X-node numbering is from west to east beginning with a fictitious first column)
j1	y-direction node number of first wet node after south boundary (= 2 in this program; later it will be converted to an array.)

jm	y-direction node number of last wet node at north boundary (Note: Y-node numbering is from south to north beginning with a fictitious first row)
k1	Layer number of first wet layer (= 2 in this program)
km	Layer number of last real (non-fictitious) layer at bottom (Note: Z-layer numbering is from top to bottom beginning with a fictitious first layer and ending with a fictitious bottom layer)
ndz	Number of real layers (= 6 in this program)
ex	Three-dimensional workspace array used for temporarily storing the sum of explicit terms in the x-momentum, y-momentum, and salt transport equations
rho0	Initial value of sigma-t (kg/m^3) assigned to all nodes in homogeneous problem or surface layer only in non-homogeneous problem (Note: Sigma-t is used in lieu of density to avoid truncation errors in calculating density gradients. Whenever density alone is needed in the computations 1000 is added to sigma-t to obtain density in kg/m^3.) (To convert density in kg/m^3 to g/cm^3 divide by 1000.)
dhro	Change in sigma-t between vertical layers used in assigning the vertical density profile in the non-homogeneous seiching test problem (= 7 kg/m^3 for non-homogeneous problem and = 0 kg/m^3 for homogeneous problem) (Note: The linear vertical density gradient used here is the same as used by Leendertse in Vol IV Rand report, p 25)
rhoair	Air density needed for wind stress calculation (= 1.3 kg/m^3)
dsal	Change in salinity between vertical layers used in assigning the vertical salinity profile in the non-homogeneous seiching test problem (= 9.18442 psu in the non-homogeneous seiching test problem when a temperature of 17 degrees centigrade is assumed; = 0 psu for the homogeneous seiching problem)
kappa	Von Karman Constant (0.41)
begind	Start time of the simulation expressed in decimal days. This is used in determining the beginning time value for the output in the 'gs' timefiles. It normally should be a Julian day. It can be a negative number or zero.
ipbin	This parameter is no longer included in the input file. It was used (prior to 8/28/04) to indicate whether the velocity and other data normally written as ASCII text into 2-D and 3-D .xml spacefiles were to be written instead into two separate sequential binary files. The program was coded so that: If ipbin = 1: Write to binary files If ipbin = 0: Write to ASCII files No option remains to write the 2d and 3d data to ASCII .xml files. The program is now coded so that when ipxml is greater than zero the binary files are written. (If ipxml = 0 then no .bin files are written.) The spacefile.xml file is always just a header file.

Appendix E: FORTRAN 77 Program for Coarsening NOS's SF Bay DEM

```
      INTEGER DEM(9999999,3),Z(9999,9999),H(9999,9999),DEMRES,COARSENESS
     &,COL,GROUP,SEARCHBOXRADIUS,DECIMETERSOUTPUT,ORIGINALDEMXYZFILE,EMP
     &TYCELLCOUNT
C
C INPUTS
C
C ORIGINAL 'DEM.XYZ' FILE: 1=YES, ORIGINAL FILE; 0=NO, MODIFIED FILE
C
      ORIGINALDEMXYZFILE=1
C
C NUMBER OF LINES IN 'DEM.XYZ': MUST BE ACCURATE
C
      IF(ORIGINALDEMXYZFILE.EQ.1)NUML=1119165
      IF(ORIGINALDEMXYZFILE.EQ.0)NUML=4625166
C
C X, Y SPACING IN 'DEM.XYZ'
C
      DEMRES=30
C
C HOLE SEARCH-BOX RADIUS
C
      SEARCHBOXRADIUS=4
C
C MAXIMUM NUMBER OF EMPTY CELLS IN SEARCH BOX TO BE CONSIDERED A HOLE
C
      MAXEMPTYCELLCOUNT=5
C
C COARSENING FACTOR FOR OUTPUT: 1, 2, 3, ...; 1 MATCHES 'DEM.XYZ'
C
      COARSENESS=1
C
C DECIMETERS OUTPUT: 1 MATCHES 'H' FILE; 0 MATCHES 'DEM.XYZ'
C
      DECIMETERSOUTPUT=1
C
C NUMBER OF COLUMNS IN 'H' FILE
C
      NCOLS=18
C
C END INPUTS
C
C INITIALIZE MINX, MINY, MAXX, MAXY
C
      MINX=2147483647
      MINY=2147483647
      MINZ=2147483647
      MAXX=-2147483648
      MAXY=-2147483648
      MAXZ=-2147483648
C
C READ X, Y, Z DATA FROM 'DEM.XYZ'
C
```

```
      OPEN(1,FILE='DEM.XYZ')
      DO L=1,NUML
      READ(1,*)DEM(L,1),DEM(L,2),DEM(L,3)
C
C FIND MINIMUM AND MAXIMUM X AND Y VALUES
C
      IF(DEM(L,1).LT.MINX)MINX=DEM(L,1)
      IF(DEM(L,2).LT.MINY)MINY=DEM(L,2)
      IF(DEM(L,3).LT.MINZ)MINZ=DEM(L,3)
      IF(DEM(L,1).GT.MAXX)MAXX=DEM(L,1)
      IF(DEM(L,2).GT.MAXY)MAXY=DEM(L,2)
      IF(DEM(L,3).GT.MAXZ)MAXZ=DEM(L,3)
      ENDDO
C
C NUMBER OF I AND J NODES IN Z ARRAY
C
      IMX=(MAXX-MINX)/DEMRES
      JMX=(MAXY-MINY)/DEMRES
C
C Z ARRAY: COLUMN 3 FROM 'DEM.XYZ'
C
      L=1
      DO I=0,IMX
      DO J=0,JMX
      IF(MINX+I*DEMRES.EQ.DEM(L,1).AND.MINY+J*DEMRES.EQ.DEM(L,2))THEN
      Z(I+1,J+1)=DEM(L,3)
      L=L+1
      ELSE
      Z(I+1,J+1)=MAXZ+1
      ENDIF
      ENDDO
      ENDDO
C
C INTERPOLATE TO FILL SINGLE-CELL HOLES IN Z ARRAY
C
      DO I=2,IMX
      DO J=2,JMX
      IF(Z(I-1,J-1).NE.MAXZ+1.AND.Z(I-1,J).NE.MAXZ+1.AND.Z(I-1,J+1).NE.M
     &AXZ+1.AND.Z(I,J-1).NE.MAXZ+1.AND.Z(I,J).EQ.MAXZ+1.AND.Z(I,J+1).NE.
     &MAXZ+1.AND.Z(I+1,J-1).NE.MAXZ+1.AND.Z(I+1,J).NE.MAXZ+1.AND.Z(I+1,J
     &+1).NE.MAXZ+1)Z(I,J)=(.5-SQRT(.125D0))*(Z(I-1,J)+Z(I,J-1)+Z(I,J+1)
     &+Z(I+1,J))+(SQRT(.125D0)-.25)*(Z(I-1,J-1)+Z(I-1,J+1)+Z(I+1,J-1)+Z(
     &I+1,J+1))+.5
      ENDDO
      ENDDO
C
C LOCATIONS OF HOLES RECORDED IN 'HOLES.XYZ'
C
      OPEN(2,FILE='HOLES.XYZ')
      DO I=SEARCHBOXRADIUS+1,IMX-SEARCHBOXRADIUS+1
      DO J=SEARCHBOXRADIUS+1,JMX-SEARCHBOXRADIUS+1
      IF(Z(I,J).EQ.MAXZ+1)THEN
      EMPTYCELLCOUNT=0
      DO K=I-SEARCHBOXRADIUS,I+SEARCHBOXRADIUS
      DO L=J-SEARCHBOXRADIUS,J+SEARCHBOXRADIUS
      IF(Z(K,L).EQ.MAXZ+1)EMPTYCELLCOUNT=EMPTYCELLCOUNT+1
      ENDDO
      ENDDO
      IF(EMPTYCELLCOUNT.LE.MAXEMPTYCELLCOUNT)WRITE(2,*)MINX+(I-1)*DEMRES
     &,MINY+(J-1)*DEMRES,Z(I,J)
```

```
      ENDIF
      ENDDO
      ENDDO
C
C NUMBER OF I AND J NODES IN H ARRAY
C
      IMX=IMX/COARSENESS+1
      JMX=JMX/COARSENESS+1
C
C H ARRAY: COARSENED Z ARRAY
C
      DO I=1,IMX
      DO J=1,JMX
      DO K=(I-1)*COARSENESS+1,I*COARSENESS
      DO L=(J-1)*COARSENESS+1,J*COARSENESS
      H(I,J)=H(I,J)-Z(K,L)*10
      ENDDO
      ENDDO
      IF(H(I,J).GE.0)H(I,J)=DBLE(H(I,J))/COARSENESS**2+.5
      IF(H(I,J).LT.0)H(I,J)=DBLE(H(I,J))/COARSENESS**2-.5
      IF(DECIMETERSOUTPUT.EQ.1)THEN
      WRITE(*,*)INT(MINX-DEMRES/2D0+(I-.5D0)*DEMRES*COARSENESS),INT(MINY
     &-DEMRES/2D0+(J-.5D0)*DEMRES*COARSENESS),-H(I,J)/10D0
      ELSEIF(H(I,J).LE.0)THEN
      WRITE(*,*)INT(MINX-DEMRES/2D0+(I-.5D0)*DEMRES*COARSENESS),INT(MINY
     &-DEMRES/2D0+(J-.5D0)*DEMRES*COARSENESS),INT(-H(I,J)/10D0+.5)
      ELSE
      WRITE(*,*)INT(MINX-DEMRES/2D0+(I-.5D0)*DEMRES*COARSENESS),INT(MINY
     &-DEMRES/2D0+(J-.5D0)*DEMRES*COARSENESS),INT(-H(I,J)/10D0-.5)
      ENDIF
      ENDDO
      ENDDO
C
C 'H' FILE FOR SI3D INPUT
C
      OPEN(3,FILE='H')
      WRITE(3,'(A,I5,A,I5,A,I5,A,I4,A/A/A)')'SFBay',DEMRES*COARSENESS,',
     &Edited & w/barriers, imx =',IMX,',jmx =',JMX,',ncols =',NCOLS,',
     &  9/10/07','HV       V   V   V   V   V   V   V   V   V   V   V   V
     &   V   V   V   V   V','HU     U z U z U z U z U z U z U z U z U z
     &U z U z U z U z U z U z U z U z U'
      DO I=1,IMX
      DO J=1,JMX
      IF(H(I,J).LE.0)H(I,J)=-90
      ENDDO
      ENDDO
      DO GROUP=0,(IMX-1)/NCOLS
      DO J=JMX,1,-1
      WRITE(3,'(I4,A$)')J,' '
      DO I=GROUP*NCOLS+1,(GROUP+1)*NCOLS-1
      IF(H(I,J).NE.0)WRITE(3,'(I4$)')H(I,J)
      ENDDO
      IF(H(I,J).NE.0)THEN
      WRITE(3,'(I4)')H(I,J)
      ELSE
      WRITE(3,*)
      ENDIF
      ENDDO
      ENDDO
      END
```